

# Metal-free reusable hollow-spherical triazine microporous organic polymer supported quinolines synthesis *via* hydrogen evolution<sup>†</sup>

Debabrat Pathak<sup>a</sup>, Bikash Kumar Kalita<sup>a</sup>, Ashish Sarmah<sup>a</sup>, Himanshu Sharma<sup>a</sup>, Bidisha Bora<sup>b</sup>, Tridib K. Goswami<sup>b</sup>, Bipul Sarma<sup>a,\*</sup>

<sup>a</sup>Department of Chemical Sciences, Tezpur University, Tezpur-784028, Assam, India.

<sup>b</sup>Department of Chemistry, Gauhati University, Guwahati-781014, Assam, India.

\*Corresponding author. Email: [bcsarma@tezu.ernet.in](mailto:bcsarma@tezu.ernet.in)

## 1. Experimental Section

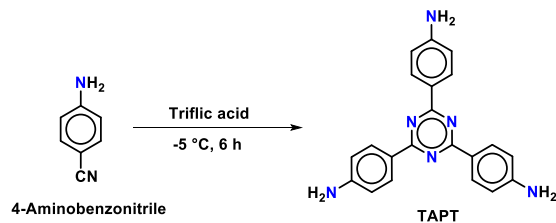
### **Materials and measurements:**

All the chemicals employed in this manuscript are brought from commercial sources and were used as such without further purification until otherwise mentioned. FT-IR spectra of the building units and synthesized MOP-TA were recorded in the range 400–4000 cm<sup>-1</sup> by preparing the sample pellets in KBr using Perkin Elmer spectrophotometer. The powder X-ray diffraction (PXRD) was recorded in D8 ADVANCE X-ray using monochromated Cu K $\alpha$  ( $\lambda = 1.542 \text{ \AA}$ ) radiation made by Bruker. Single crystal X-ray diffractions were collected on a Bruker SMART APEX-II CCD diffractometer using Mo K $\alpha$  ( $\lambda = 0.71073 \text{ \AA}$ ) radiation. All the structures were solved and refined using SHELXL. Thermogravimetric analyses (TGA) were performed on a Shimadzu 60 thermal analyser at a heating rate of 10 °C min<sup>-1</sup> under continuous nitrogen flow. The porosity and rigidity of MOP-TA has been measured recording the N<sub>2</sub> adsorption-desorption isotherm of it at Quantachrome (Version 3.0) surface area analyser. The liquid nitrogen used in the measurement was of ultra-high purity (99.999% pure) and the refrigerated bath of liquid nitrogen (77 K) further controls the temperature during the process. Field emission scanning electron microscope (FESEM) images were recorded in Gemini 500 FE-SEM (software: SmartSEM User Interface) and high-resolution transmission electron microscope (TEM) images were recorded in JEOL JEM 2100 at an accelerating voltage of 200 kV to examine the surface and bulk morphology. Solid state <sup>13</sup>C cross polarizing magic angle spinning (<sup>13</sup>C CP-MAS) NMR data has been recorded in Jeol 400 MHz spectrometer employing 4 nm MAS probe with spin rate of 5000 Hz. The progress of the reactions was monitored by TLC using TLC silica gel F254 250  $\mu$ m pre-coated-plates from Merck and the product formation was confirmed by NMR spectrometer (Bruker AVANCE NEO NMR SPECT. 400 MHz), (JEOL ECS-400, DELTA, VERSION-4.3.6), (Bruker ADVANCE III HD NMR SPECT.

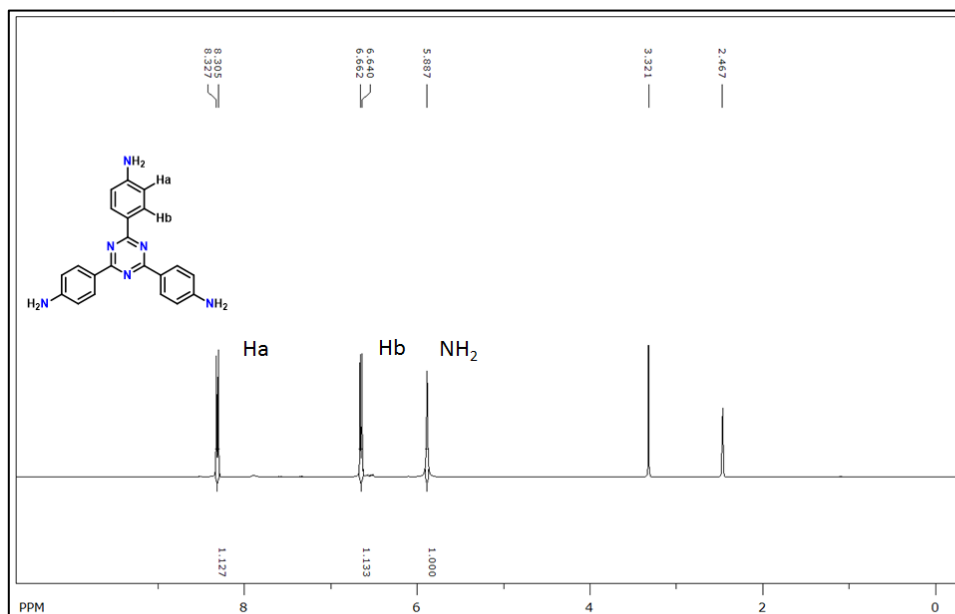
600 MHz) and HRMS (Xevo G2-XS QToF (Waters) mass spectrometer using electron spray ionization mass).

**<sup>1</sup>H & <sup>13</sup>C{<sup>1</sup>H} NMR of 2,4,6-tris-(4-aminophenyl)-1,3,5-triazine (TAPT):**

<sup>1</sup>H NMR (400MHz, DMSO-d<sub>6</sub>) δ (ppm): 8.31 (d, 6H, J=8), 6.65 (d, 6H J= 8), 5.89 (s, 6H). <sup>13</sup>C{<sup>1</sup>H} (101MHz, DMSO-d<sub>6</sub>) δ (ppm): 170.1, 153.5, 130.7, 123.4, 113.6.



Scheme S1. Synthesis of 2,4,6-tris-(4-aminophenyl)-1,3,5-triazine (TAPT).



(a)

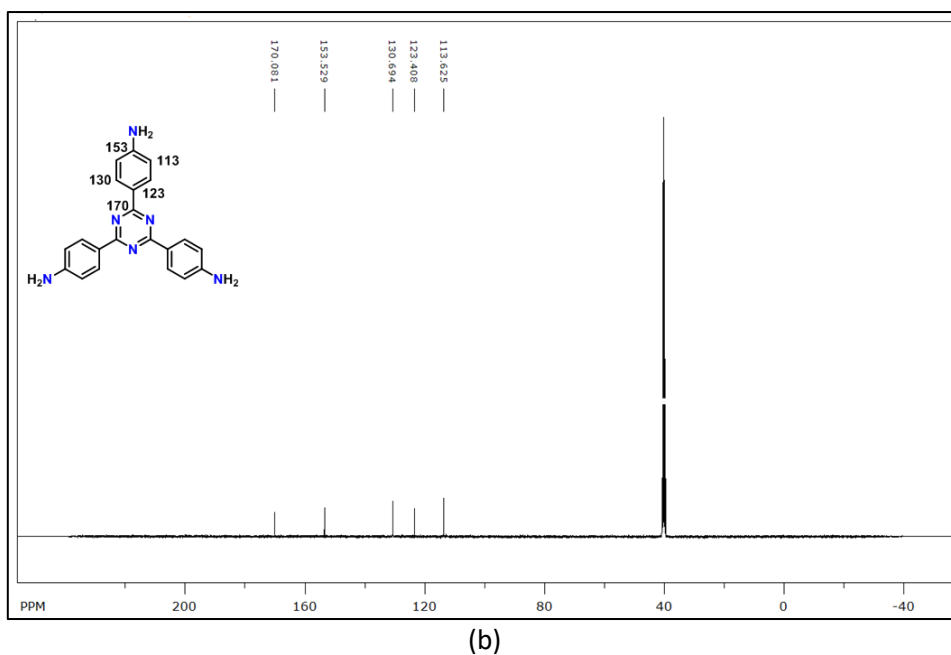


Figure S1. (a)  $^1\text{H}$  NMR (400 MHz) and (b)  $^{13}\text{C}$  NMR (101 MHz) spectra of TAPT in  $\text{DMSO-d}_6$ .

## 2. FT-IR analysis

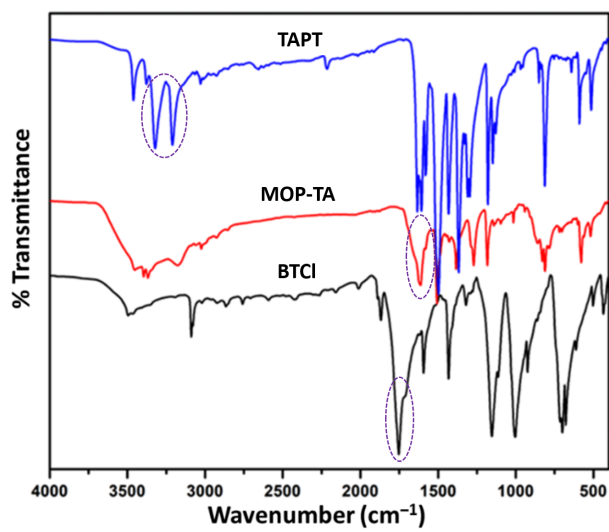


Figure S2. FT-IR spectra of TAPT and MOP-TA, BTCI.

## 3. FESEM analysis

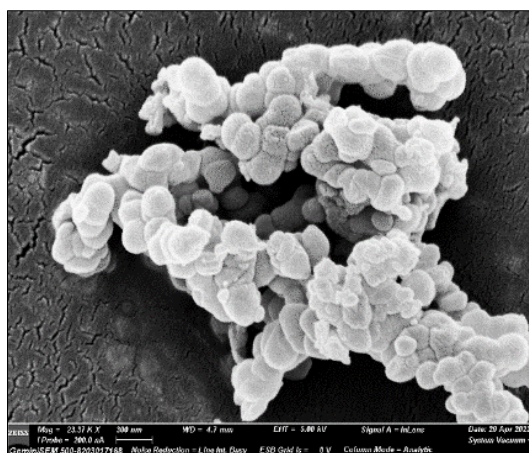


Figure S3. FESEM imaging demonstrated MOP-TA having globular surface morphology.

#### 4. TGA analysis

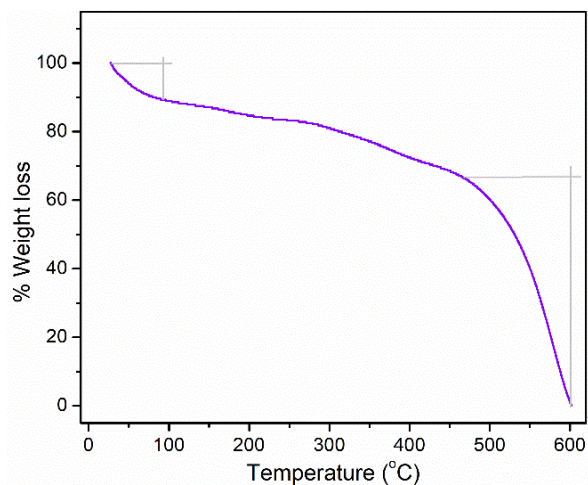


Figure S4. TGA thermogram of MOP-TA.

#### 5. Stability test with FT-IR and PXRD analysis

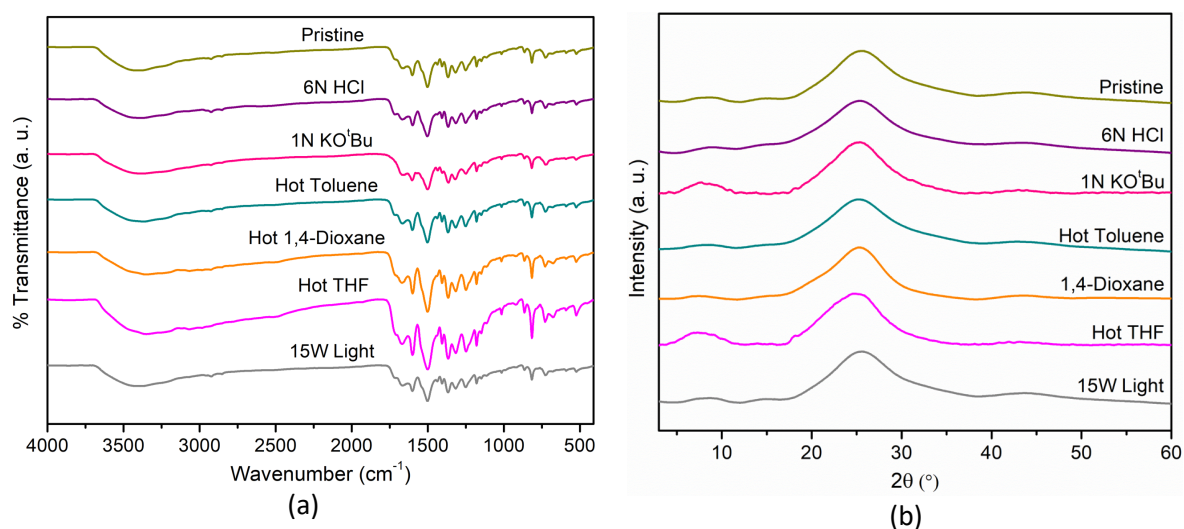
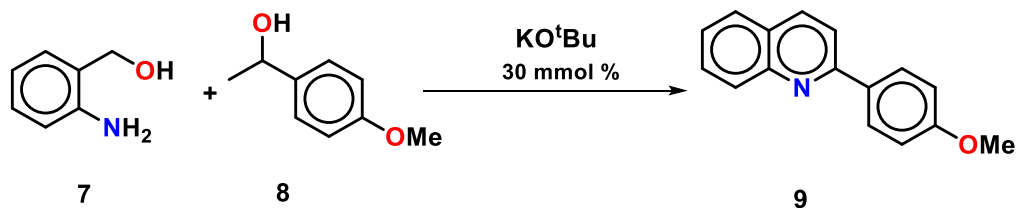


Figure S5. FT-IR spectra (a) and PXRD pattern (b) of MOP-TA after treating it with various physical and chemical environment for two days showed consistent structural stability..



## 6. Green matrix determination



	7	8	KO <sup>t</sup> Bu	Toluene	9
Quantity	1.230 g	1.824 g	0.336 g	7.800 g	2.085 g
	Total reactant = 11.190 g				

E factor: Mass of total waste ÷ mass of product

$$= (11.190 - 2.085) \div 2.085$$

$$= 4.367 \text{ kg waste/1 kg product}$$

Atom Economy: Molecular mass of product ÷ molecular mass of reactants × 100

$$= [235.1 \div (123.07 + 152.08)] \times 100 \%$$

$$= 85.43 \%$$

Atom Efficiency: Percentage yield × [atom economy ÷ 100]

$$= 88.68 \times (85.43 \div 100)$$

$$= 75.76 \%$$

Carbon Efficiency: [No. of carbon atoms in the reactants ÷ No. of carbon atoms in the products] × 100

$$= (16 \div 16) \times 100 \%$$

$$= 100 \%$$

Excess Reactant Factor: (Stoichiometric mass of reactant + excess mass of reactant) ÷ stoichiometric mass of reactant

$$= [(1.230 + 1.824)] \div 2.750$$

$$= 1.04$$

Reaction Mass Efficiency: [Actual mass of desired product ÷ mass of reactants] × 100

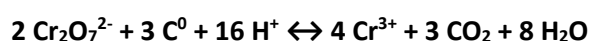
$$= [2.085 \div (1.230 + 1.824)] \times 100 \%$$

$$= 68.27 \%$$

## 7. Total organic carbon determination

The modified Walkley and Black method of redox titration were used to determine the total organic carbon for the representative substrates of the concerned reaction. Carbon balance is a measure to quantify the efficiency of reaction in terms of carbon emission to the surroundings. Hence, it is expressed as the sum of the total organic carbons from all the possible products dividing it by the total carbons from the reactant. In this method, 1 N  $K_2Cr_2O_7$ , and conc.  $H_2SO_4$  (98%) is used as a digesting agent followed by the use of reducing titrant 0.5 M  $Fe(NH_4)_2(SO_4)_2$  solution that converts excess Cr(VI) to Cr(III). To a known amount of sample, 10 mL of 1 N  $K_2Cr_2O_7$  solution and 20 mL of conc.  $H_2SO_4$  is added, subjected to a temperature of 140 °C for 3-4 minutes, swirled, and allowed to stand for half an hour for complete digestion. Once the solution attained room temperature, 200 mL of distilled water and 10 mL of ortho-Phosphoric acid (for an intense colour change) is further added to it. The addition of 1mL of Diphenylamine as an indicator makes the solution dark violet or blue in colour which is finally titrated against 0.5M  $Fe(NH_4)_2(SO_4)_2$  solution till a bright green solution appears.

The involved redox chemical equation is



Therefore,

1mL of 1N  $K_2Cr_2O_7$  = 0.003 g of organic carbon (OC)

Thus,

$$\%OC = \frac{(B-S) \times M[Fe(II)] \times 0.003 \times 100}{\text{Amount of sample in g}}$$

Where, B = Titrant value of Blank Solution

S = Titrant value of Substrate Solution

M [Fe(II)] = Concentration of  $Fe(NH_4)_2(SO_4)_2$  solution.

A blank titration was carried out without any sample to ascertain the volume of  $Fe(NH_4)_2(SO_4)_2$  solution required to reduce the 10 mL of 1N  $K_2Cr_2O_7$  solution used. The readings were collected in thrice for the concordant values. For the blank sample the titrant value, B was found to be 18.9 mL. The concordant titrant values (S) during the annulation of 2-(*p*-anisyl)quinoline, before the reaction and after the reaction, are tabulated below.

**Table S1.** Carbon balance or total organic carbon for during synthesis of 2-(*p*-anisyl)quinoline.

Entry	Weight Taken	Before Reaction	After Reaction	
-------	--------------	-----------------	----------------	--

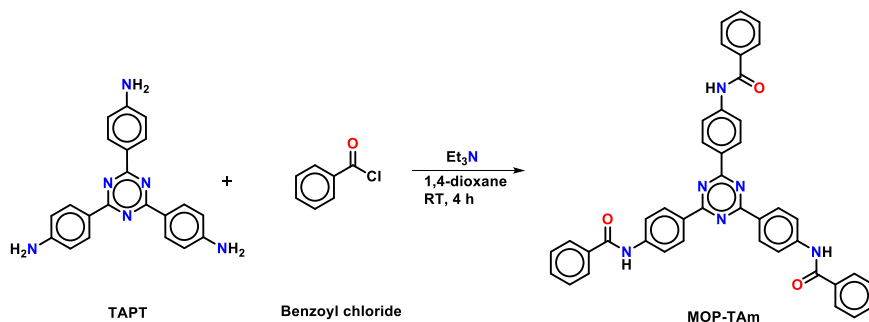
		Titrant value of 0.5 N Fe (NH <sub>4</sub> ) <sub>2</sub> (SO <sub>4</sub> ) <sub>2</sub> (mL) <b>S</b>	OC content quantity on reactant side(mg)	Titrant value of 0.5 N Fe (NH <sub>4</sub> ) <sub>2</sub> (SO <sub>4</sub> ) <sub>2</sub> (mL) <b>S</b>	OC content quantity on reactant side(mg)	% Carbon Balance
<b>Scheme 2</b>	30 mg	5.2	20.55	5.3	20.40	99.27

### 8. Synthesis of nitrogen rich monomer unit (MOP-TAm)

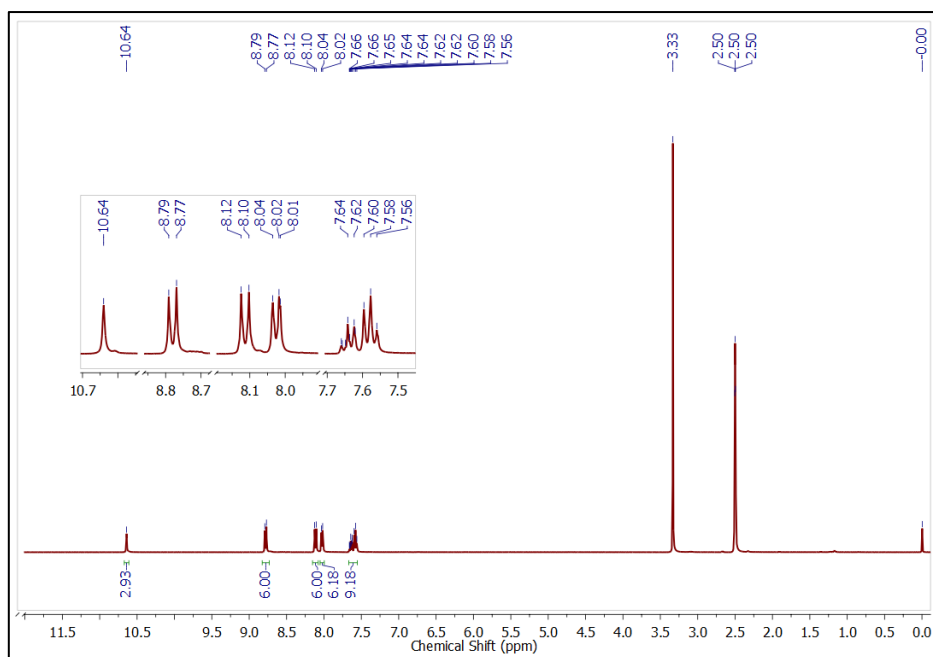
MOP-TAm is synthesized using reported procedure. Dissolved 200 mg (0.56 mmol) of TAPT in 15 mL of dry 1,4-dioxane and adding 1 mL of triethylamine (TEA). To it 170  $\mu$ L (1.68 mmol) of benzoyl chloride (PhCOCl) was slowly added in nitrogenous environment and left with continuous stirring for 4 h (Scheme S3). The desired precipitate of MOP-TAm is then filtered and washed with 1,4-dioxane. It is then dried in desiccator and characterized with <sup>1</sup>H NMR.

<sup>1</sup>H NMR (DMSO-d<sub>6</sub>, 400 MHz),  $\delta$  (ppm): 10.64 (s, 3H, -NH-), 8.78 (d, *J* = 8.8 Hz, 6H), 8.11 (d, *J* = 8.8 Hz, 6H), 8.03 (d, *J* = 7.9 Hz, 6H), 7.67 – 7.55 (m, 9H).

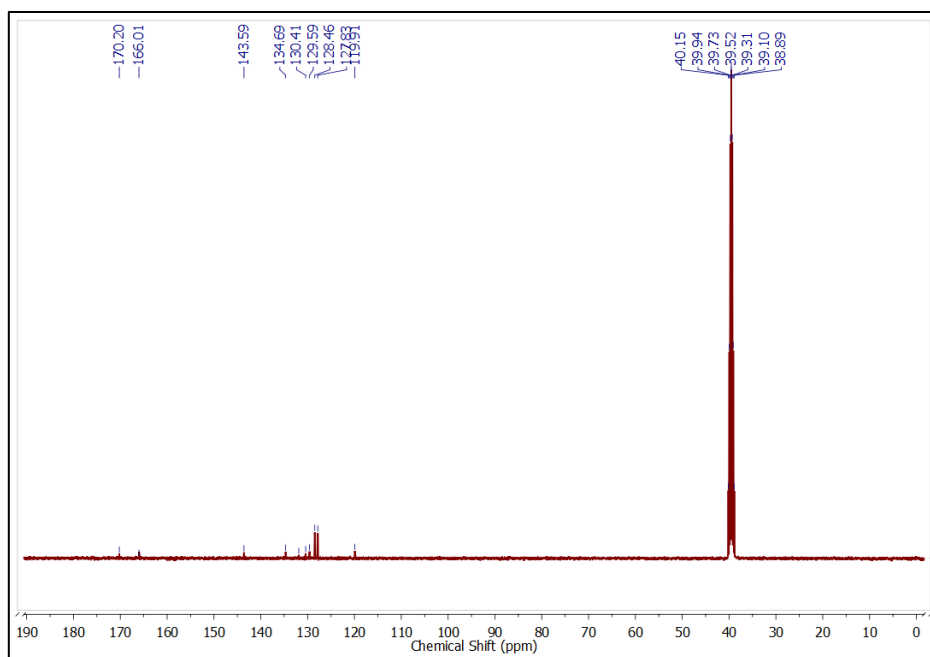
<sup>13</sup>C{<sup>1</sup>H} NMR (DMSO-d<sub>6</sub>, 101 MHz),  $\delta$  (ppm): 170.2, 166.0, 143.6, 134.7, 131.9, 130.4, 129.6, 128.5, 127.8, 119.9.



Scheme S2. Synthesis of monomeric unit of the triazine based porous organic polymer, MOP-TAm.



(a)



(b)

Figure S6. (a)  $^1\text{H}$  (400 MHz,  $\text{DMSO-d}_6$ ) and (b)  $^{13}\text{C}\{^1\text{H}\}$  (101 MHz,  $\text{DMSO-d}_6$ ) NMR of MOP-TAm.

**9. Table S2.** Catalytic conversion comparison of both MOP-TA and MOP-TAm under same reaction condition.

Entry	Catalyst	% Conversion
6a	MOP-TA	93%
	MOP-TAm	12%
6c	MOP-TA	96%
	MOP-TAm	15%
6d	MOP-TA	86%

	MOP-TAm	<b>4%</b>
<b>6g</b>	MOP-TA	<b>90%</b>
	MOP-TAm	<b>7%</b>
<b>6i</b>	MOP-TA	<b>82%</b>
	MOP-TAm	<b>trace</b>
<b>6j</b>	MOP-TA	<b>84%</b>
	MOP-TAm	<b>trace</b>
<b>6l</b>	MOP-TA	<b>90%</b>
	MOP-TAm	<b>10%</b>
<b>6p</b>	MOP-TA	<b>96%</b>
	MOP-TAm	<b>13%</b>
<b>6u</b>	MOP-TA	<b>96%</b>
	MOP-TAm	<b>12%</b>
<b>6v</b>	MOP-TA	<b>96%</b>
	MOP-TAm	<b>14%</b>

**10. Table S3.** Comparison of MOP-TA with other reported catalyst during quinoline synthesis

<b>Catalyst</b>	<b>Substrate</b>	<b>Reaction Condition</b>	<b>Yields/ Remarks</b>	<b>Ref</b>
[IrCl(cod)] <sub>2</sub>	2-aminoalcohol + ketone	2-aminoalcohol (2 mmol), ketone (4 mmol), KOH (0.4 mmol), T (100 °C)	Up to 91% / Additives= PPh <sub>3</sub> (0.08 mmol)	1
Pd-nano	2-aminoalcohol + ketone	2-aminoalcohol (1 mmol), ketone (2 mmol), KOH (3 mmol), T (100 °C), Solvent (Toluene or Dioxane), t (24 h)	Up to 85%	1
FeCl <sub>3</sub>	Aniline + aldehyde + Ethyl lactate	Aniline (0.2 mmol), aldehyde (0.2 mmol), Ethyl lactate (2 mL), T (110 °C), t (12 h)	Up to 79%	2
Pyridine	2-aminoalcohol + ketone	2-aminoalcohol (0.81 mmol), ketone (0.97 mmol), KOH (0.16 mmol), T (135 °C), Solvent (1,4-dioxane), Ar atmosphere	Up to 92%	3
Silica sulfuric acid	Aldehyde + aniline + pyruvic acid	Ethanol, T (78 °C), t (3.5 h)	Up to 84%	4

RuCl <sub>2</sub> (PPh <sub>3</sub> ) <sub>3</sub>	Alcohols	KOH, 1-dodecene, T (80 °C), t (20 h)	Up to 90%	5
Yb(Pfb) <sub>3</sub>	Aldehyde + aniline + Phenylacetylene	T (120 °C), t (12 h)	Up to 92%	6
Fe(OTs) <sub>3</sub> ·6H <sub>2</sub> O	Alcohol + ketone	DTBP as oxidant (0.6 mmol), DMSO (0.8 mL), T (110 °C) t (20 h), air	Up to 81%	7
Ru(PPh <sub>3</sub> ) <sub>3</sub> Cl <sub>2</sub>	Nitroaldehyde + alcohol	K <sub>2</sub> CO <sub>3</sub> (0.5 equiv.), additives, T (150 °C), t (24 h)	Up to 74%	8
Anthraquinone	Alcohols	NaOH (2 equiv.), DMSO as oxidant, hv (LEDs 450-460 nm), t (6 h)	Up to 95%	9
MOP-TA	Alcohols	KO <sup>t</sup> Bu (30 mol%), Toluene, T (85 °C), t (3 h)	Up to 93% No oxidant, No metal	This work

### 11. Interaction of the substrate molecule over MOP-TA

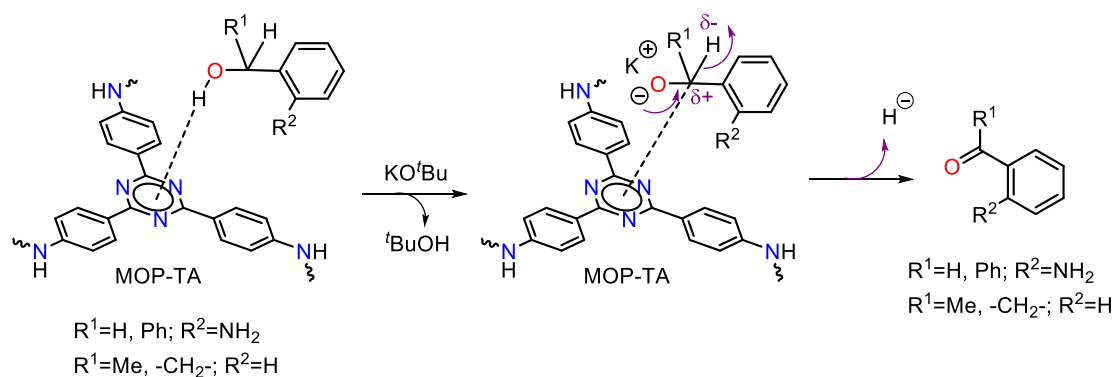
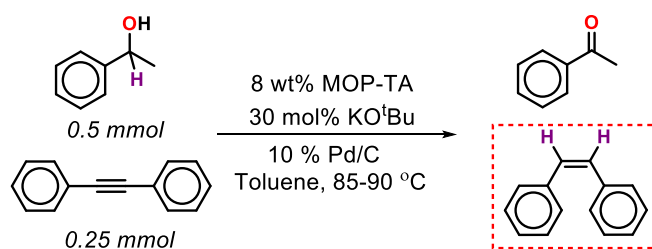


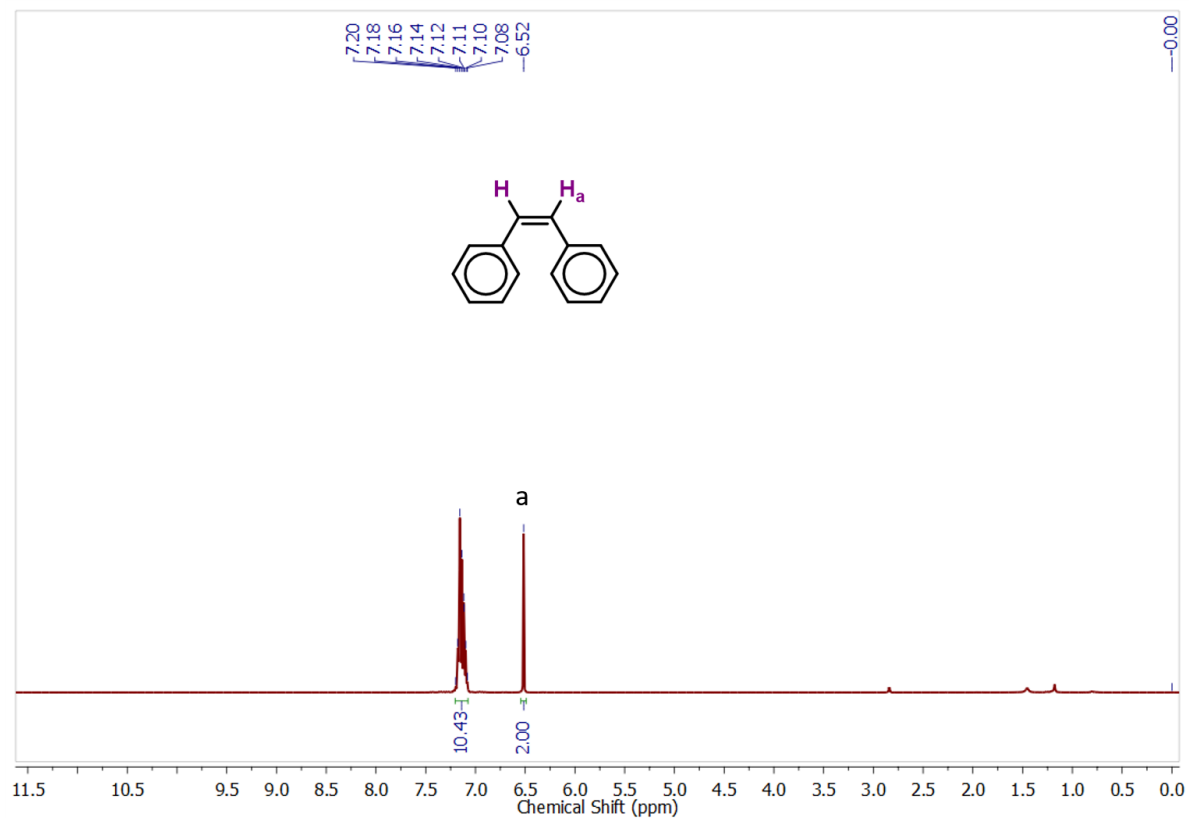
**Figure S7.** Detailed interaction between MOP-TA and the substrates.

### 12. In-situ reduction of diphenylacetylene in detecting hydrogen evolution

In a 20 mL Schlenk tube 0.5 mmol of 1-phenylethanol, 0.25 mmol of diphenylacetylene, 30 mol% of KO<sup>t</sup>Bu, 8 wt% of MOP-TA, 10 mol% of Pd/C (10% Pd/C) and 2 mL of toluene were added and heated at 85-90 °C for 8 h. The reaction is monitored using TLC. The reaction mixture was purified using column chromatography and characterized by NMR spectroscopy.

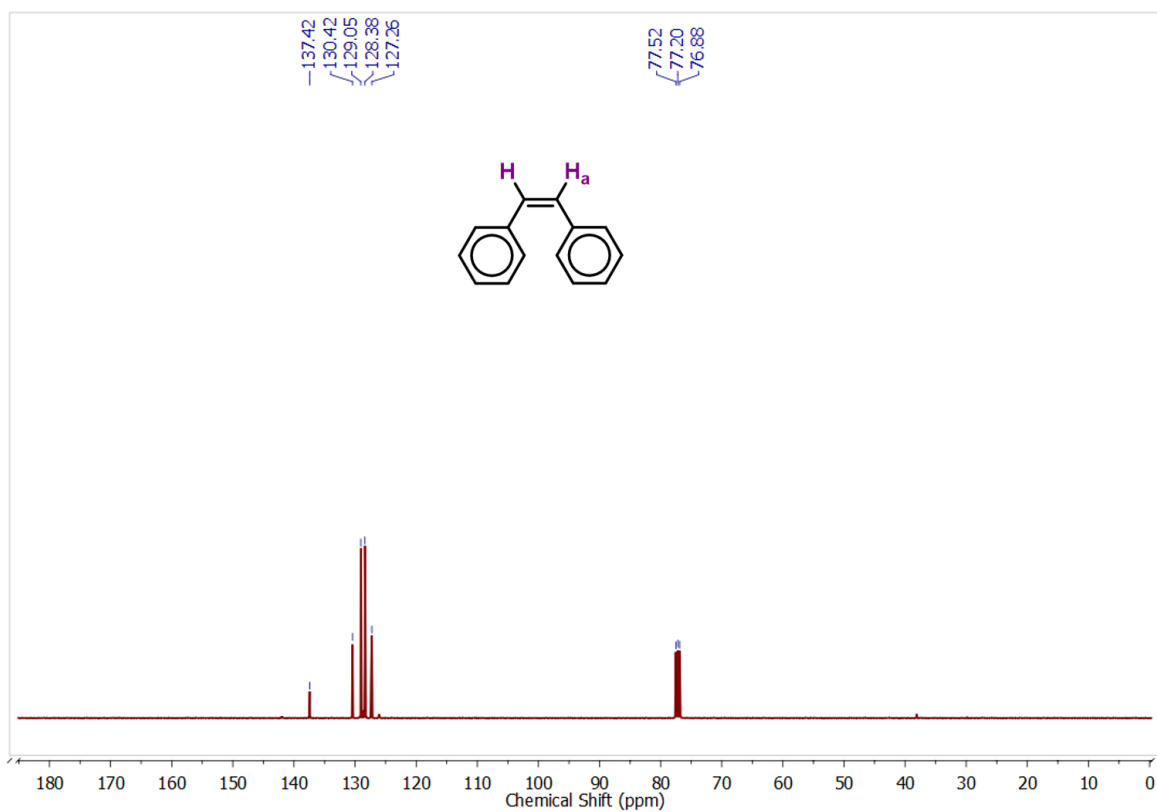


Scheme S3. *In-situ* reduction of diphenylacetylene to cis-stilbene.



(a)





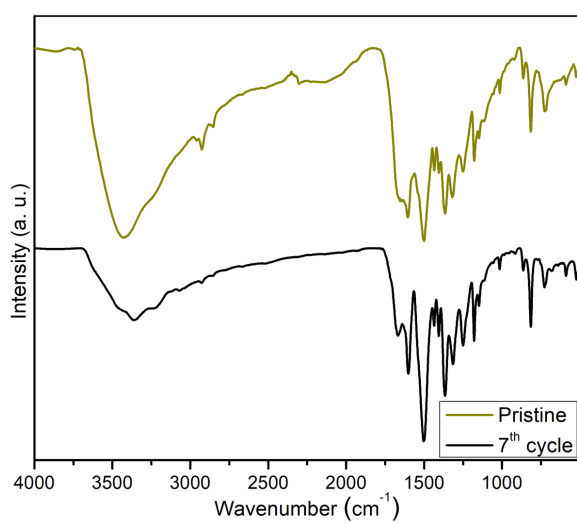
(b)

**Figure S8.** (a) <sup>1</sup>H NMR (400 MHz) and (b) <sup>13</sup>C{<sup>1</sup>H} NMR (101 MHz) of *cis*-stilbene at CDCl<sub>3</sub>.

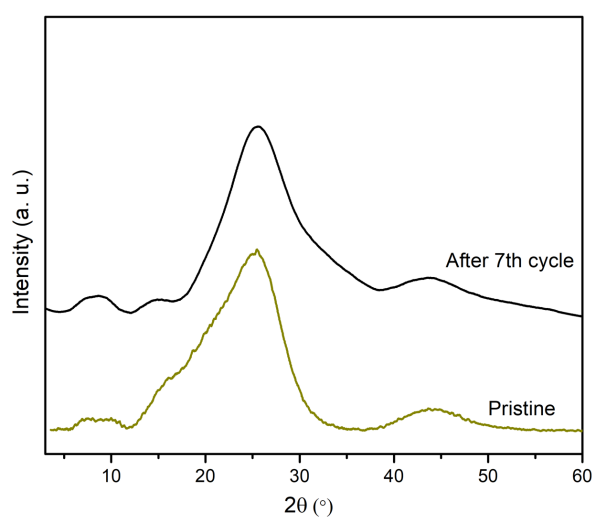
<sup>1</sup>H NMR (400 MHz, CDCl<sub>3</sub>) δ (ppm): 7.20-7.08 (m, 10H), 6.52 (s, 2H).

<sup>13</sup>C{<sup>1</sup>H} NMR (101 MHz, CDCl<sub>3</sub>) δ (ppm): 137.4, 130.4, 129.0, 128.4, 127.3.

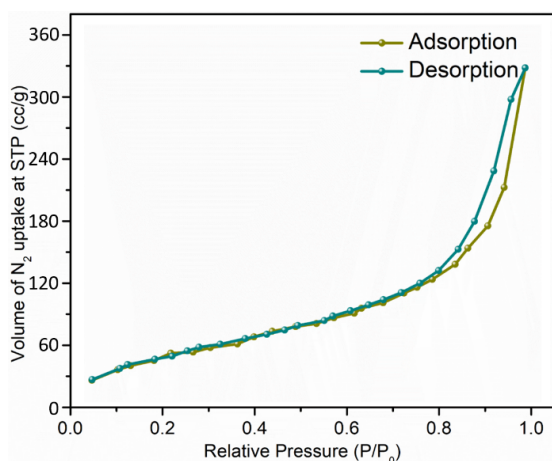
### 13. FT-IR and PXRD of reused catalyst



(a)



(b)



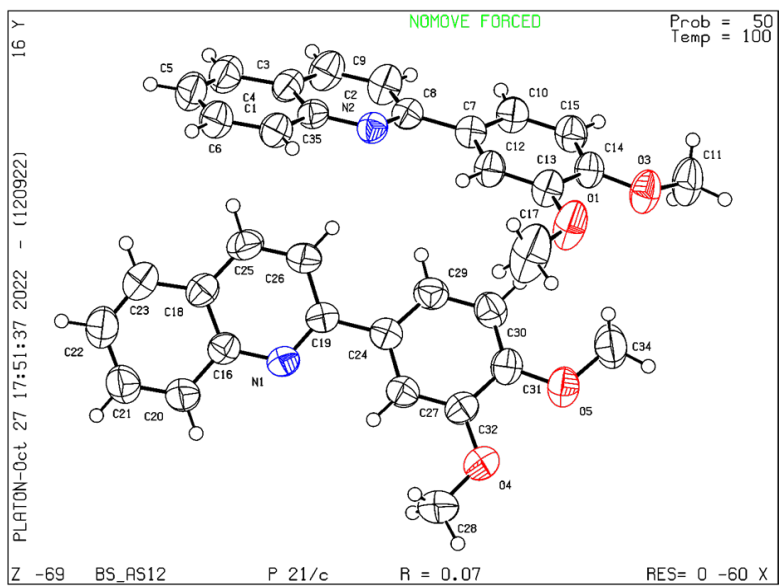
(c)

**Figure S9.** Overlay FT-IR (a) and PXRD pattern (b) of reused catalyst after 7<sup>th</sup> cycle. (c) BET adsorption-desorption isotherm with N<sub>2</sub> at 77 K of MOP-TA after 5<sup>th</sup> catalytic cycle.

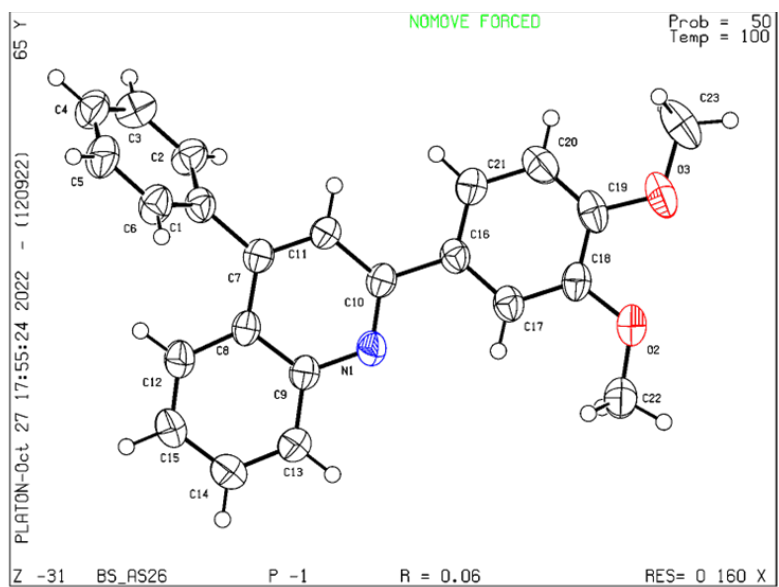
**14. Table S4.** Crystallographic parameters.

Crystal Data	<b>3k</b>	<b>3u</b>	<b>3v</b>
Formula Unit	C <sub>17</sub> H <sub>15</sub> NO <sub>2</sub>	C <sub>23</sub> H <sub>19</sub> NO <sub>2</sub>	C <sub>23</sub> H <sub>17</sub> N
Formula Weight (g/mol)	265.30	341.39	307.38
Crystal system	Monoclinic	Triclinic	Monoclinic
T [K]	100	100	296
<i>a</i> [Å]	10.6990 (9)	7.804 (11)	14.1830 (3)
<i>b</i> [Å]	24.6110 (19)	10.261 (14)	12.8550 (3)
<i>c</i> [Å]	11.4440 (9)	11.611 (16)	8.8411 (19)
$\alpha$ [°]	90	100.605 (13)	90
$\beta$ [°]	112.405 (19)	102.623 (13)	98.111 (6)
$\gamma$ [°]	90	94.906 (13)	90
Volume [Å <sup>3</sup> ]	2786 (4)	884 (2)	1595.7 (6)
Space group	<i>P</i> 2 <sub>1</sub> / <i>c</i>	<i>P</i> $\bar{1}$	<i>P</i> 2 <sub>1</sub> / <i>c</i>
Z	8	2	4
D <sub>cal</sub> [g/cm <sup>3</sup> ]	1.265	1.282	1.279
$\mu$ (mm <sup>-1</sup> )	0.083	0.082	0.074
Reflns. collected	5470	3418	3136
Unique observed	3217	1894	2265
R1 [I > $\sigma$ (I)]	0.0693	0.0569	0.0425
wR2	0.1997	0.1647	0.1161
CCDC No.	2219983	2219981	2219982

**15. ORTEP diagram**



6k



6u

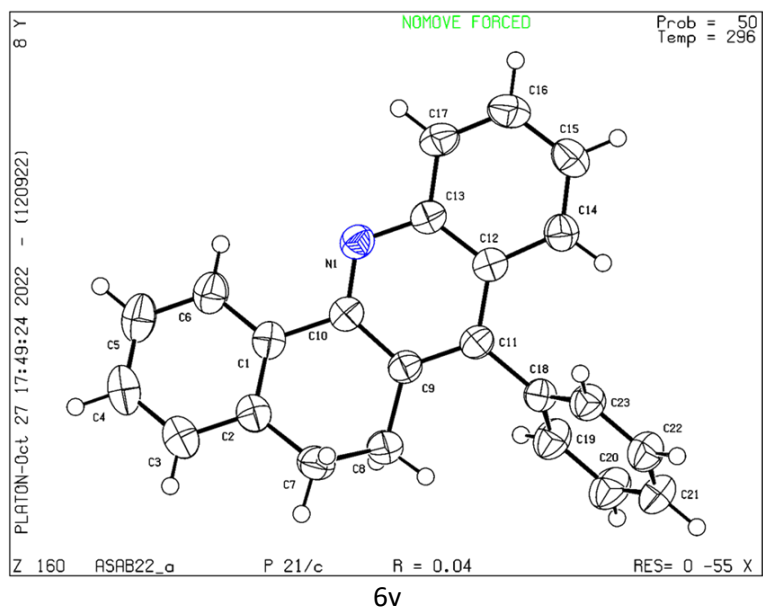
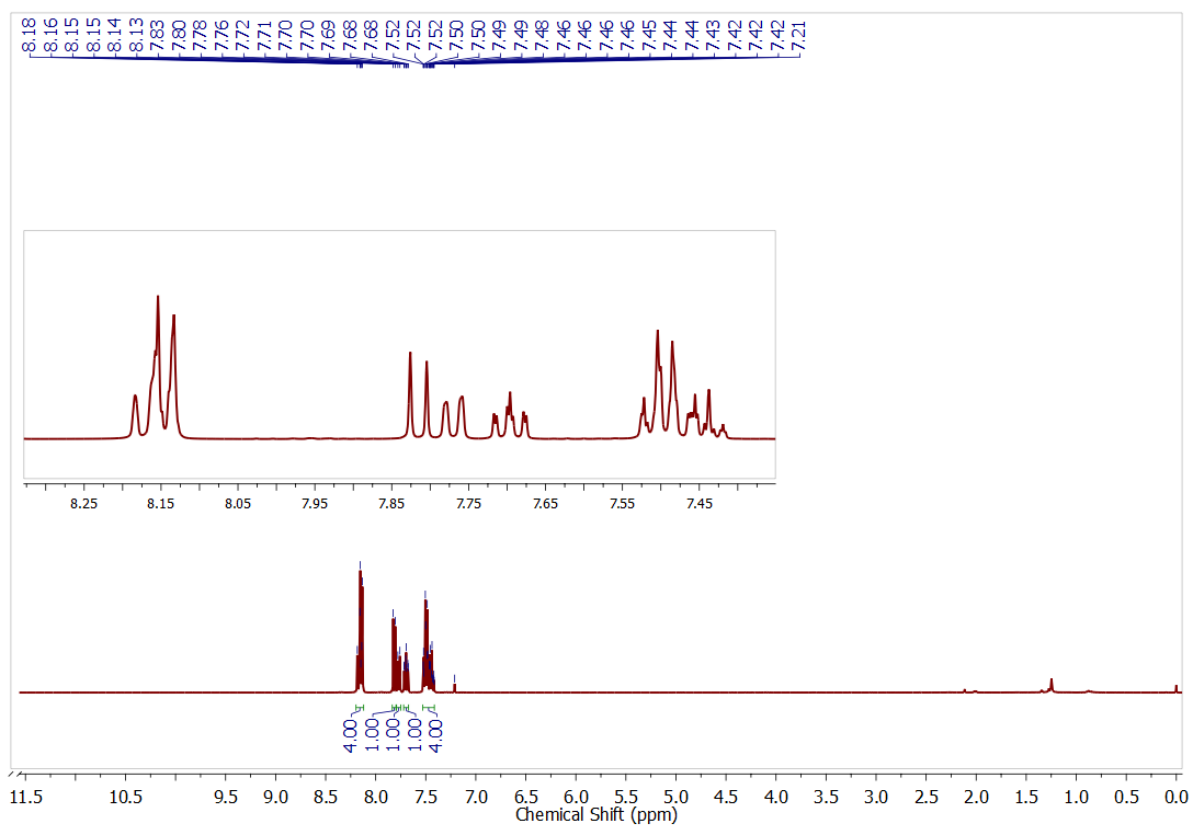
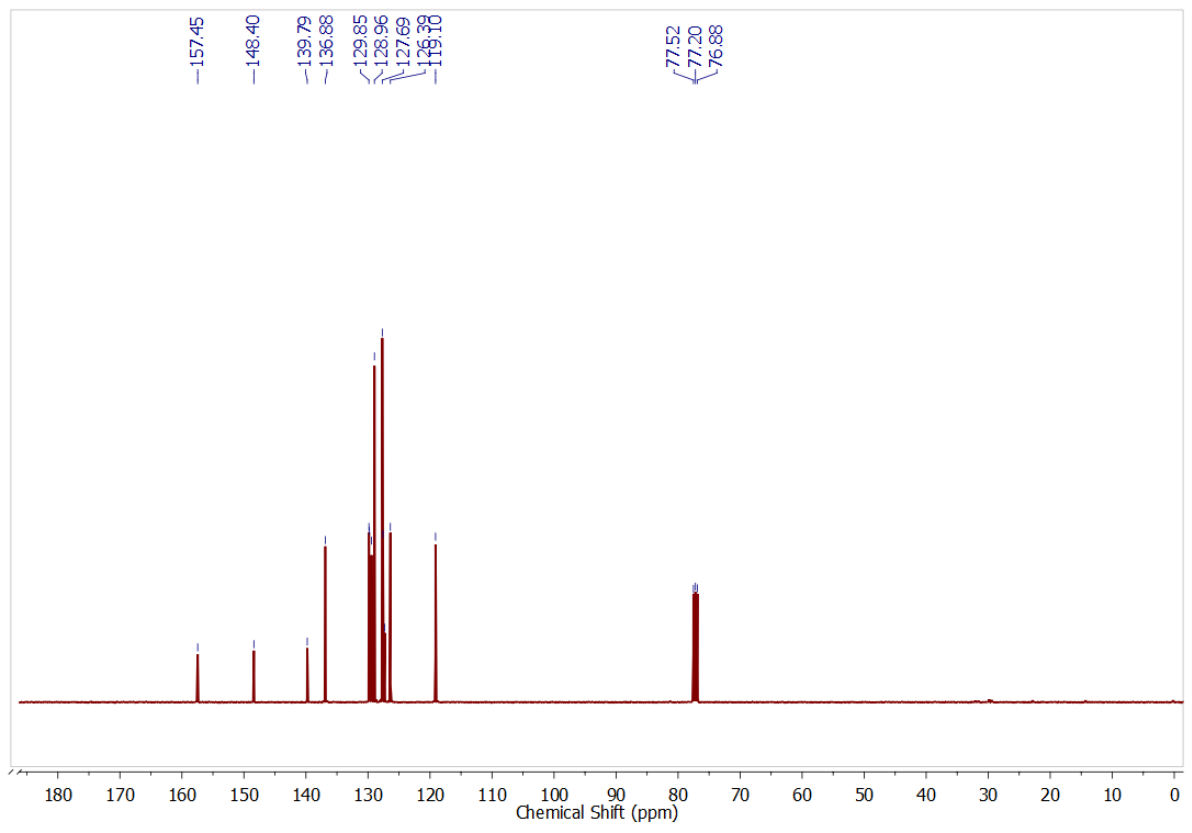


Figure S10. ORTEP diagram of 6k, 6u and 6v.

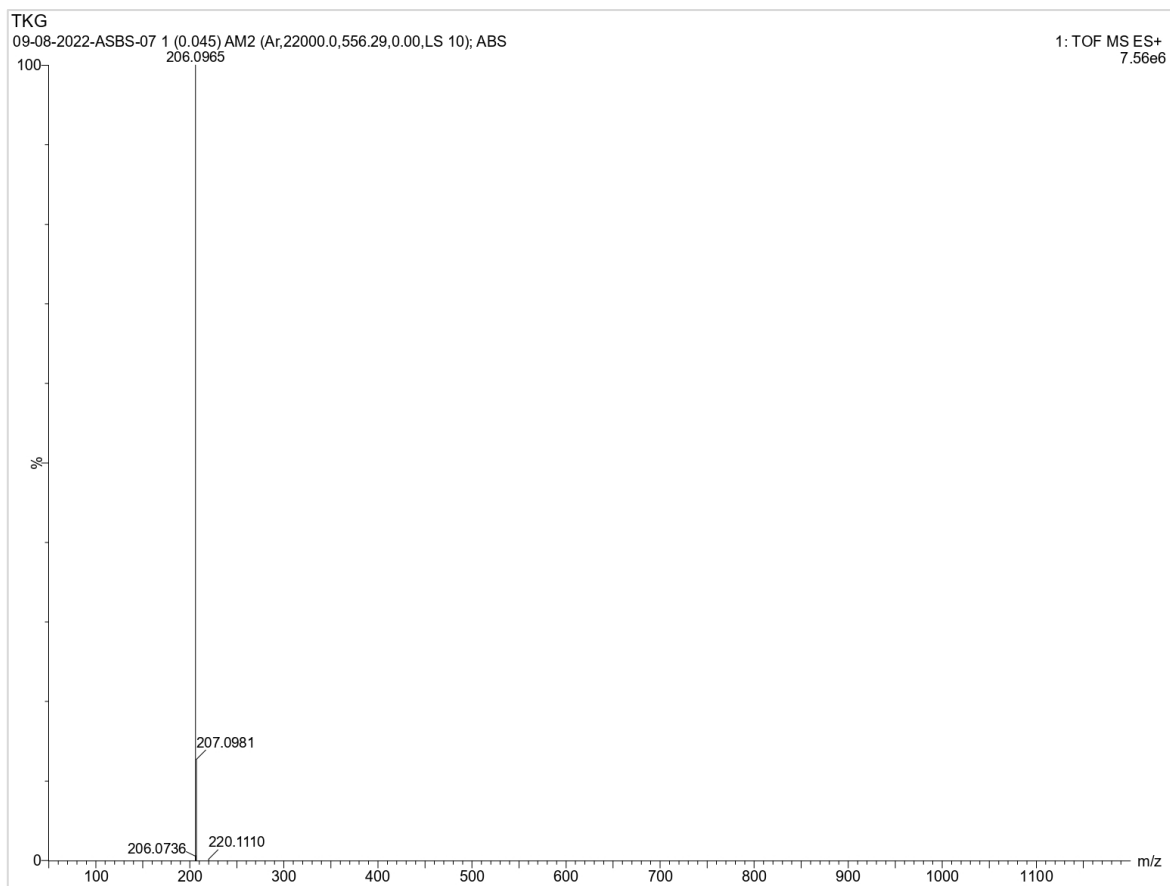
## 16. NMR Spectra and HRMS.



(a)

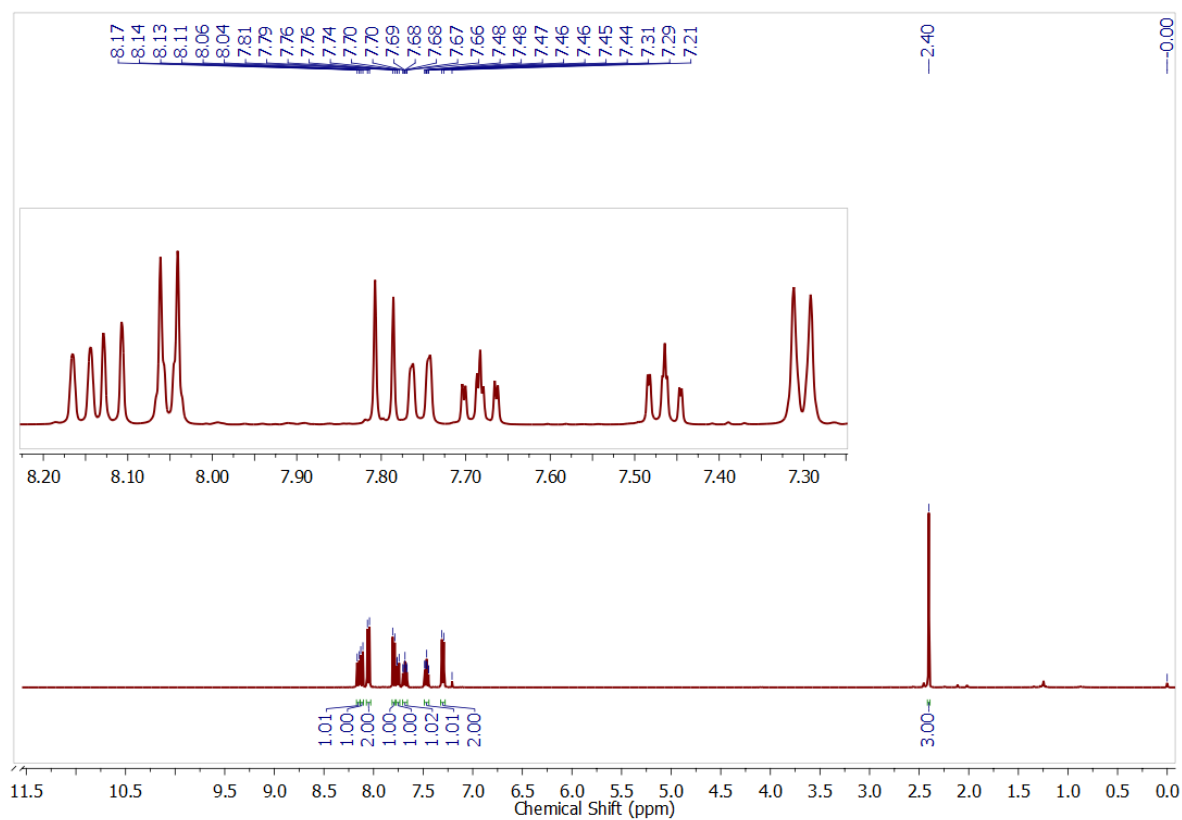


(b)

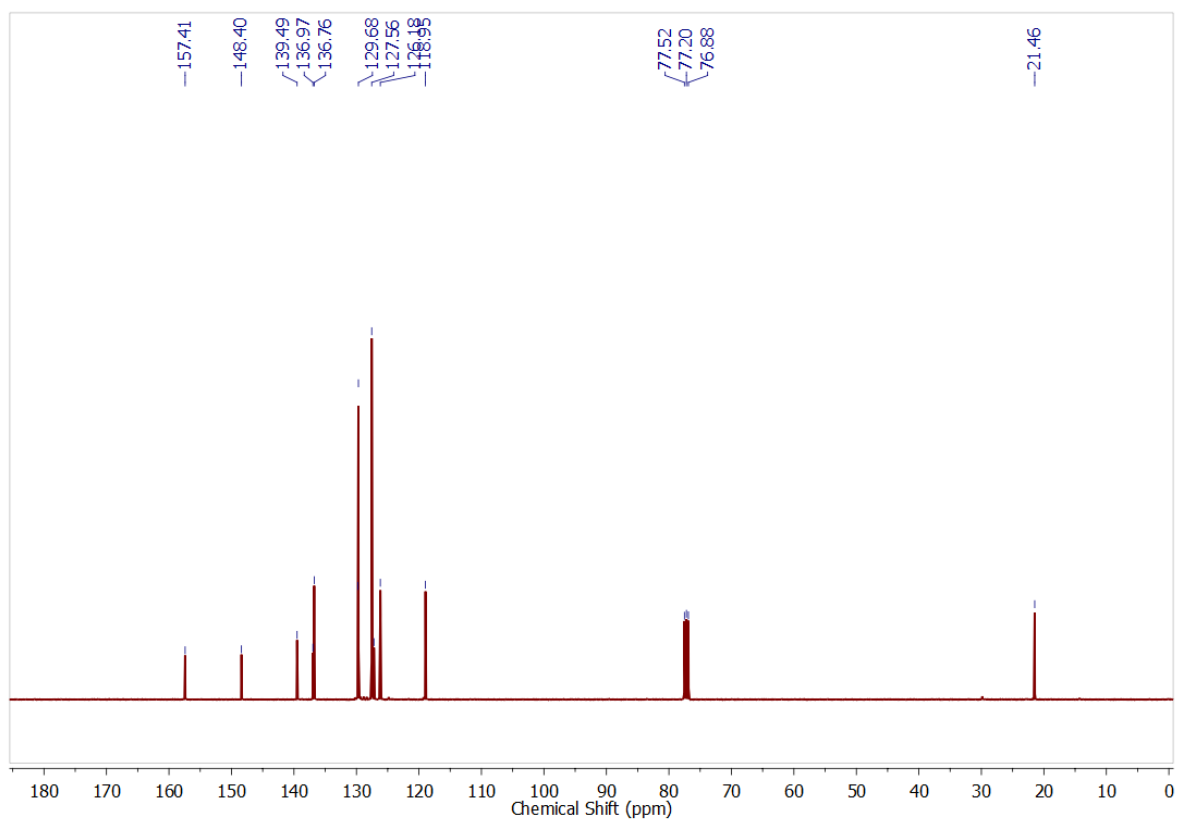


(c)

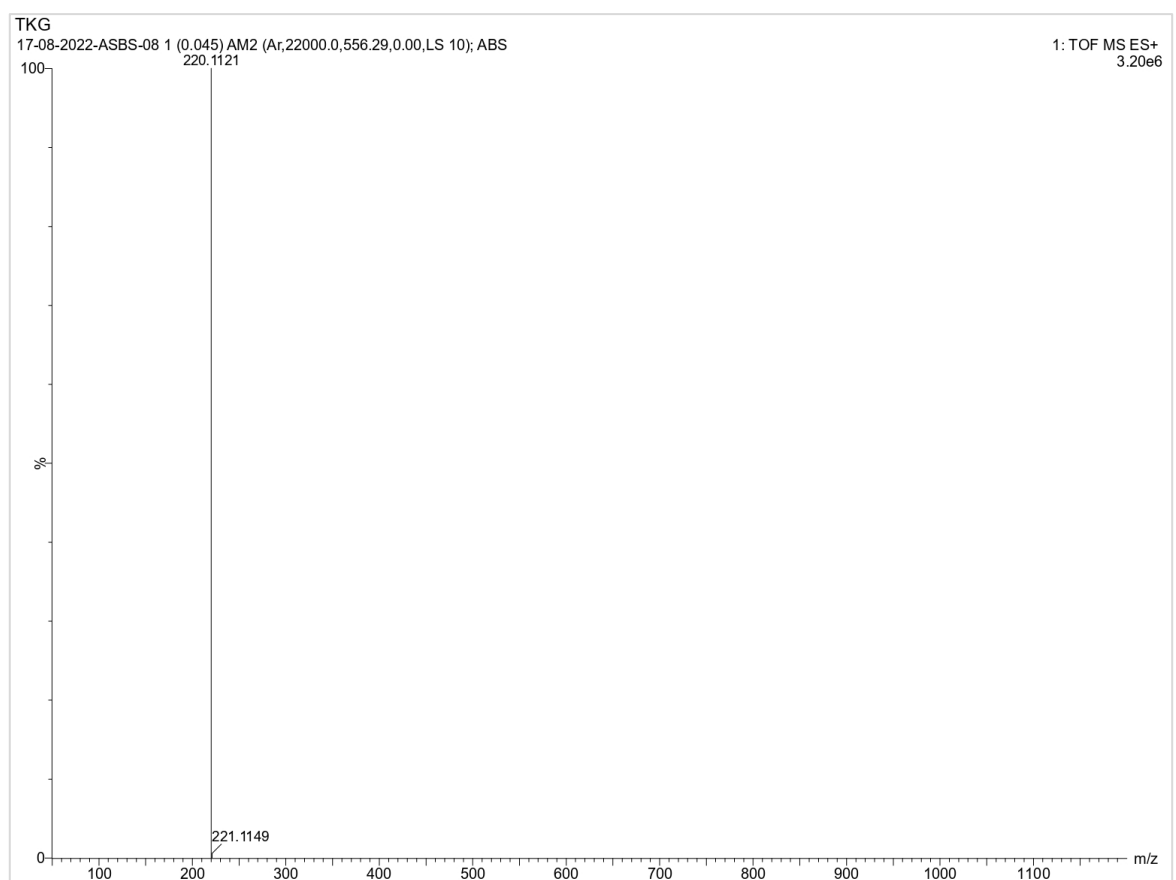
Figure S11. (a)  $^1\text{H}$ , (b)  $^{13}\text{C}\{^1\text{H}\}$  NMR and (c) HRMS of **6a**.



(a)



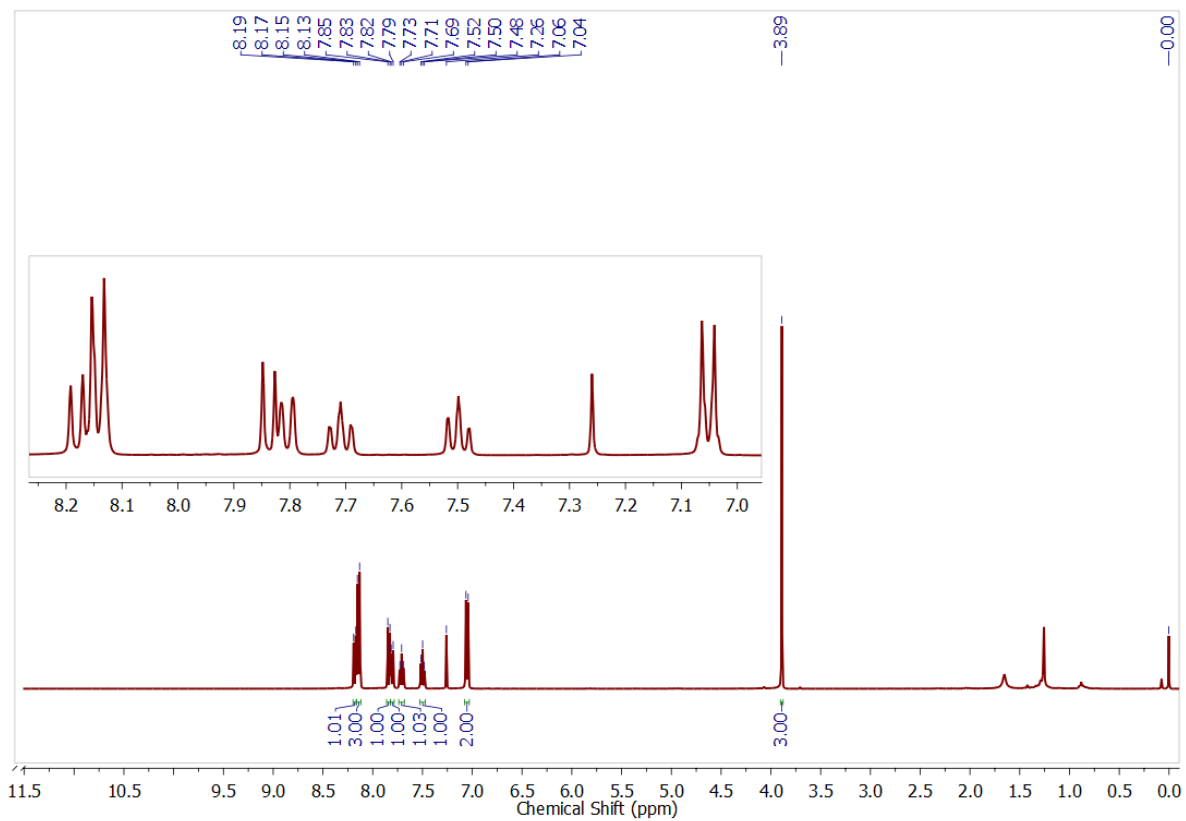
(b)



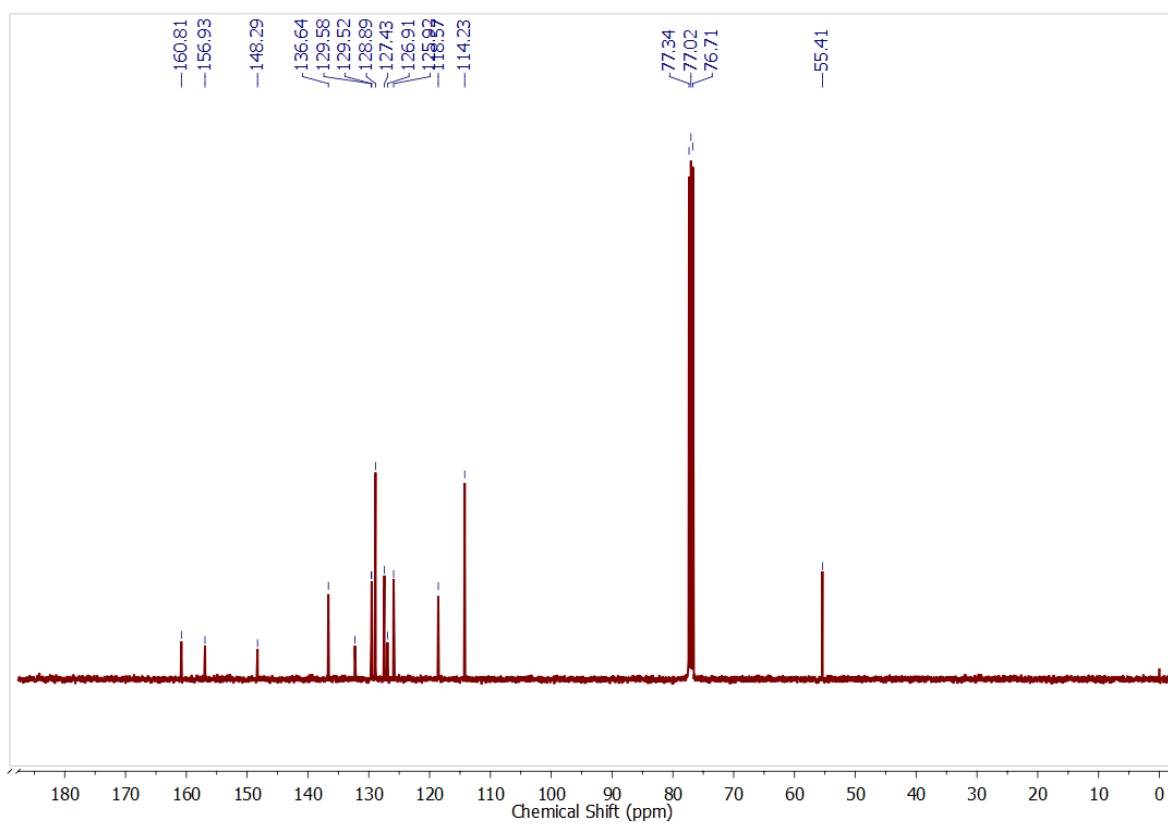
(c)

Figure S12. (a)  $^1\text{H}$ , (b)  $^{13}\text{C}\{^1\text{H}\}$  NMR and (c) HRMS of **6b**.

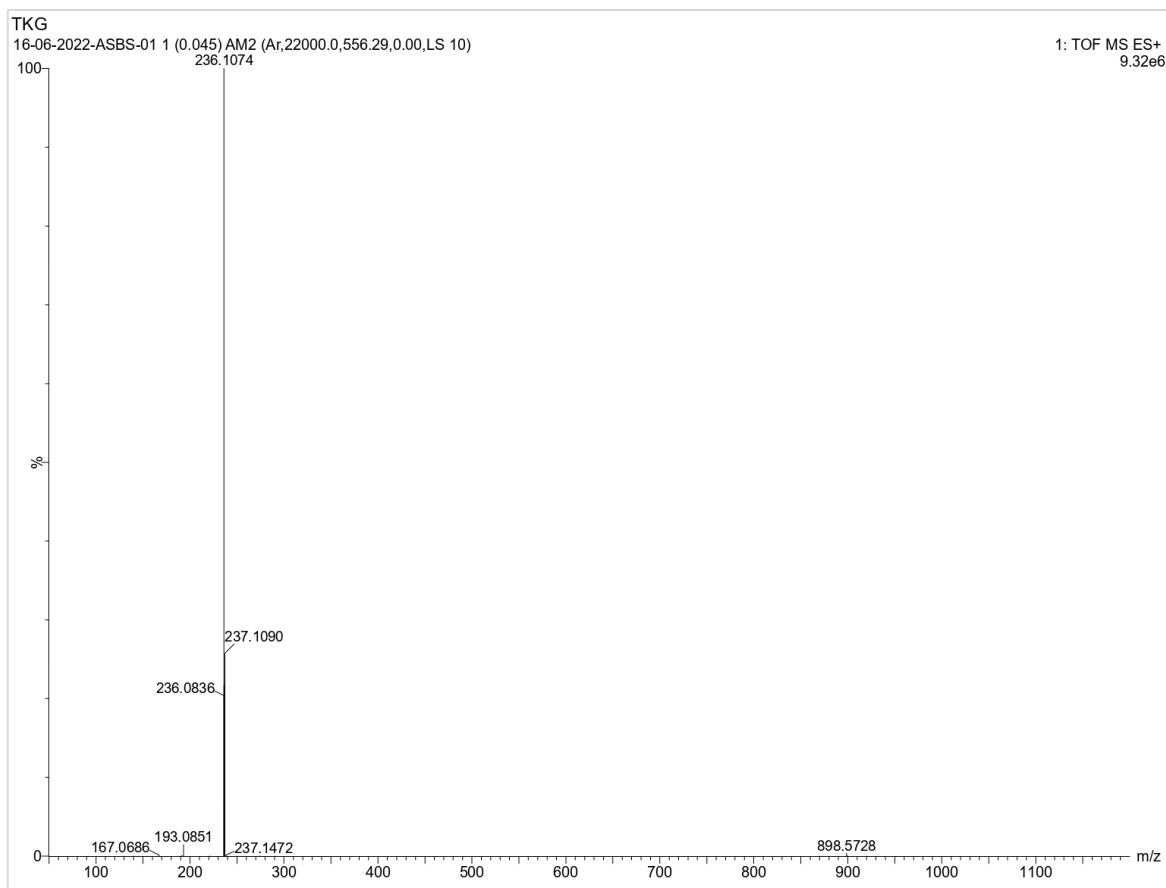




(a)

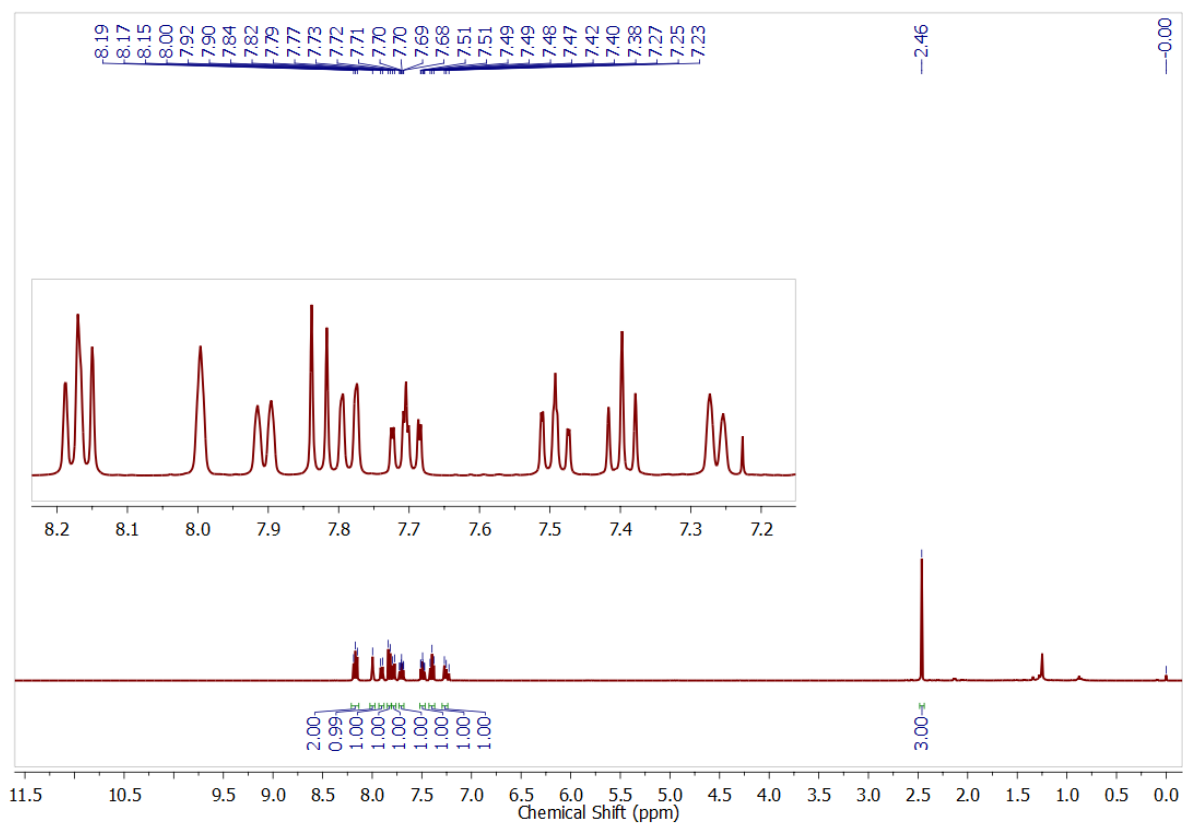


(b)

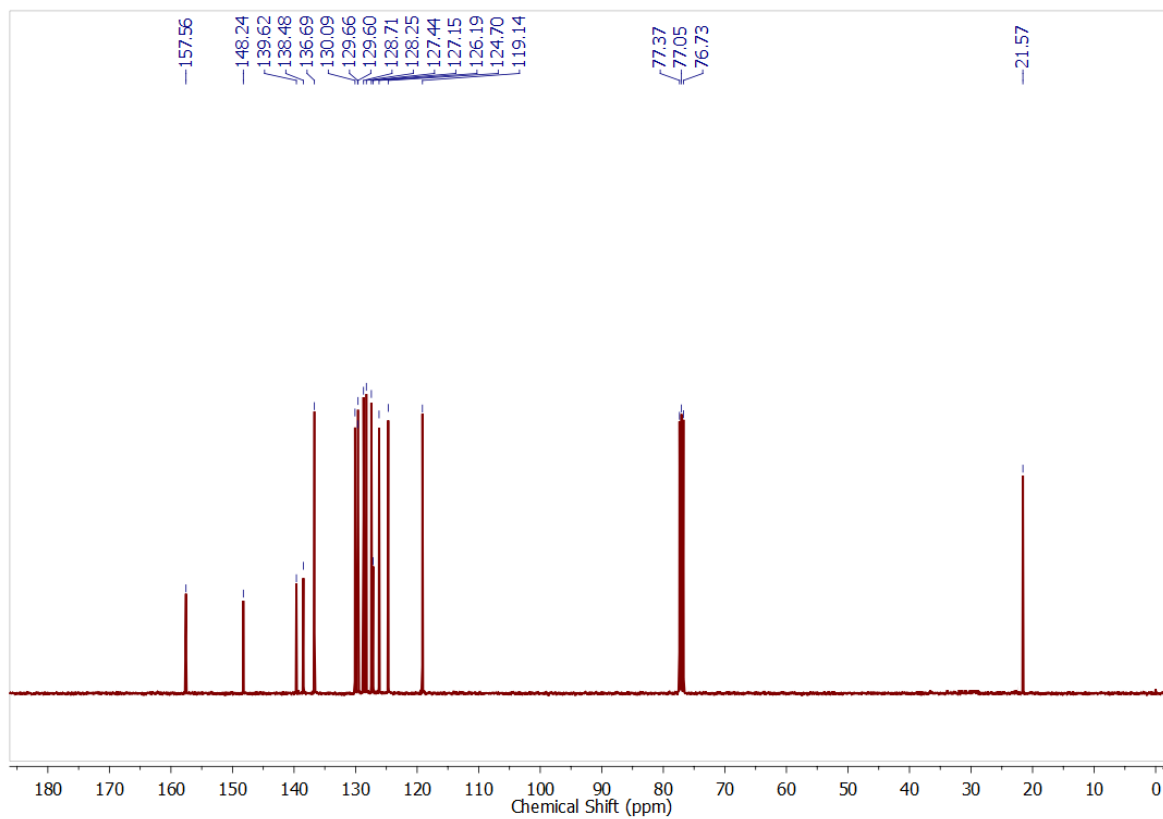


(c)

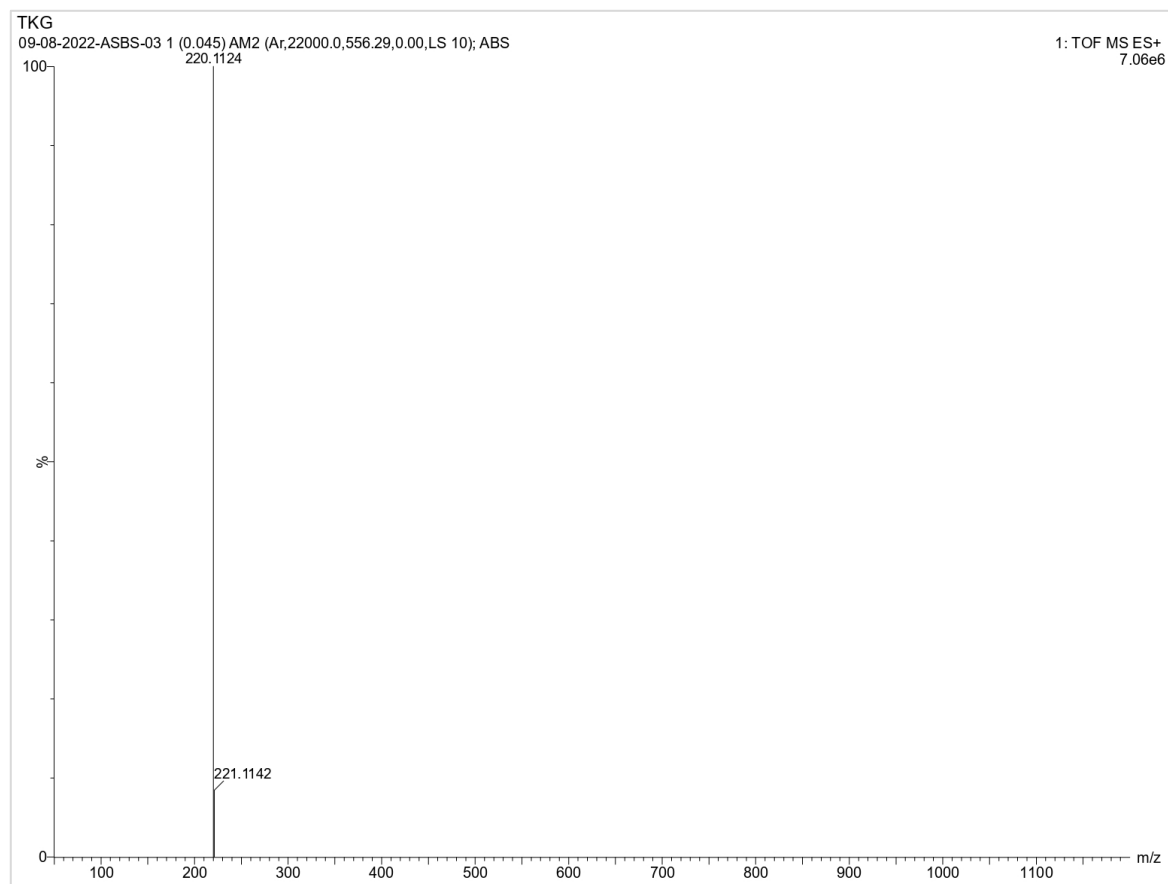
Figure S13. (a)  $^1\text{H}$ , (b)  $^{13}\text{C}\{^1\text{H}\}$  NMR and (c) HRMS of **6c**.



(a)

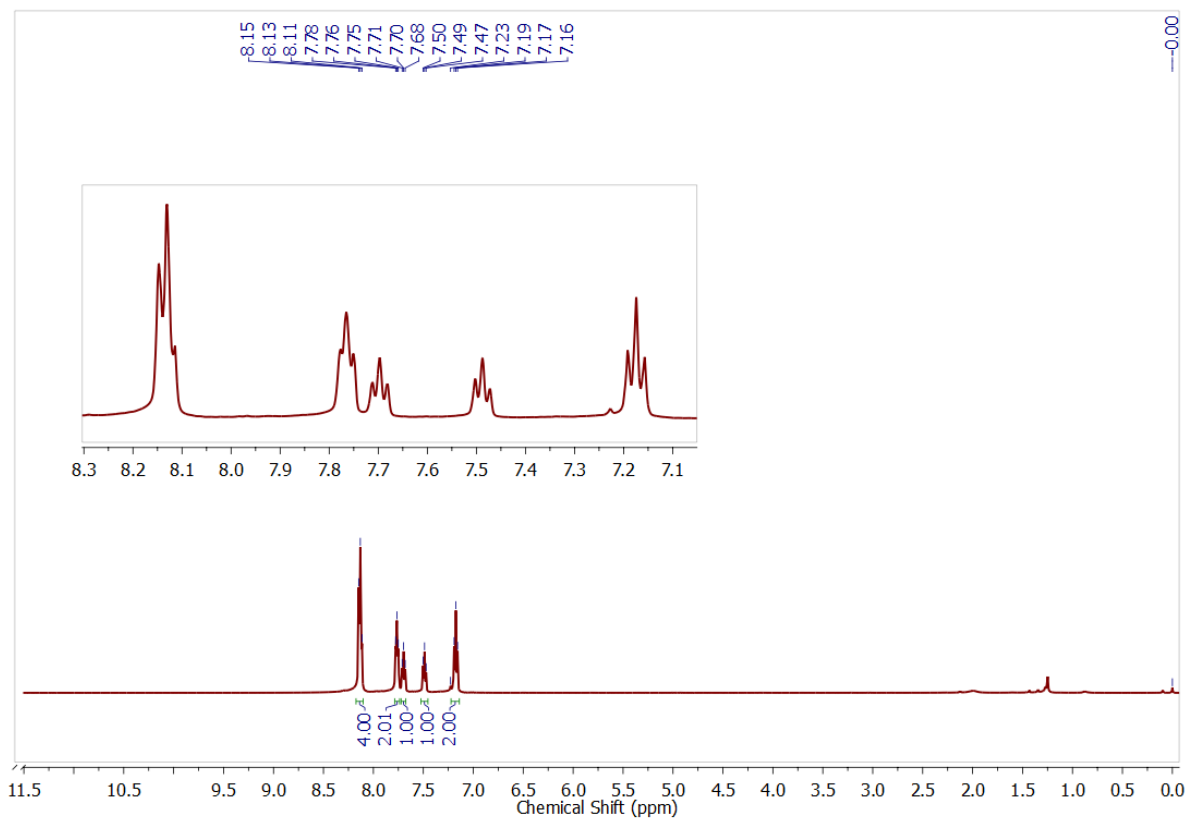


(b)

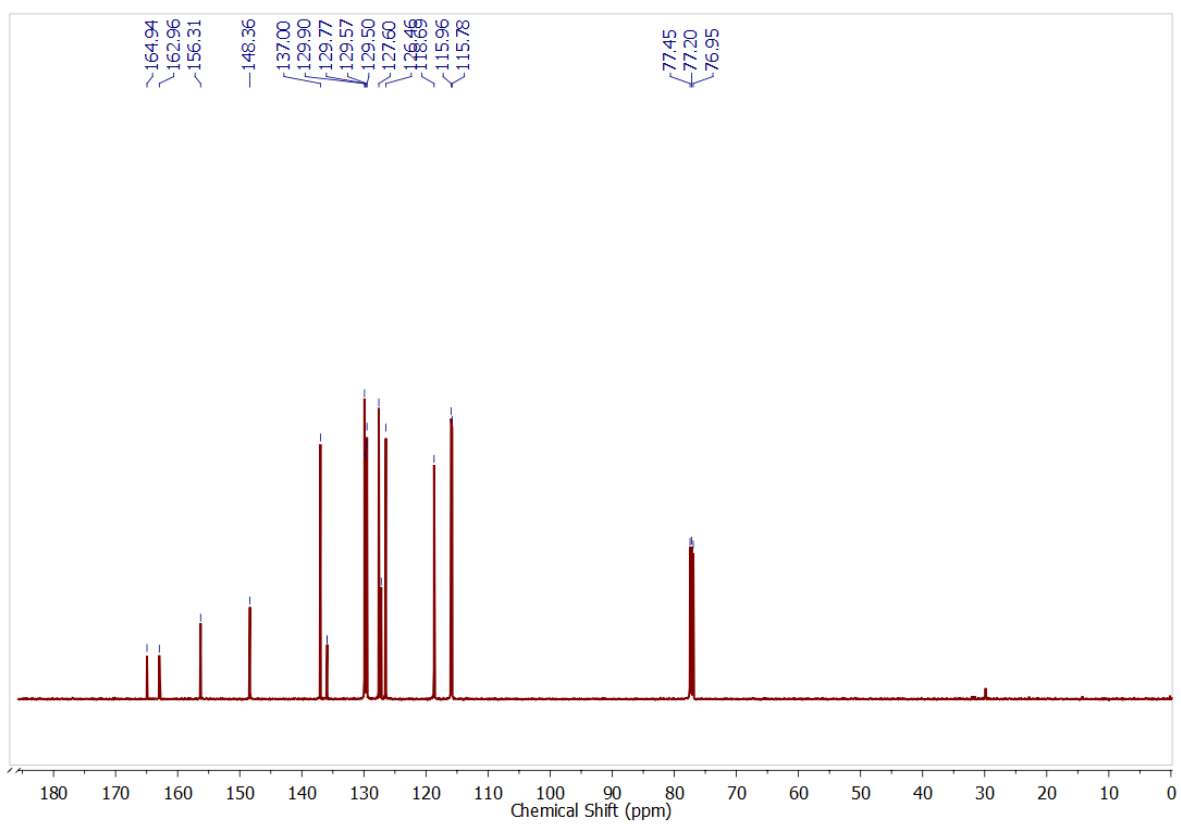


(c)

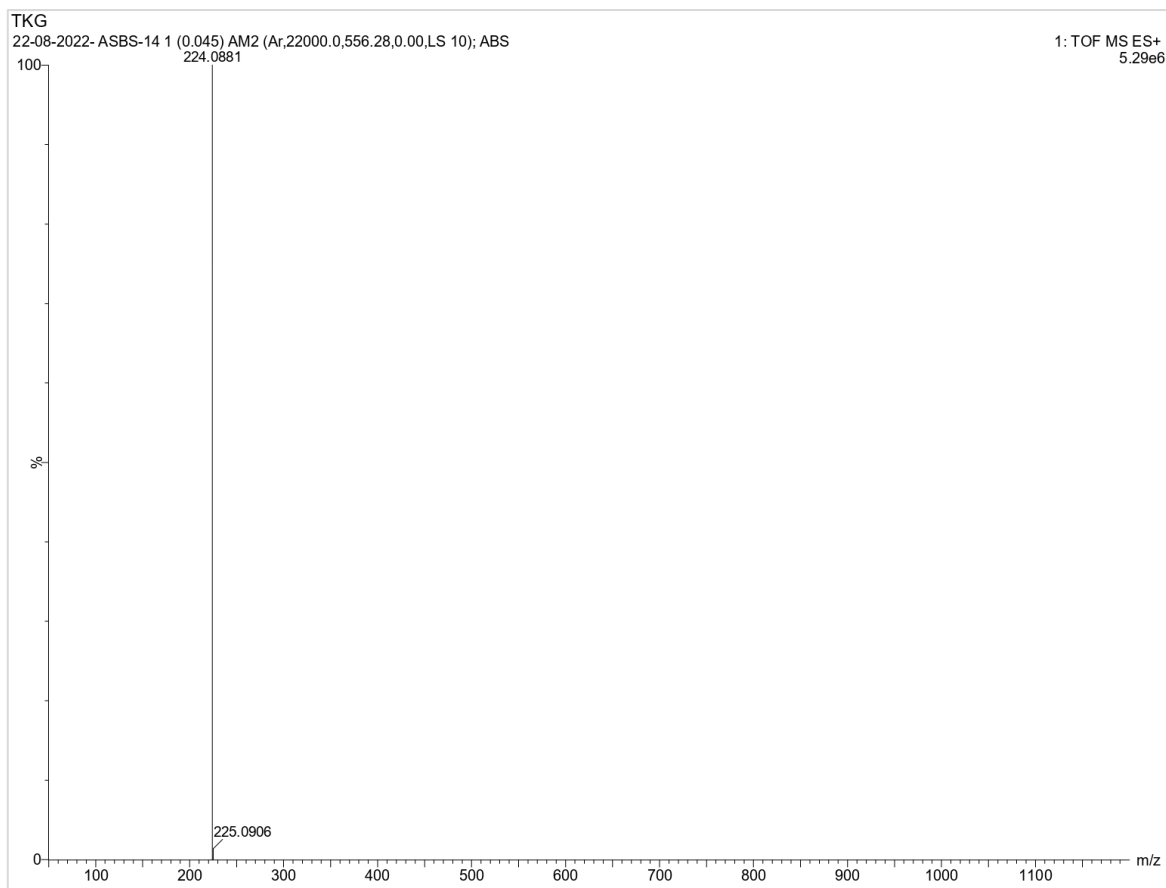
Figure S14. (a)  $^1\text{H}$ , (b)  $^{13}\text{C}\{^1\text{H}\}$  NMR and (c) HRMS of **6d**.



(a)

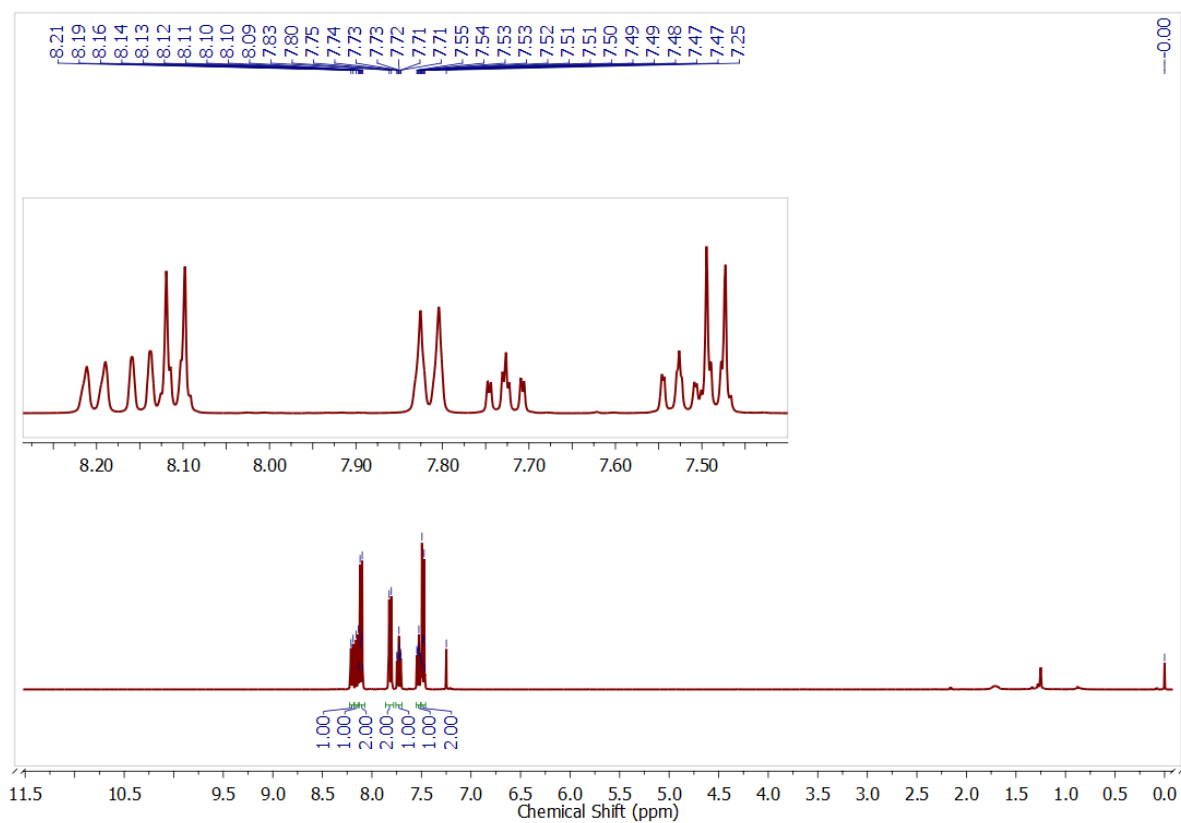


(b)

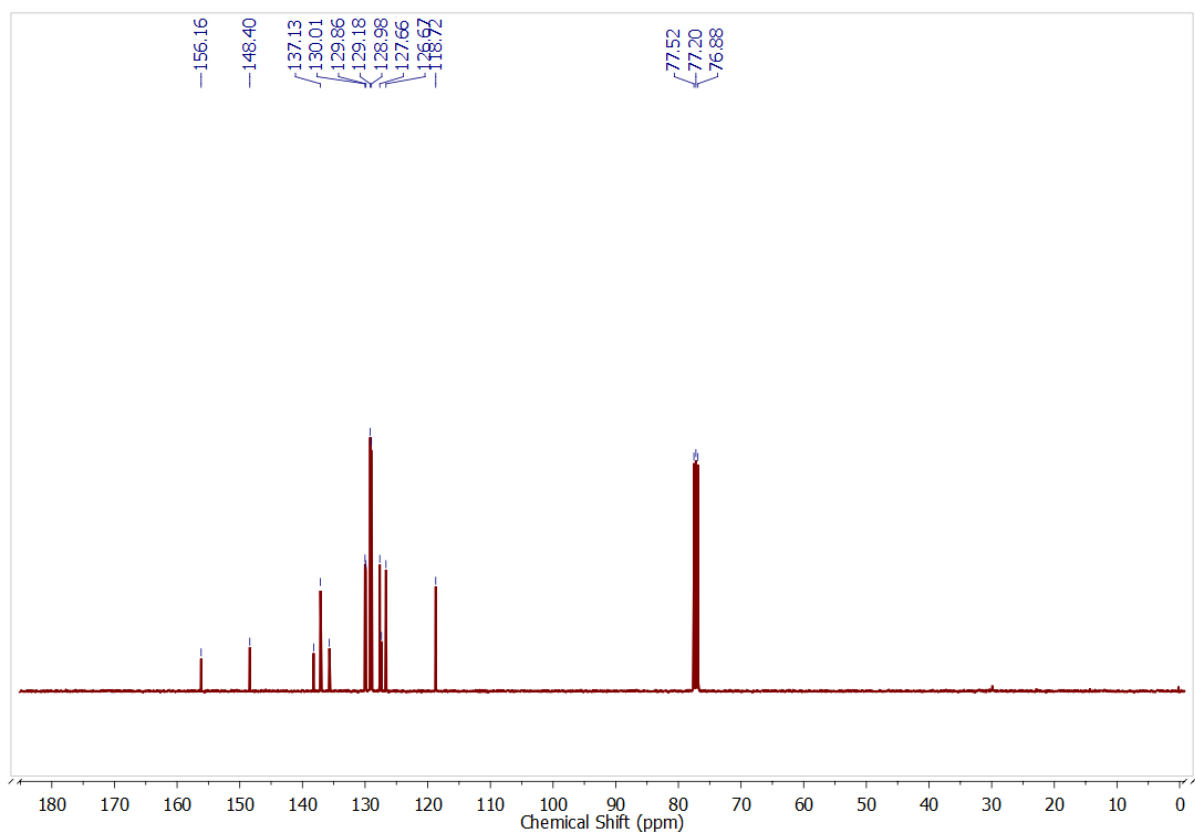


(c)

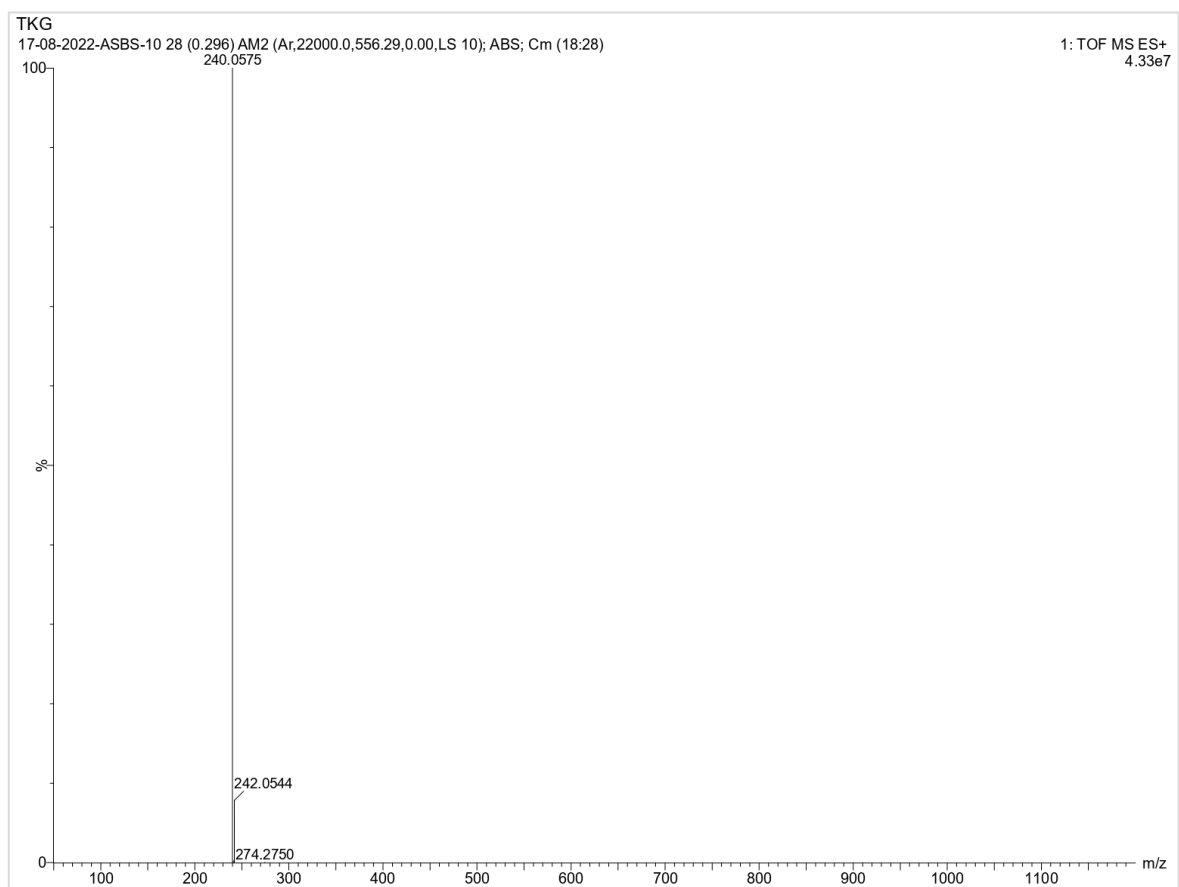
Figure S15. (a)  $^1\text{H}$ , (b)  $^{13}\text{C}\{^1\text{H}\}$  NMR and (c) HRMS of **6e**.



(a)

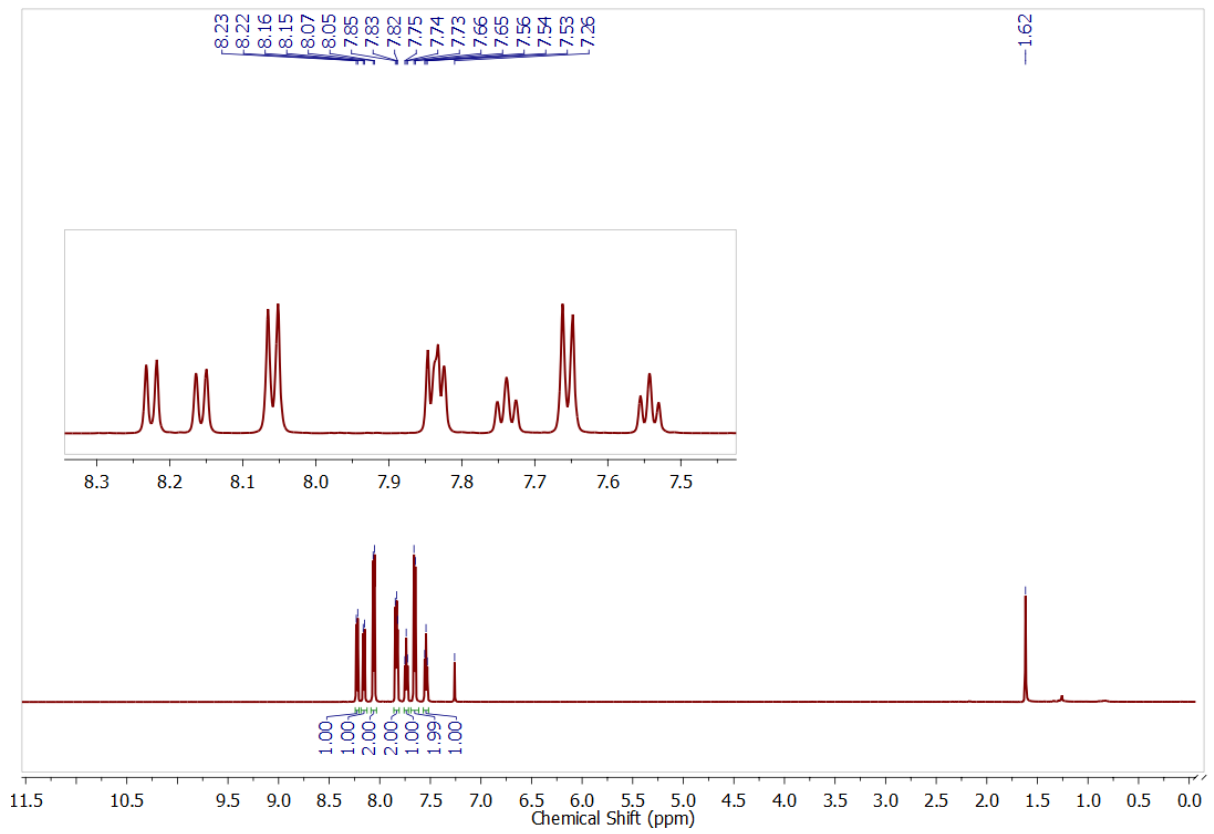


(b)

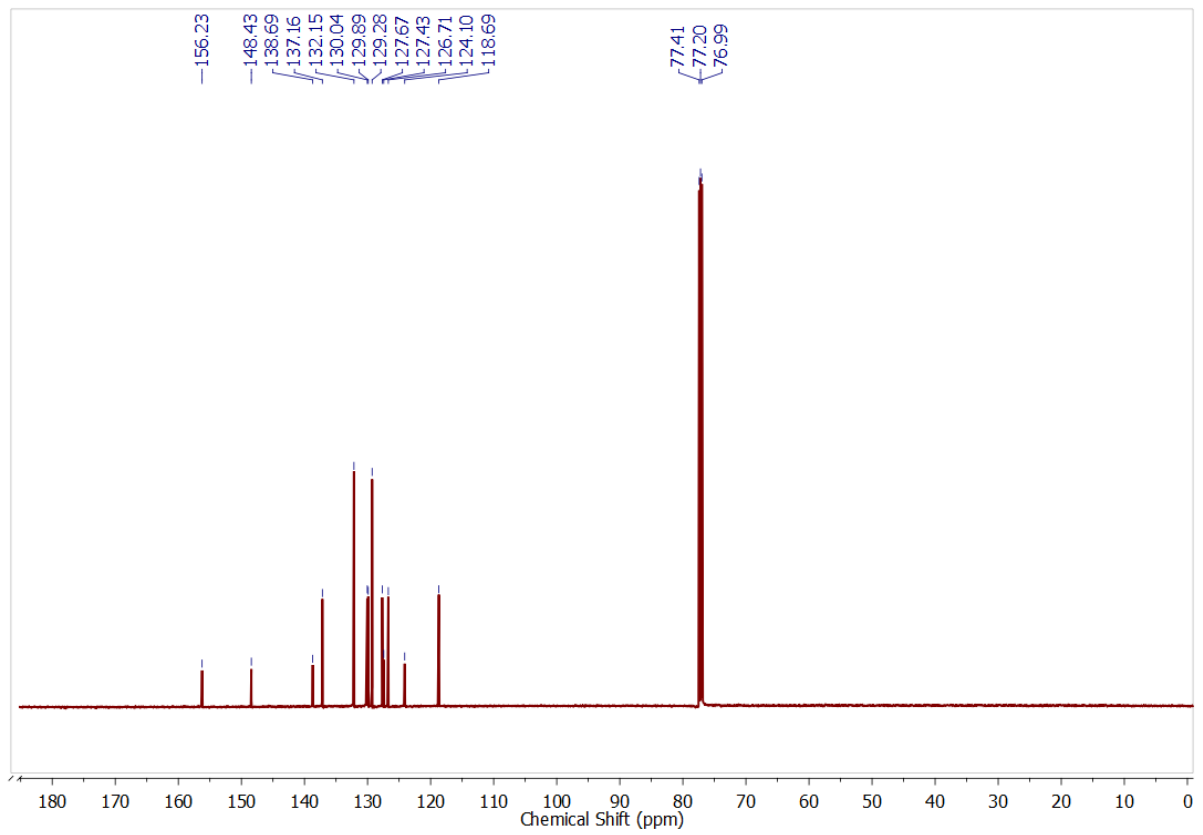


(c)

Figure S16. (a)  $^1\text{H}$ , (b)  $^{13}\text{C}\{^1\text{H}\}$  NMR and (c) HRMS of **6f**.

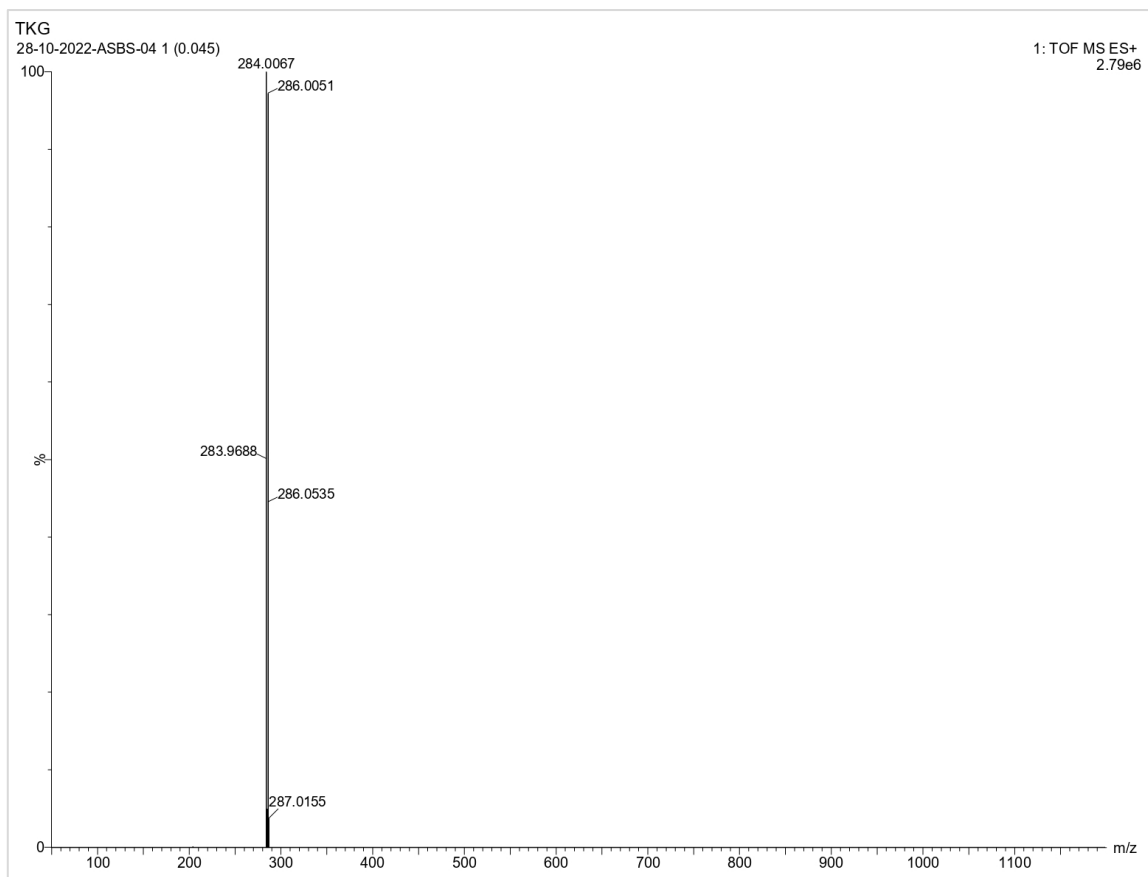


(a)



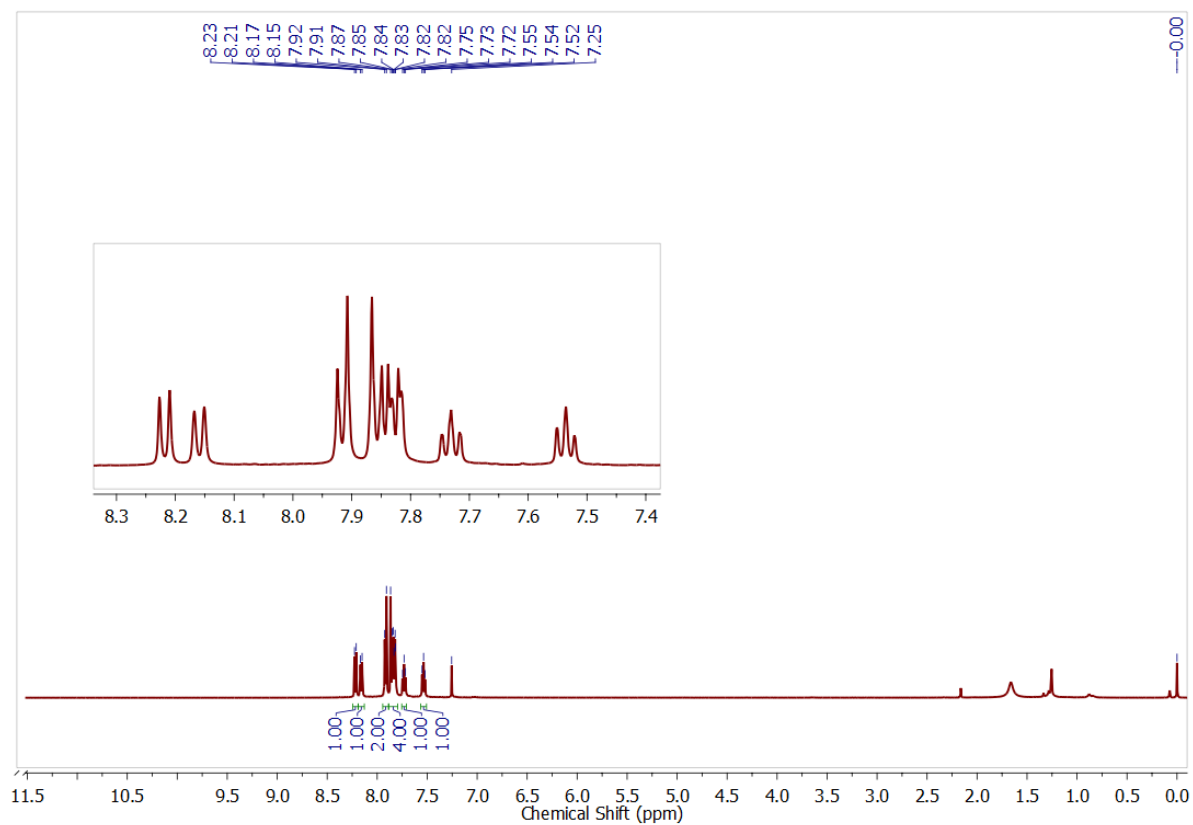
(b)



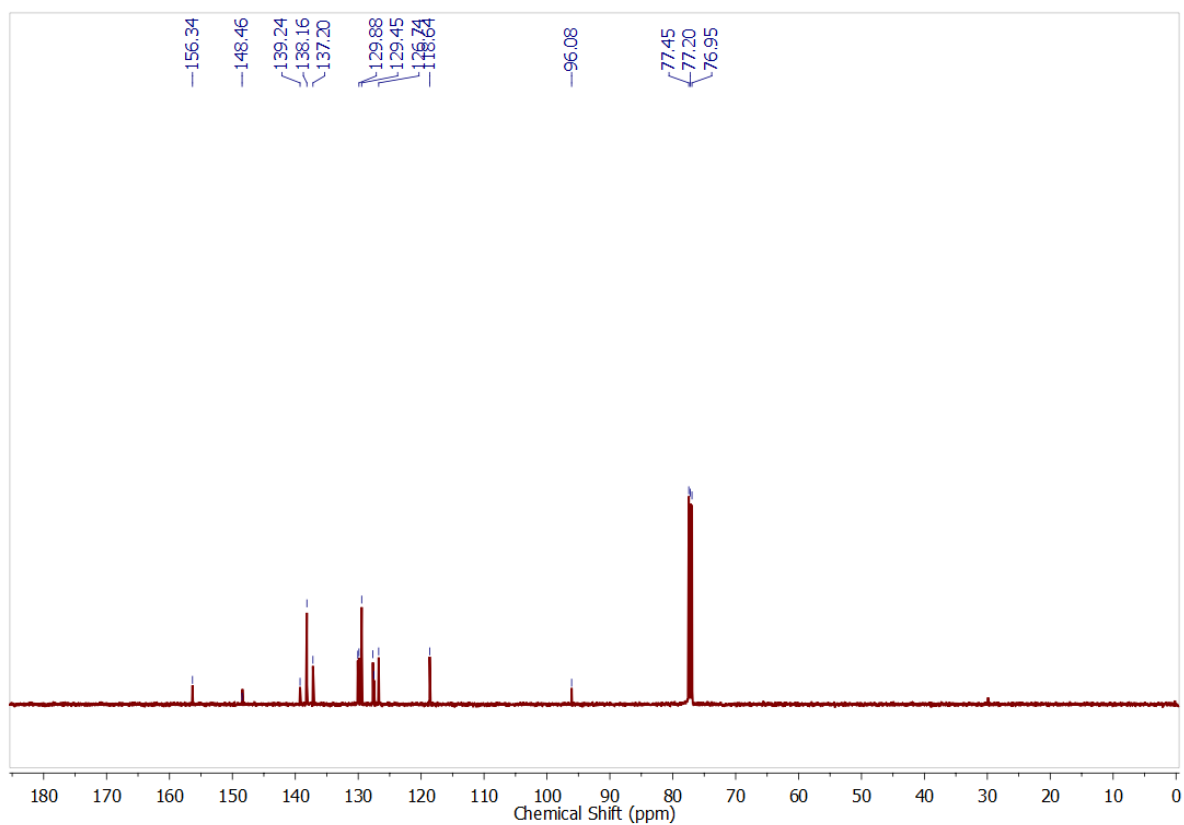


(c)

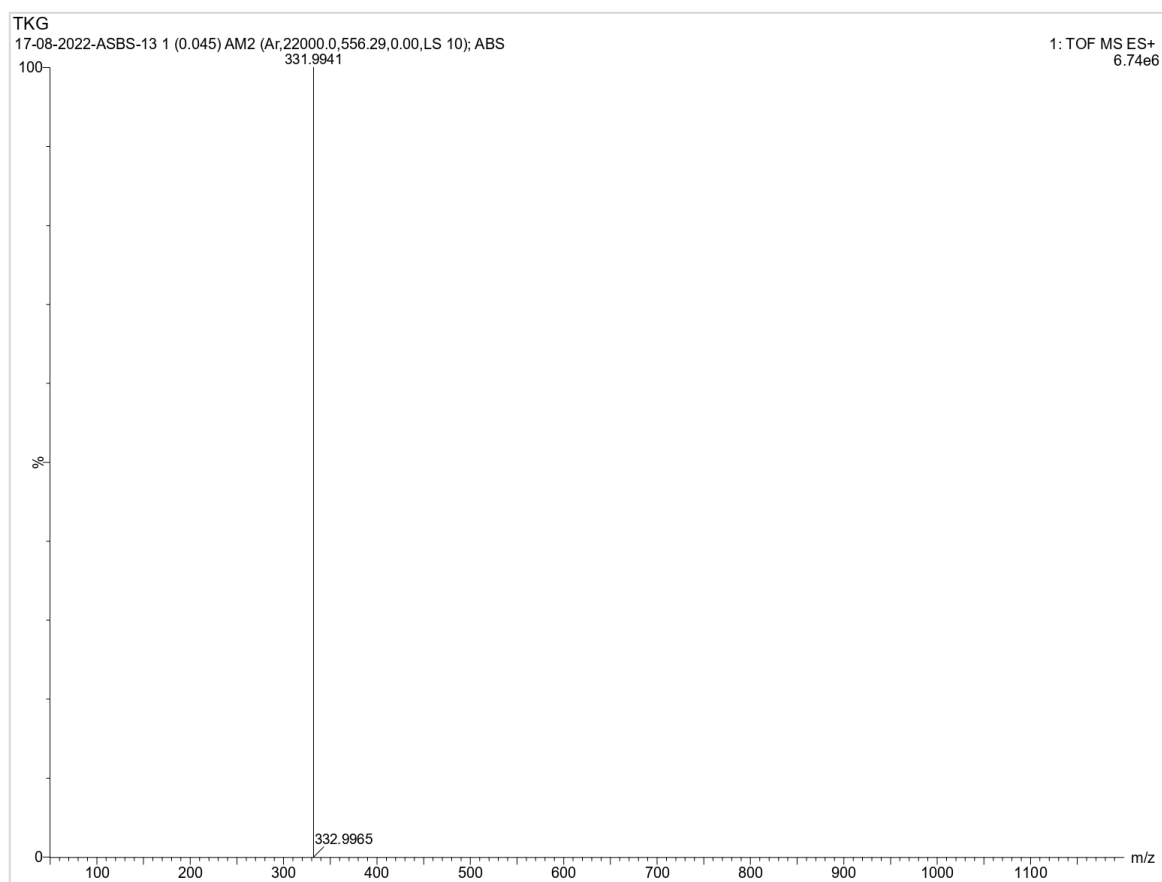
Figure S17. (a)  $^1\text{H}$ , (b)  $^{13}\text{C}\{^1\text{H}\}$  NMR and (c) HRMS of **6g**.



(a)

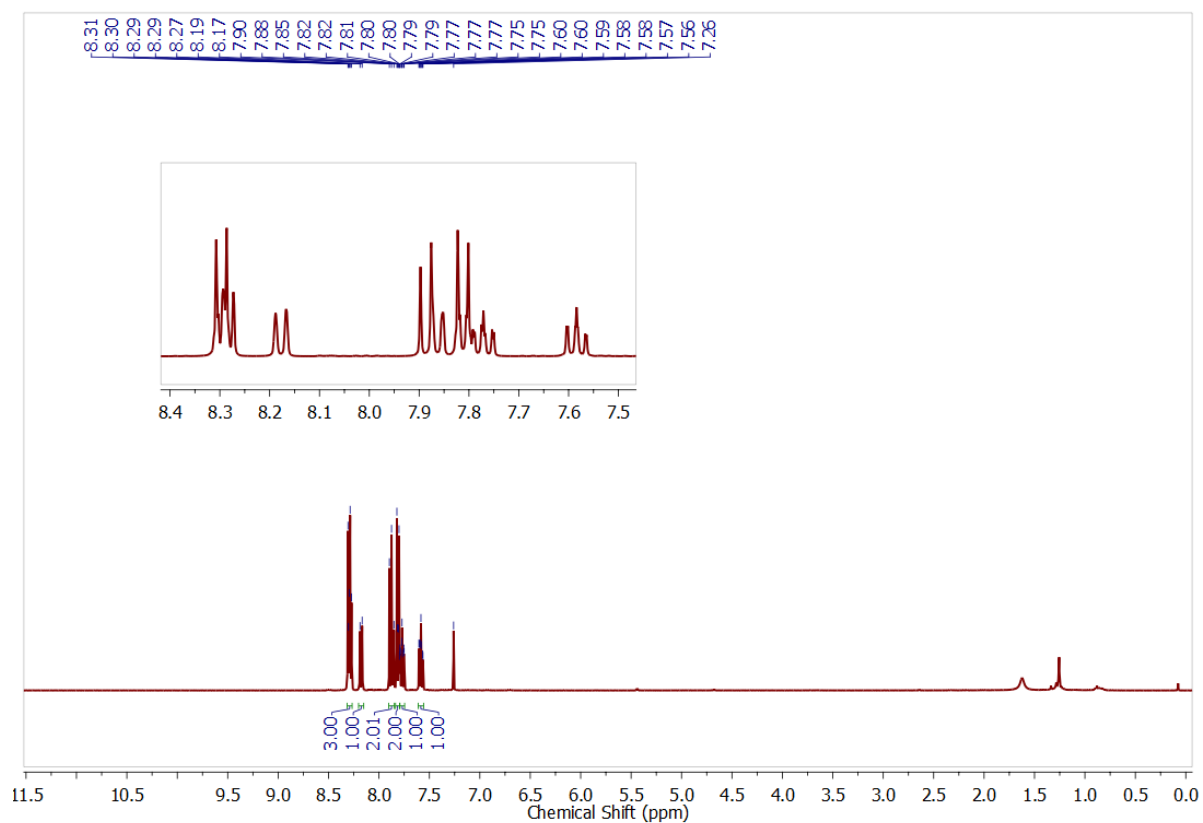


(b)

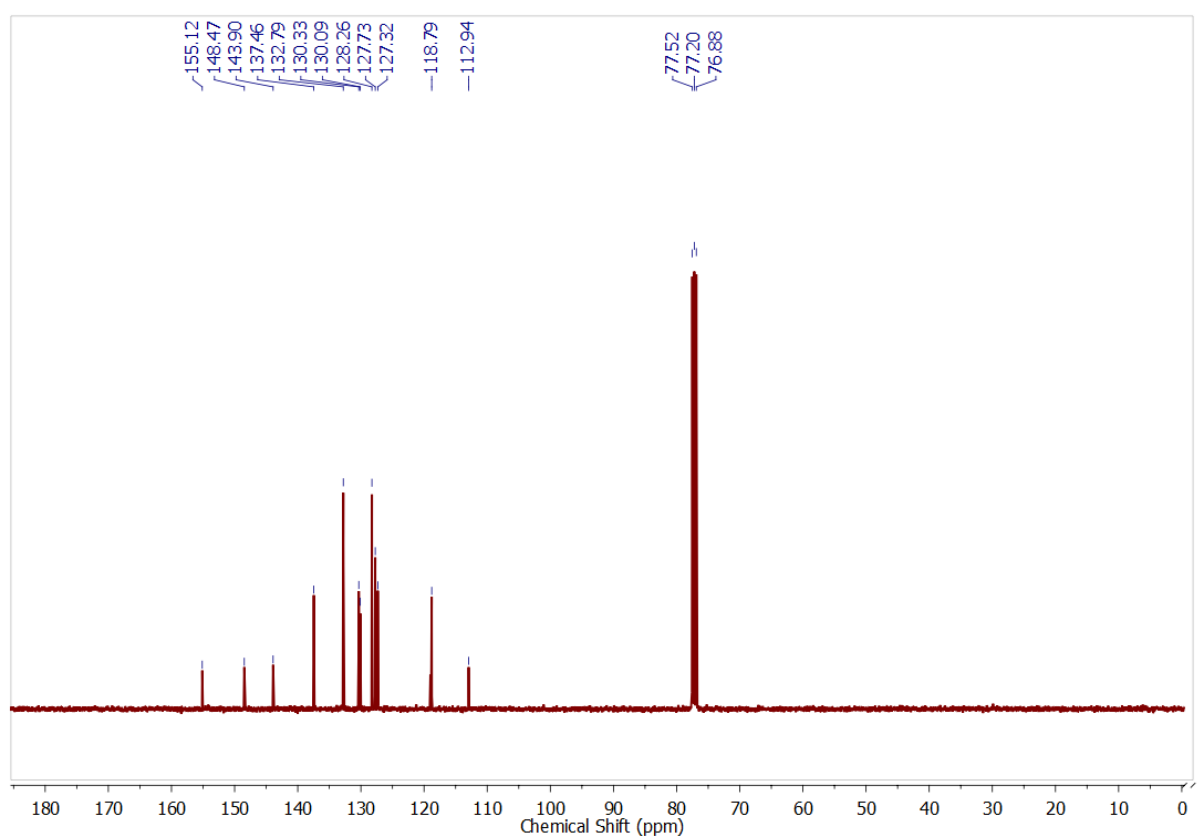


(c)

Figure S18. (a)  $^1\text{H}$ , (b)  $^{13}\text{C}\{^1\text{H}\}$  NMR and (c) HRMS of **6h**.

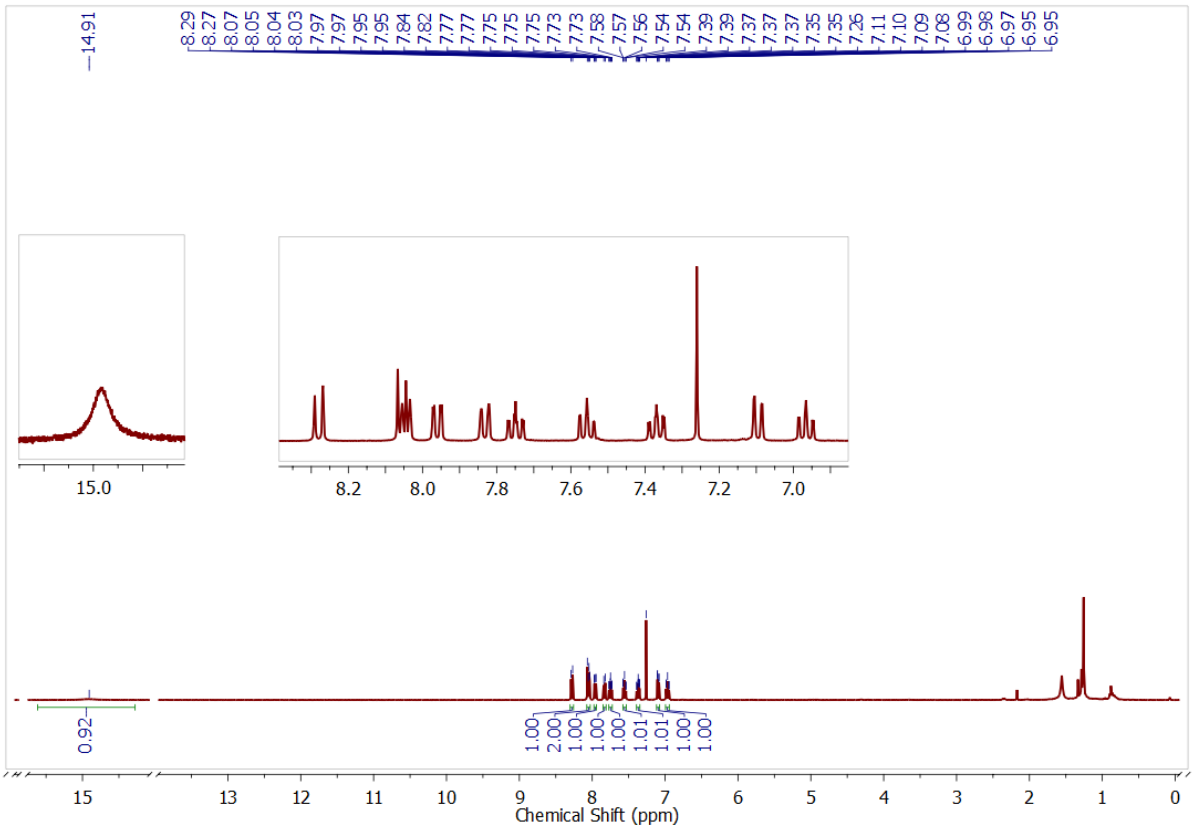


(a)

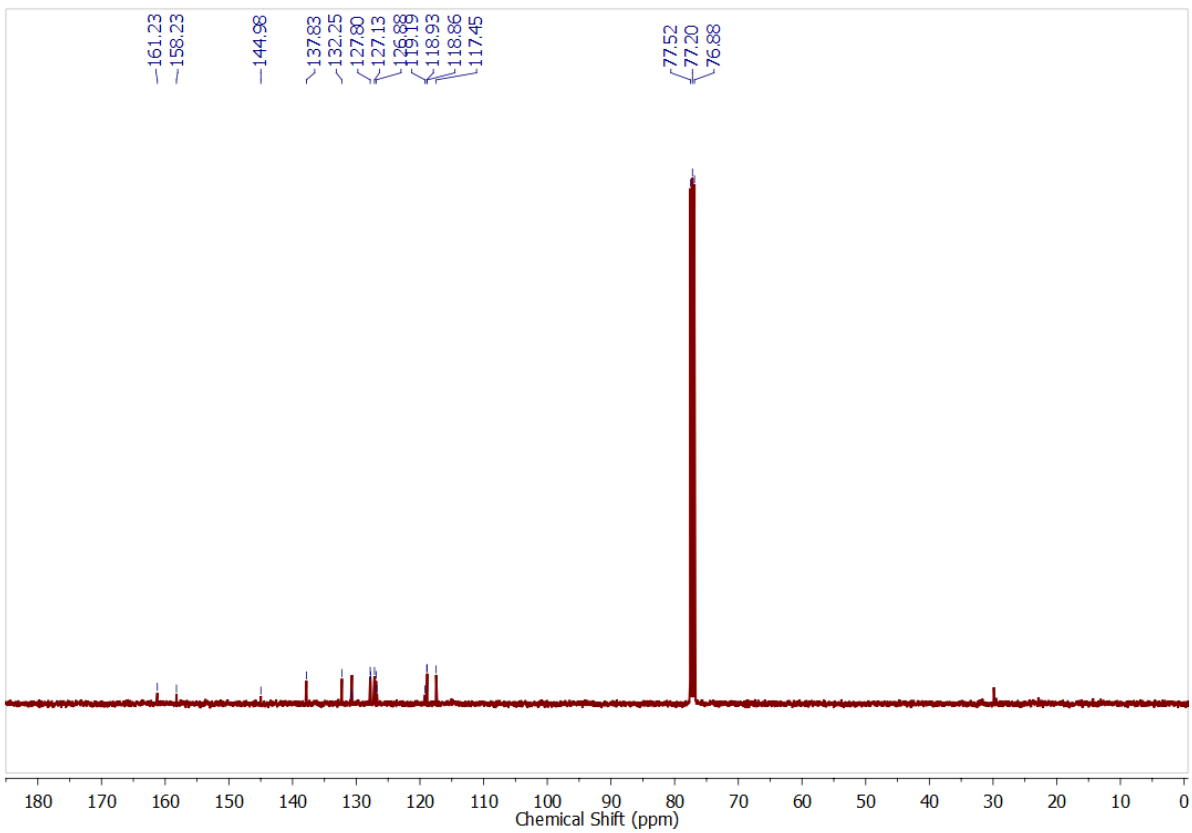


(b)

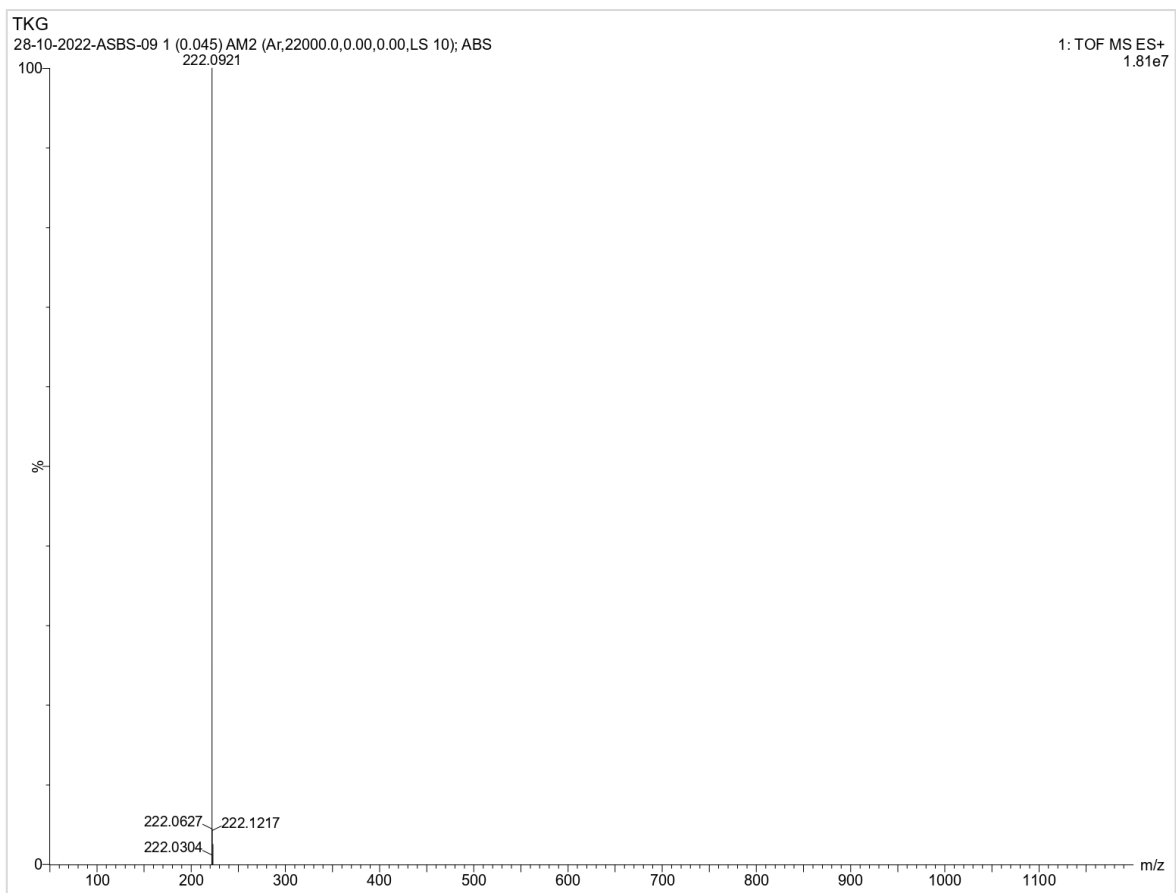
Figure S19. (a)  $^1\text{H}$ , and (b)  $^{13}\text{C}\{^1\text{H}\}$  NMR of **6i**.



(a)

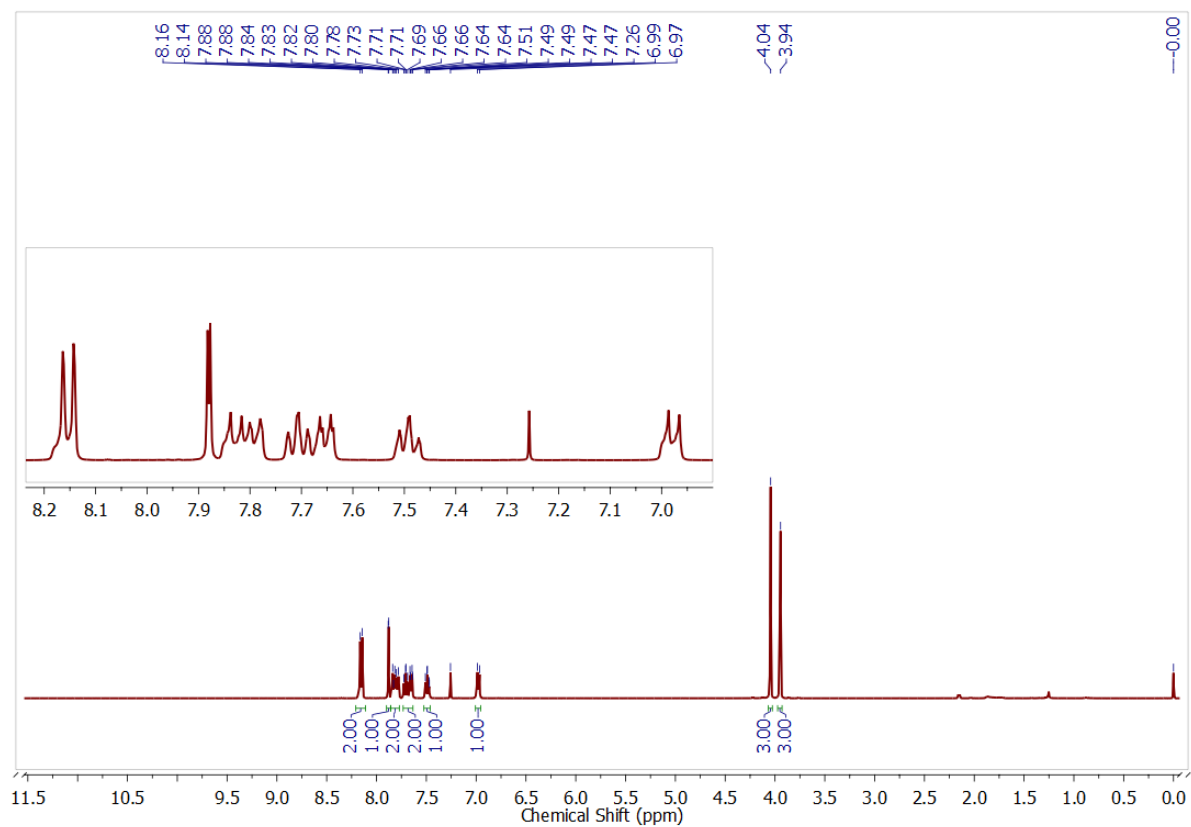


(b)

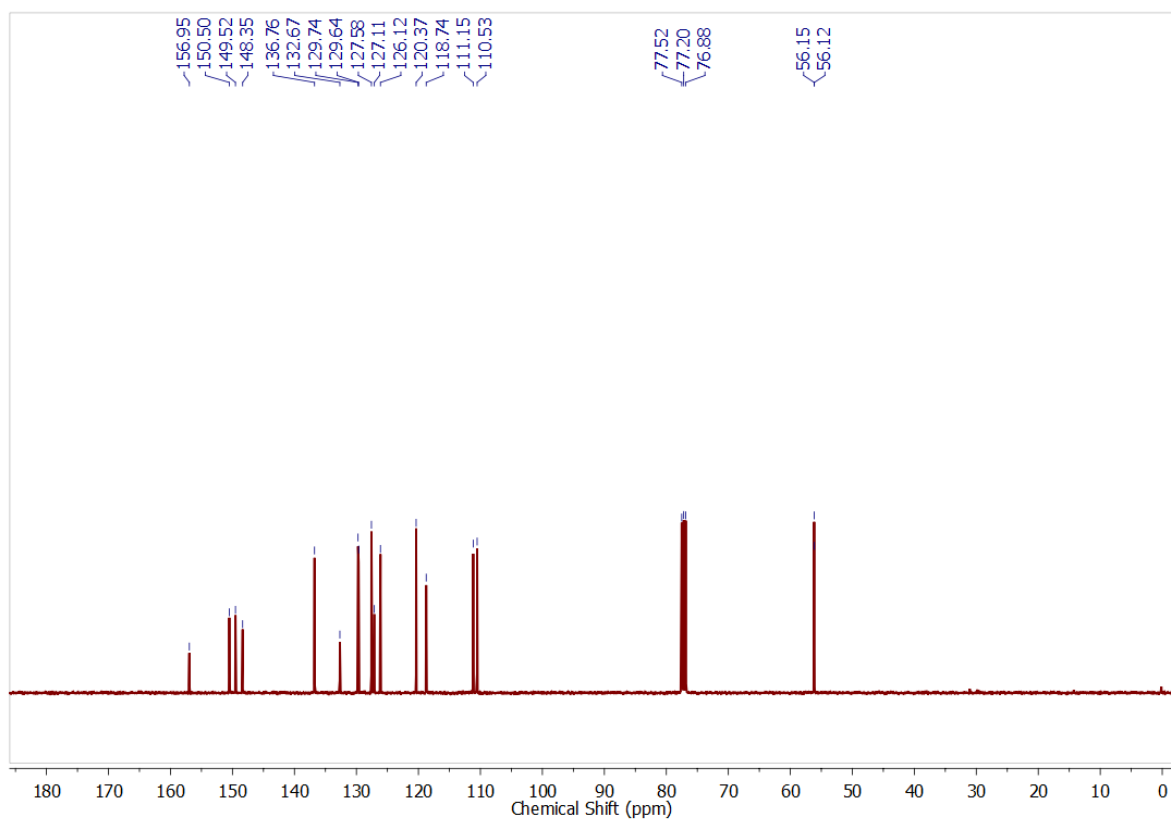


(c)

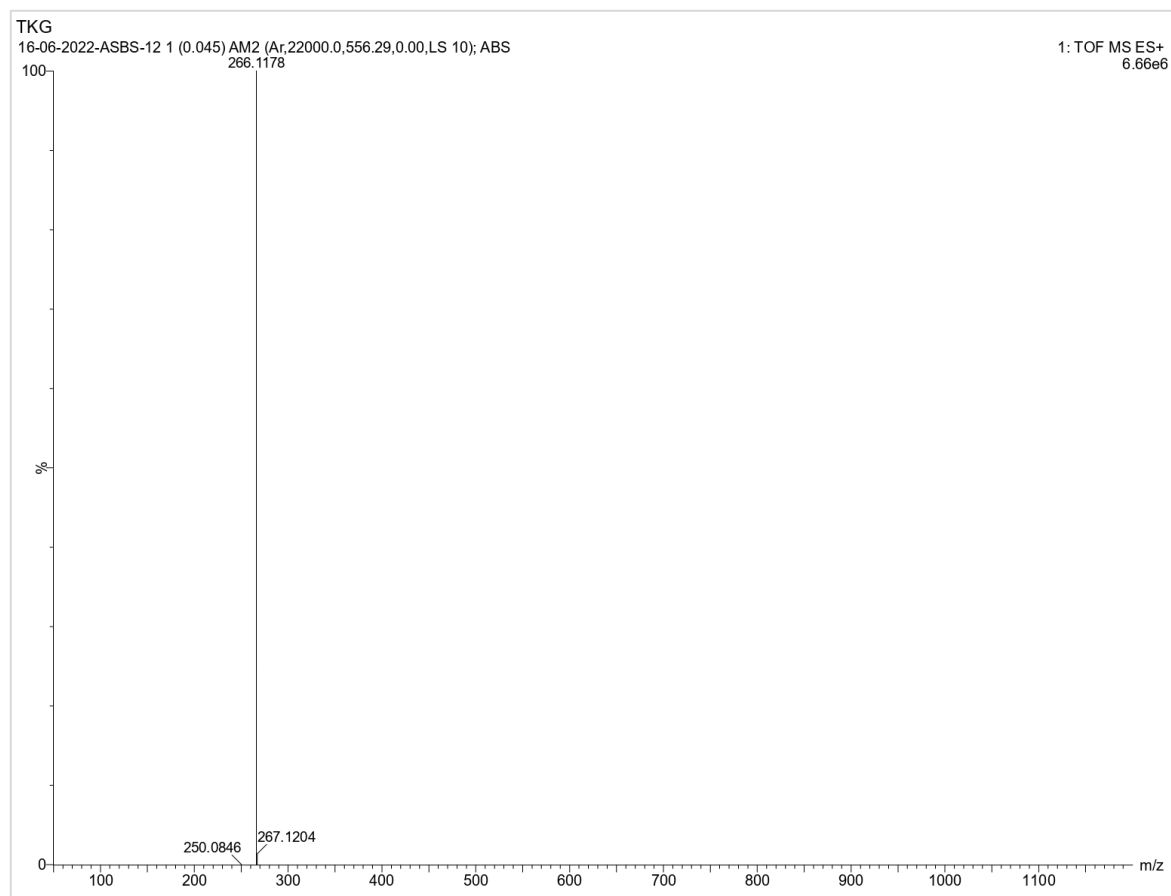
Figure S20. (a)  $^1\text{H}$ , (b)  $^{13}\text{C}\{^1\text{H}\}$  NMR and (c) HRMS of **6j**.



(a)

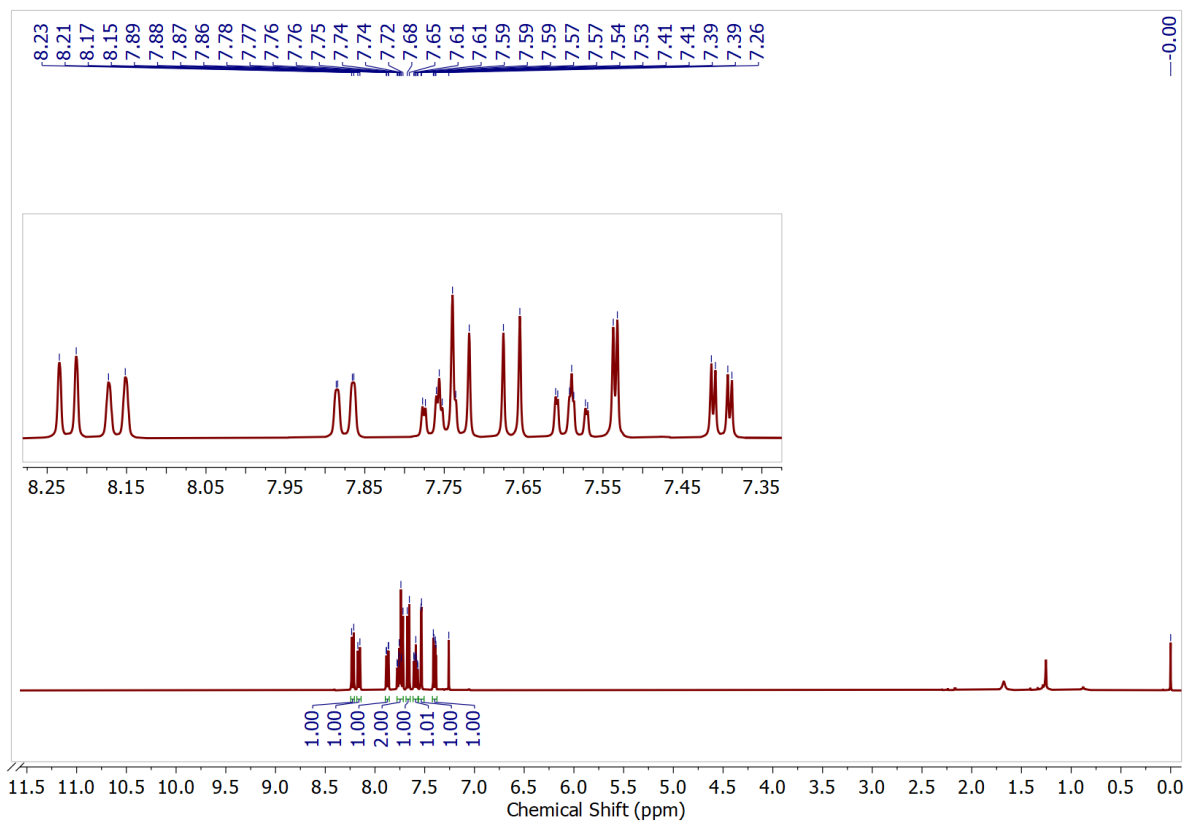


(b)

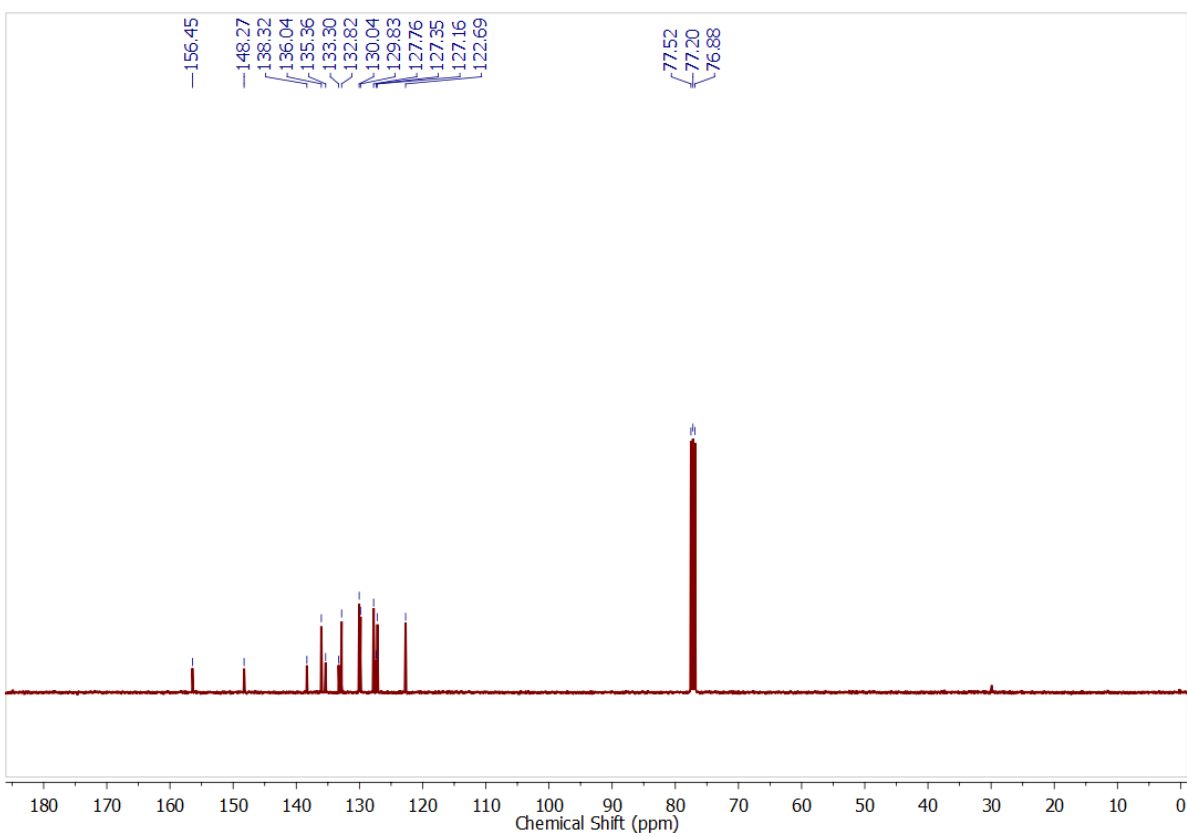


(c)

Figure S21. (a)  $^1\text{H}$ , (b)  $^{13}\text{C}\{^1\text{H}\}$  NMR and (c) HRMS of **6k**.

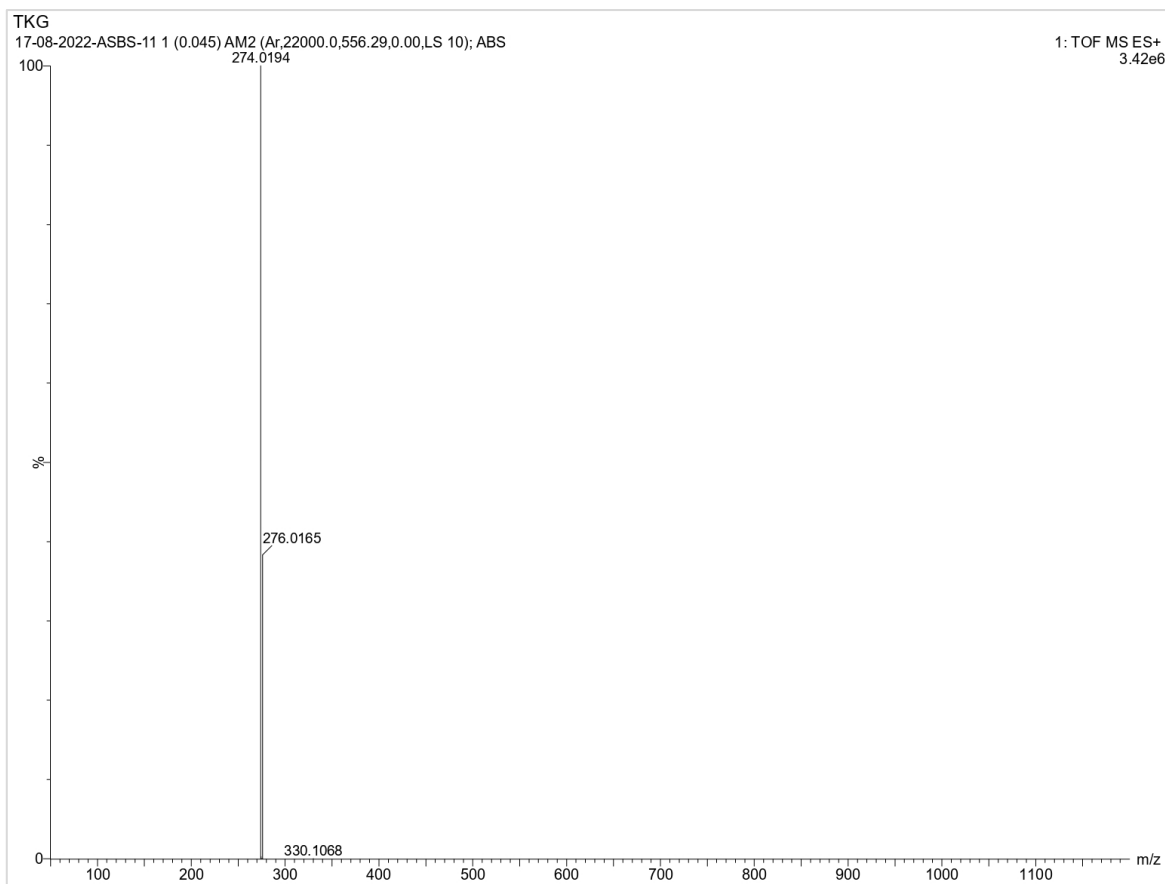


(a)



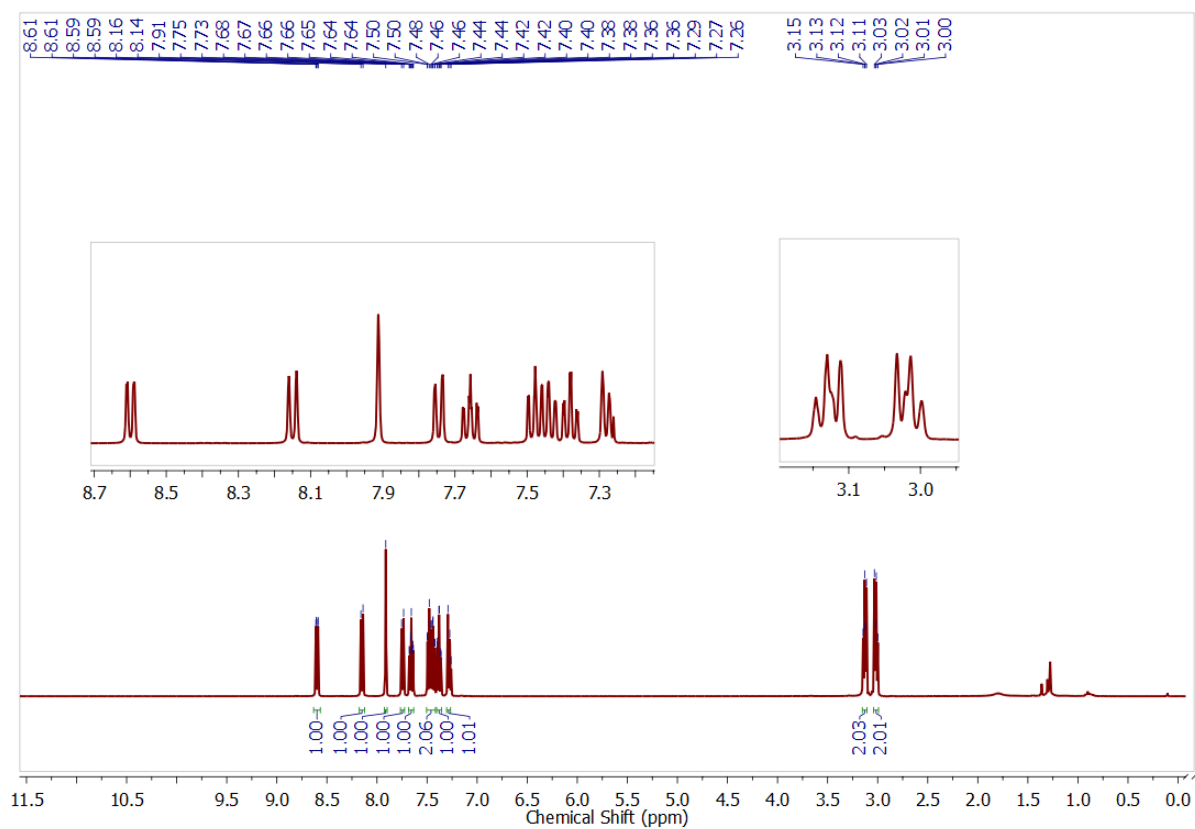
(b)



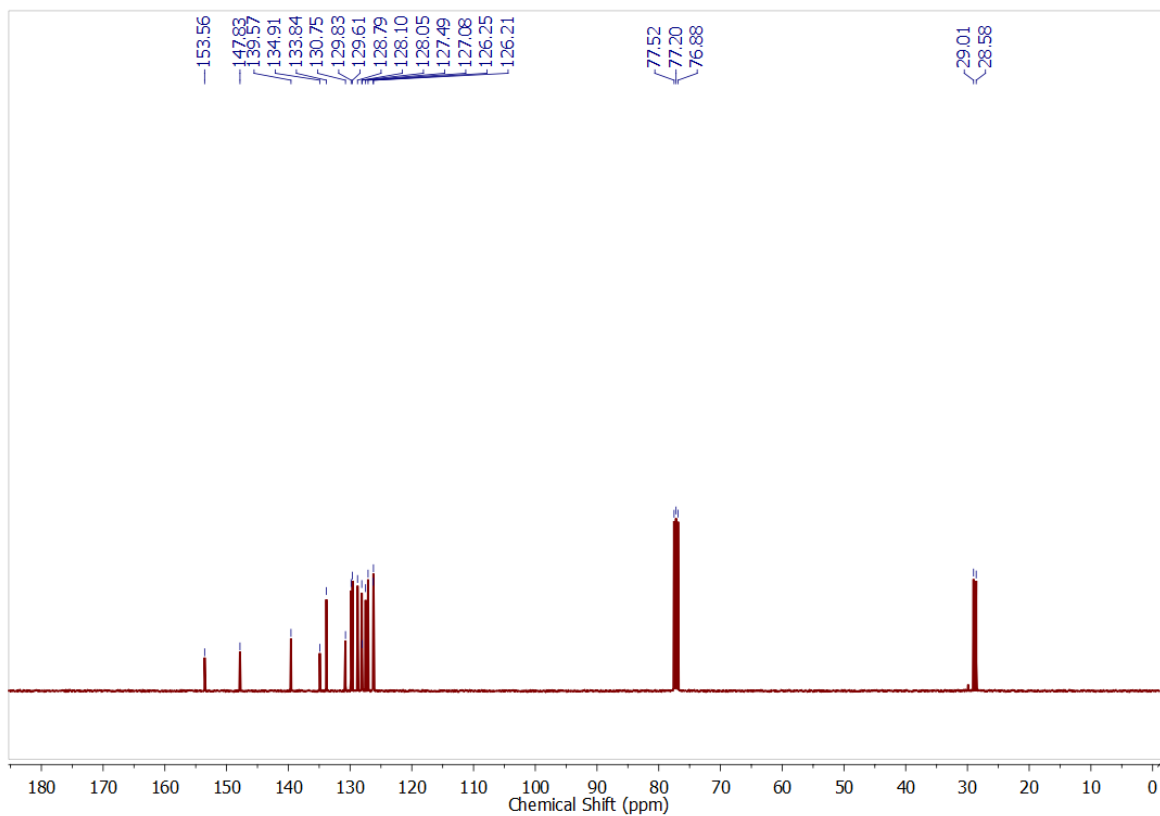


(c)

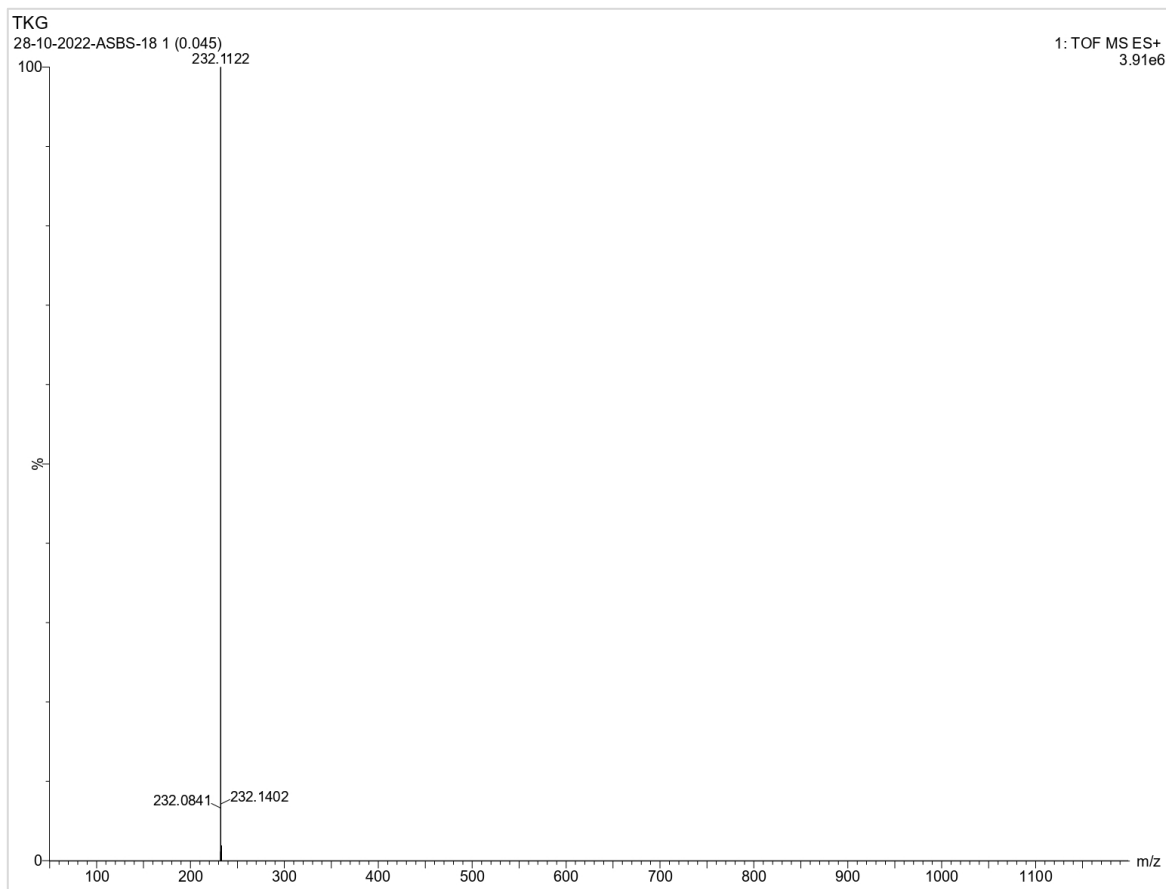
Figure S22. (a)  $^1\text{H}$ , (b)  $^{13}\text{C}\{^1\text{H}\}$  NMR and (c) HRMS of **6I**.



(a)

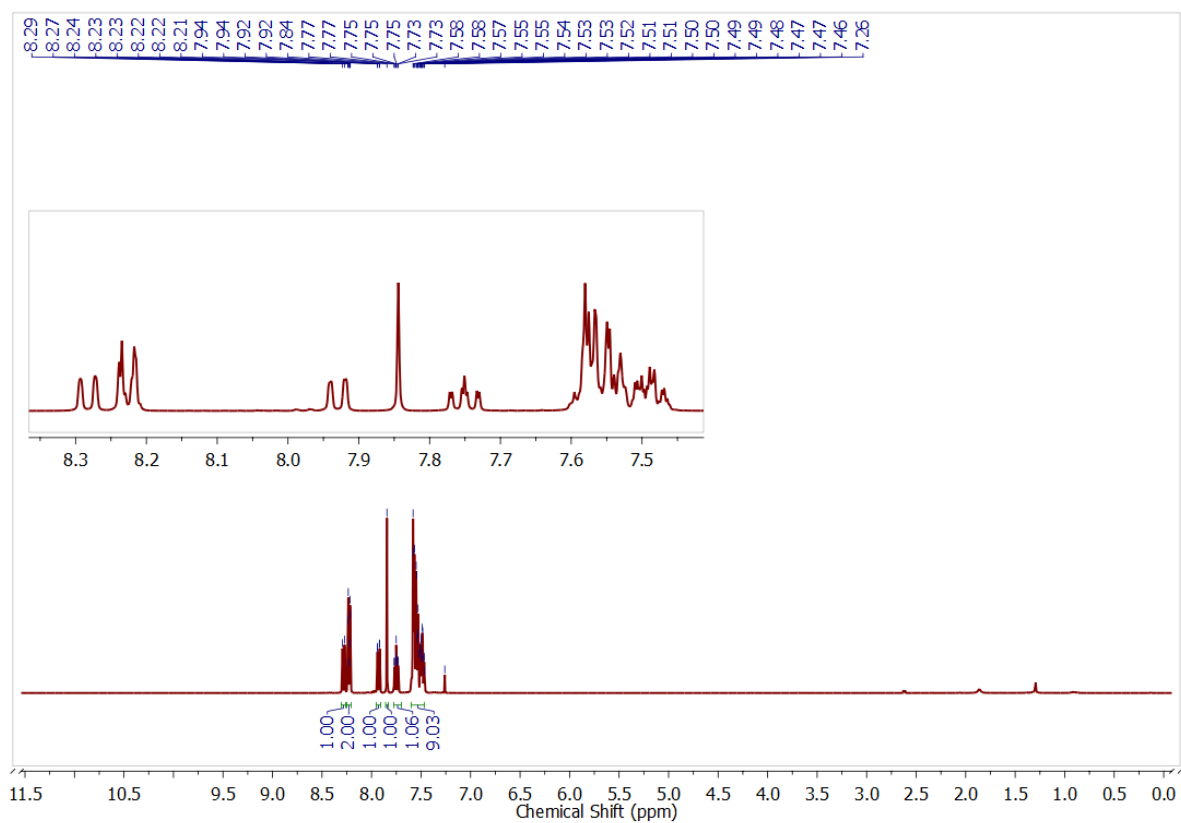


(b)

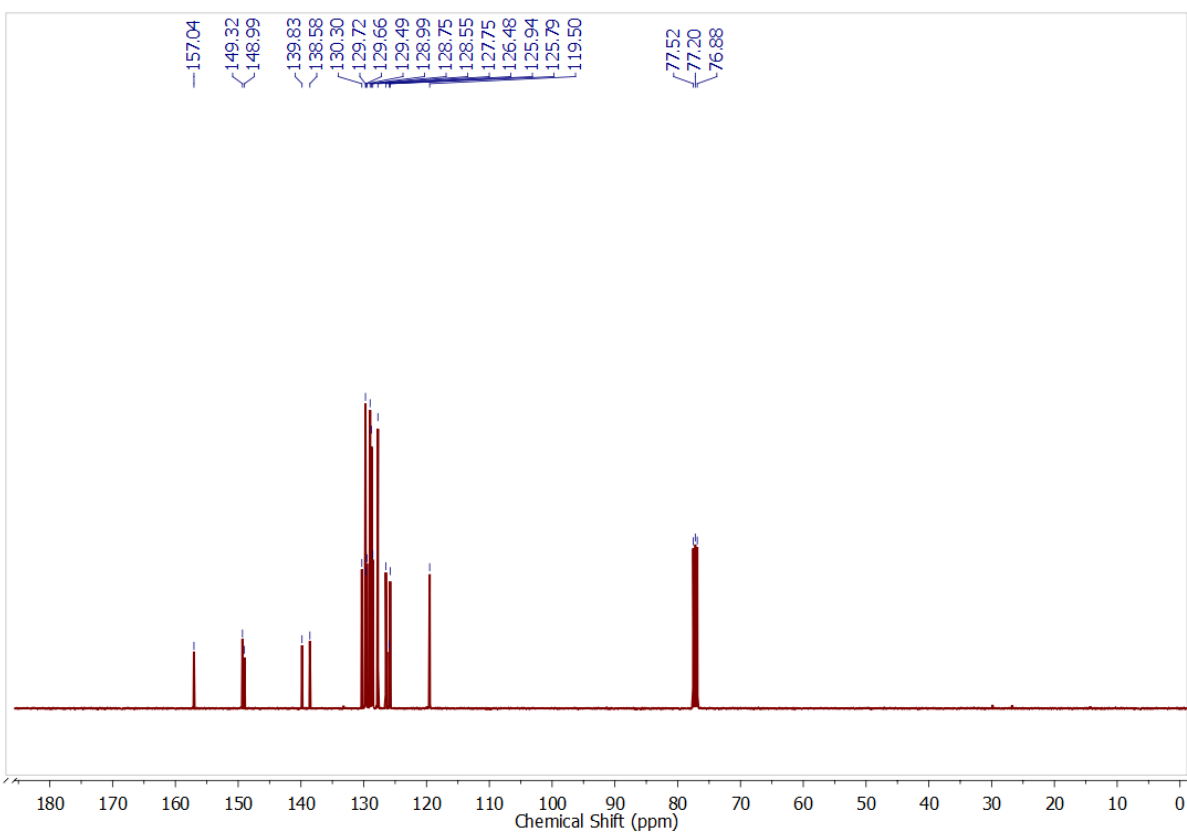


(c)

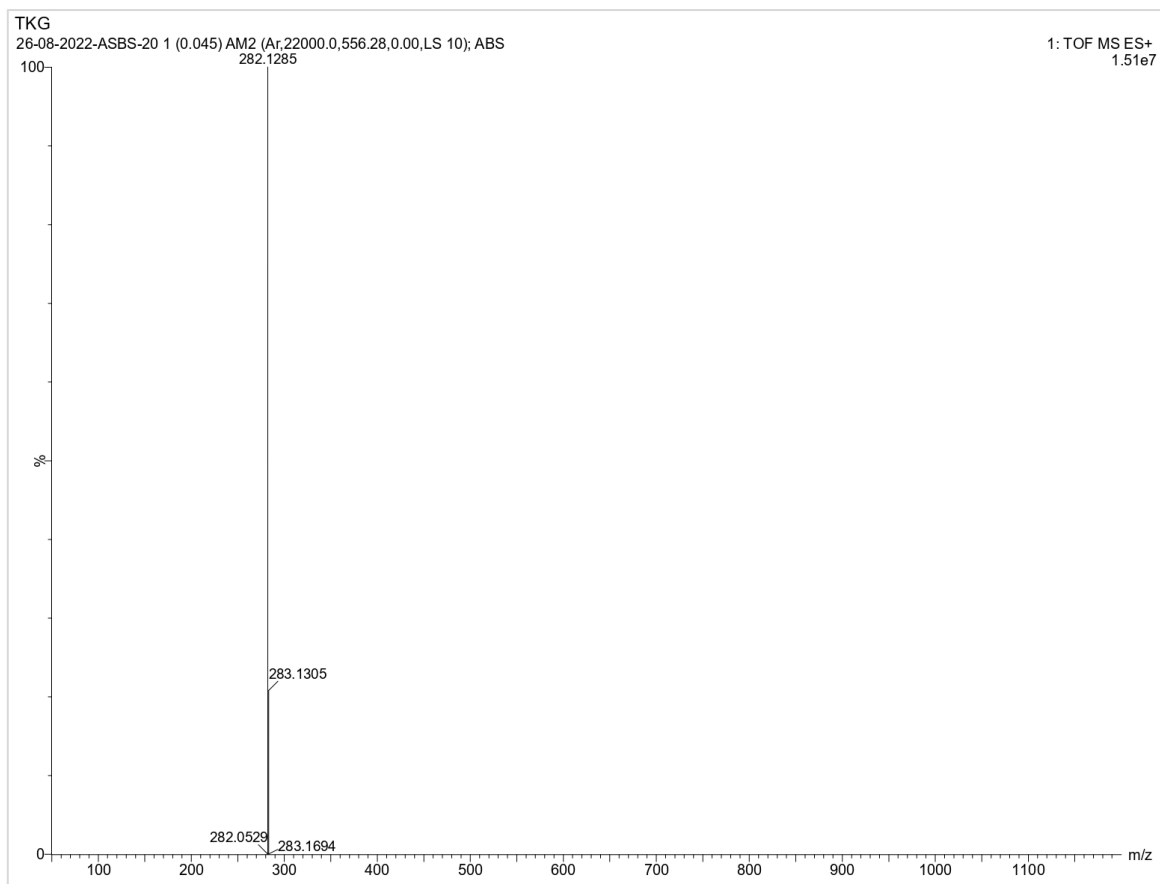
Figure S23. (a)  $^1\text{H}$ , (b)  $^{13}\text{C}\{^1\text{H}\}$  NMR and (c) HRMS of **6m**.



(a)

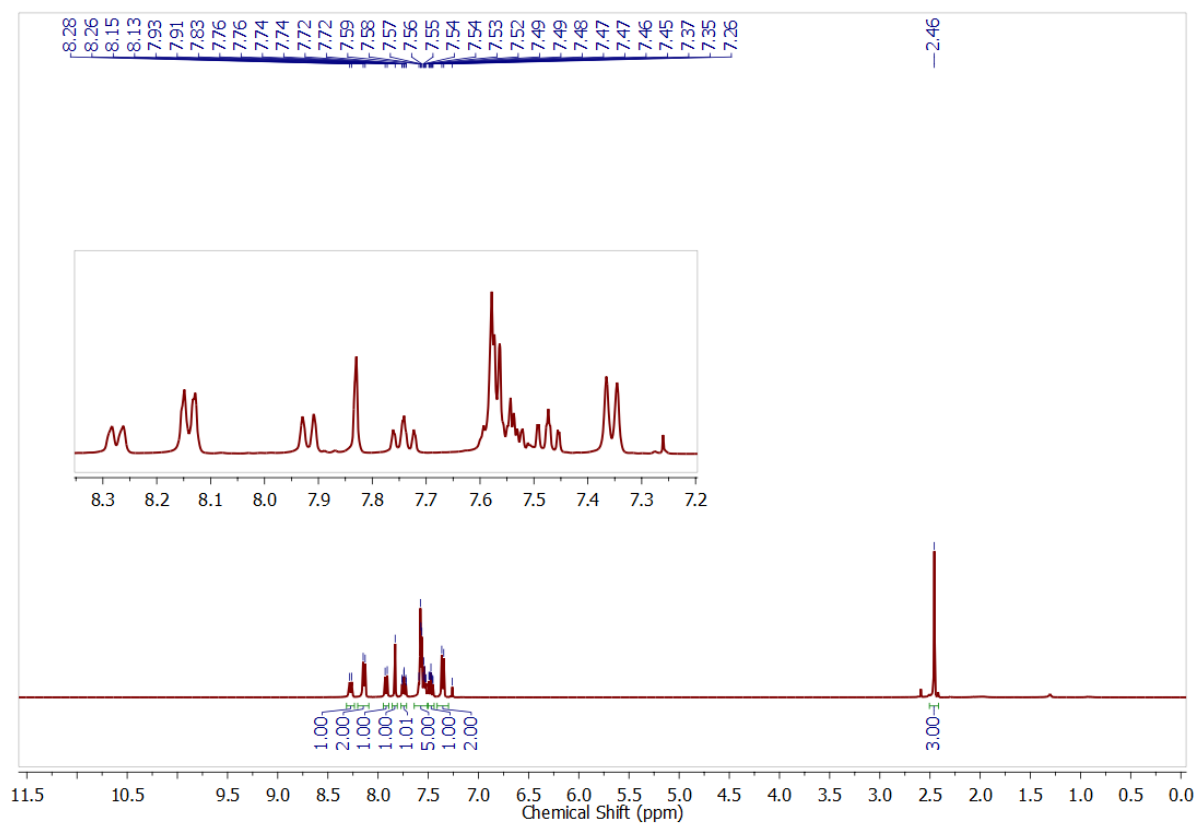


(b)

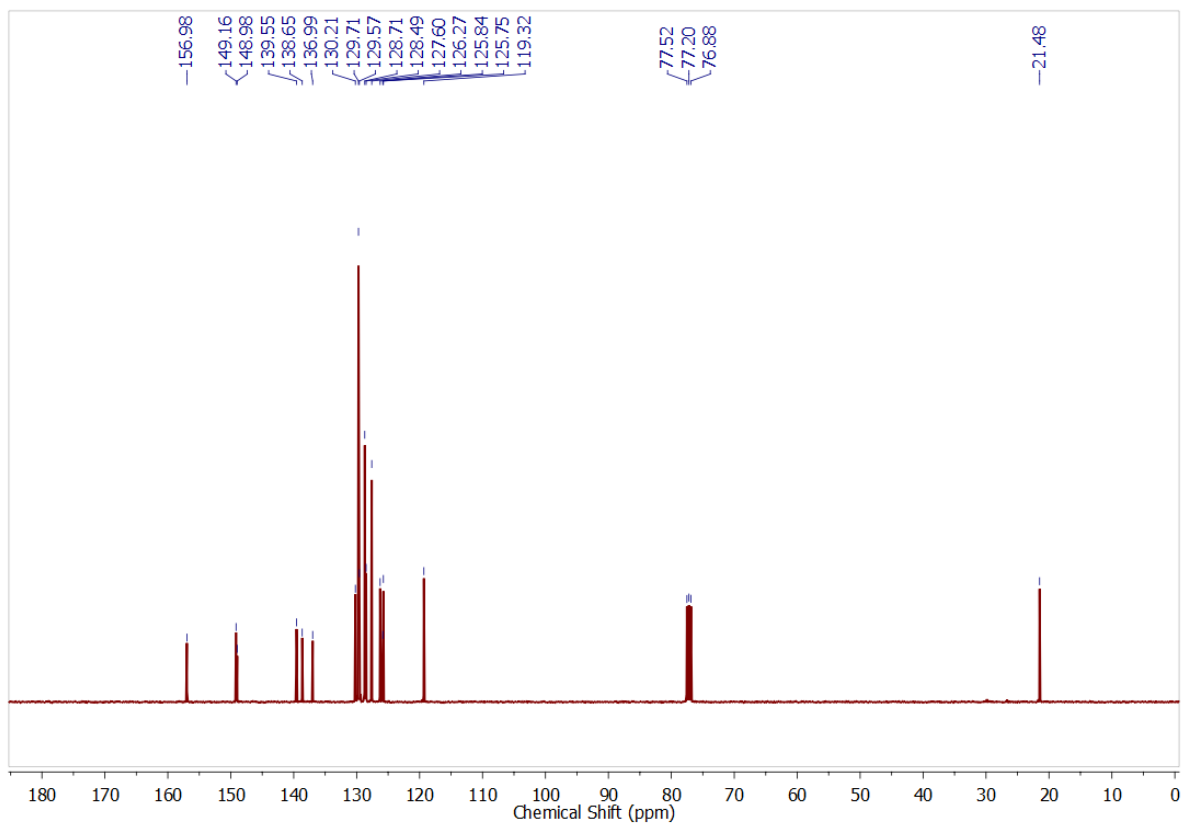


(c)

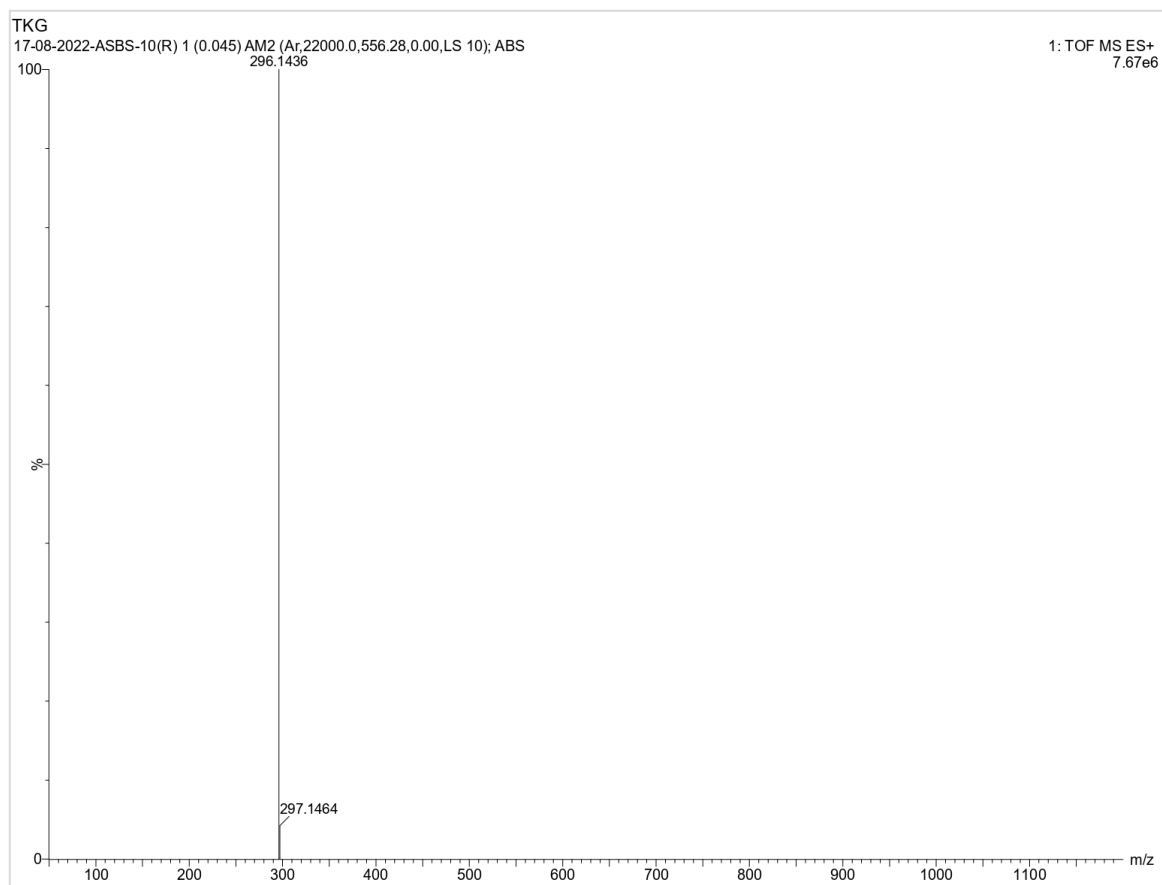
Figure S24. (a)  $^1\text{H}$ , (b)  $^{13}\text{C}\{^1\text{H}\}$  NMR and (c) HRMS of **6n**.



(a)

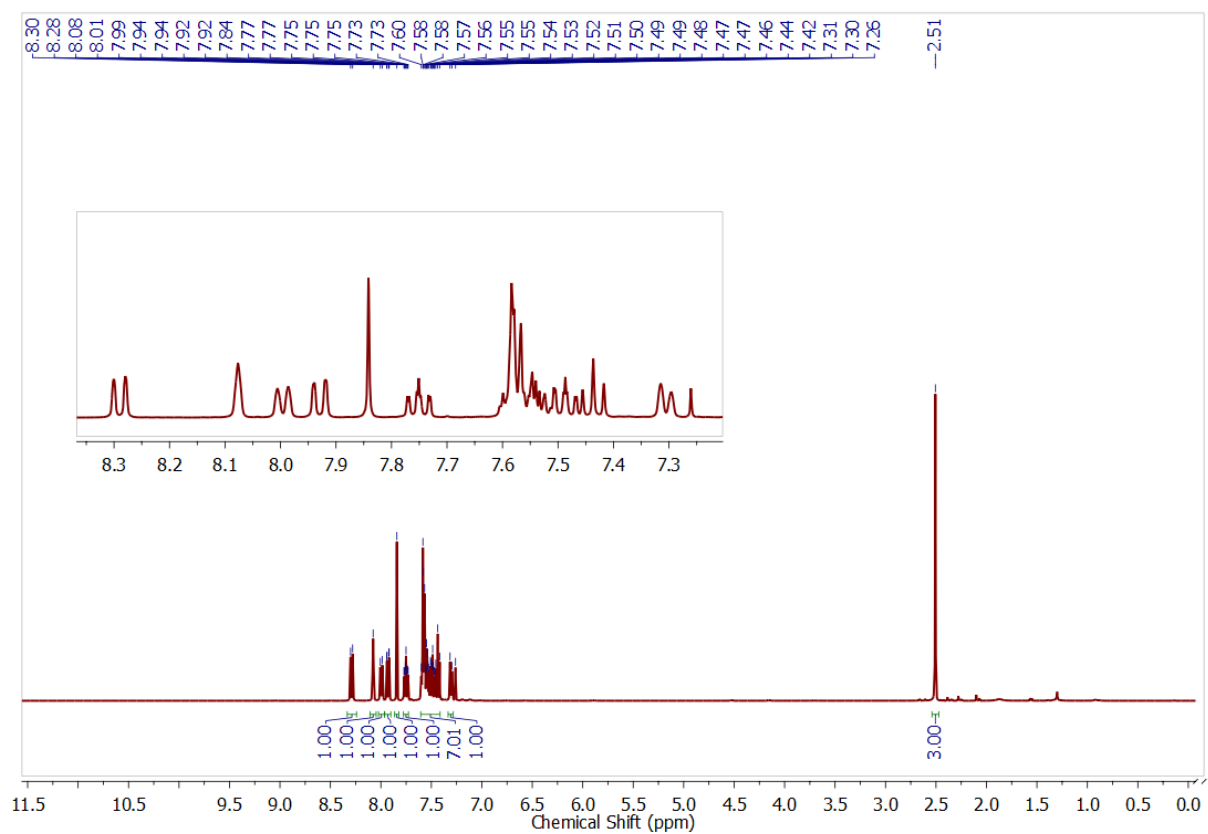


(b)

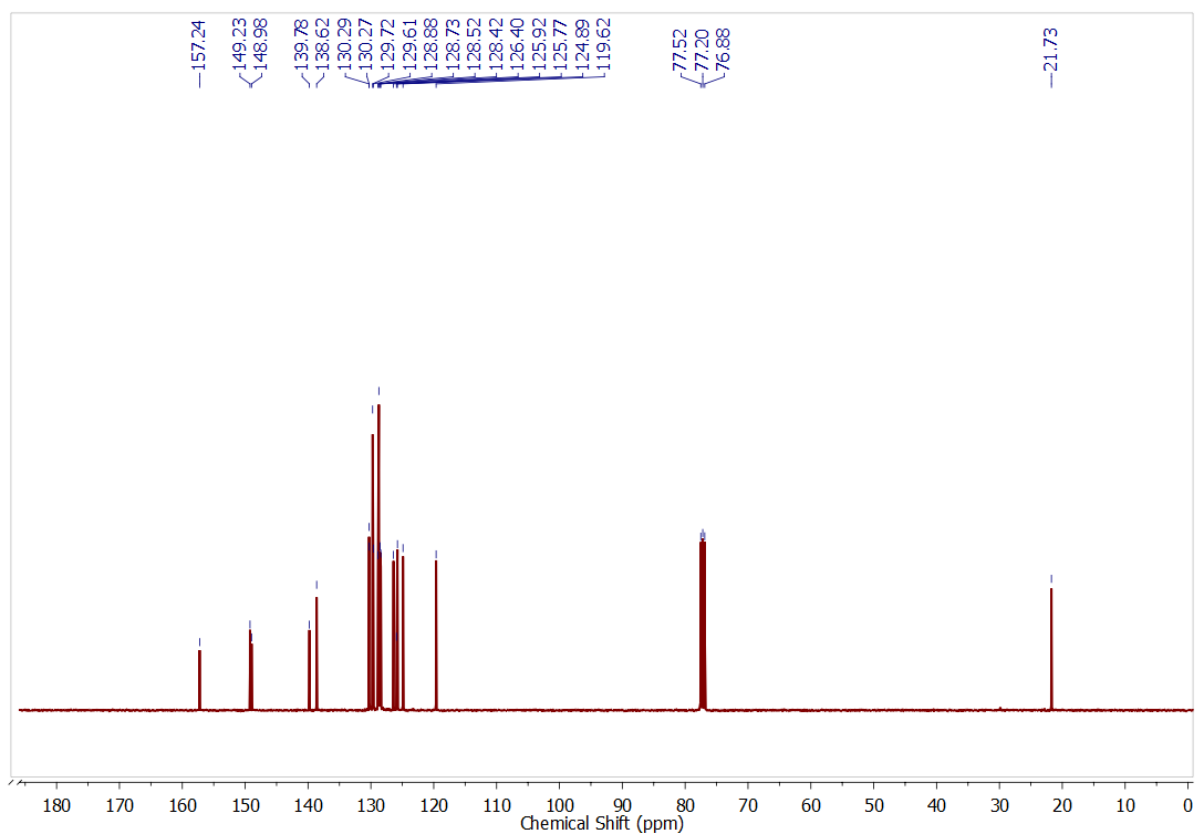


(c)

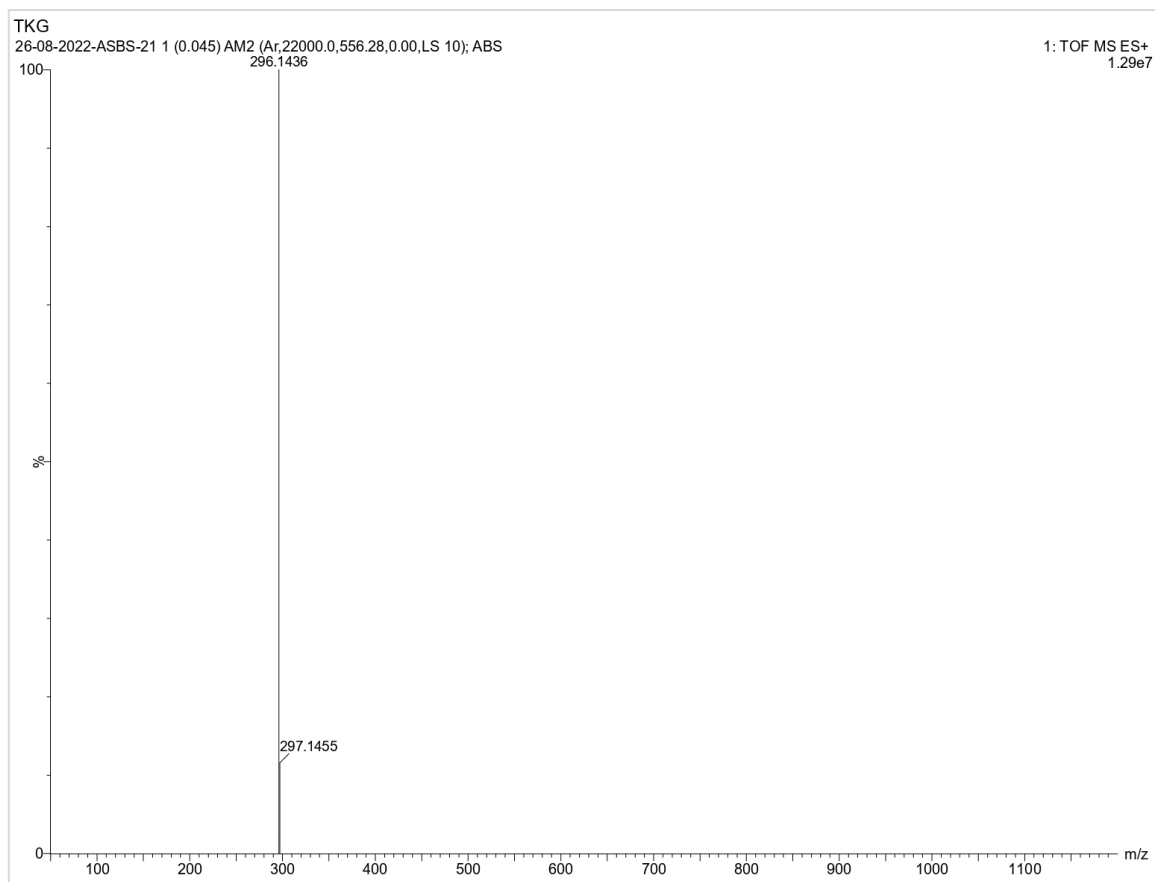
Figure S25. (a)  $^1\text{H}$ , (b)  $^{13}\text{C}\{^1\text{H}\}$  NMR and (c) HRMS of **6o**.



(a)

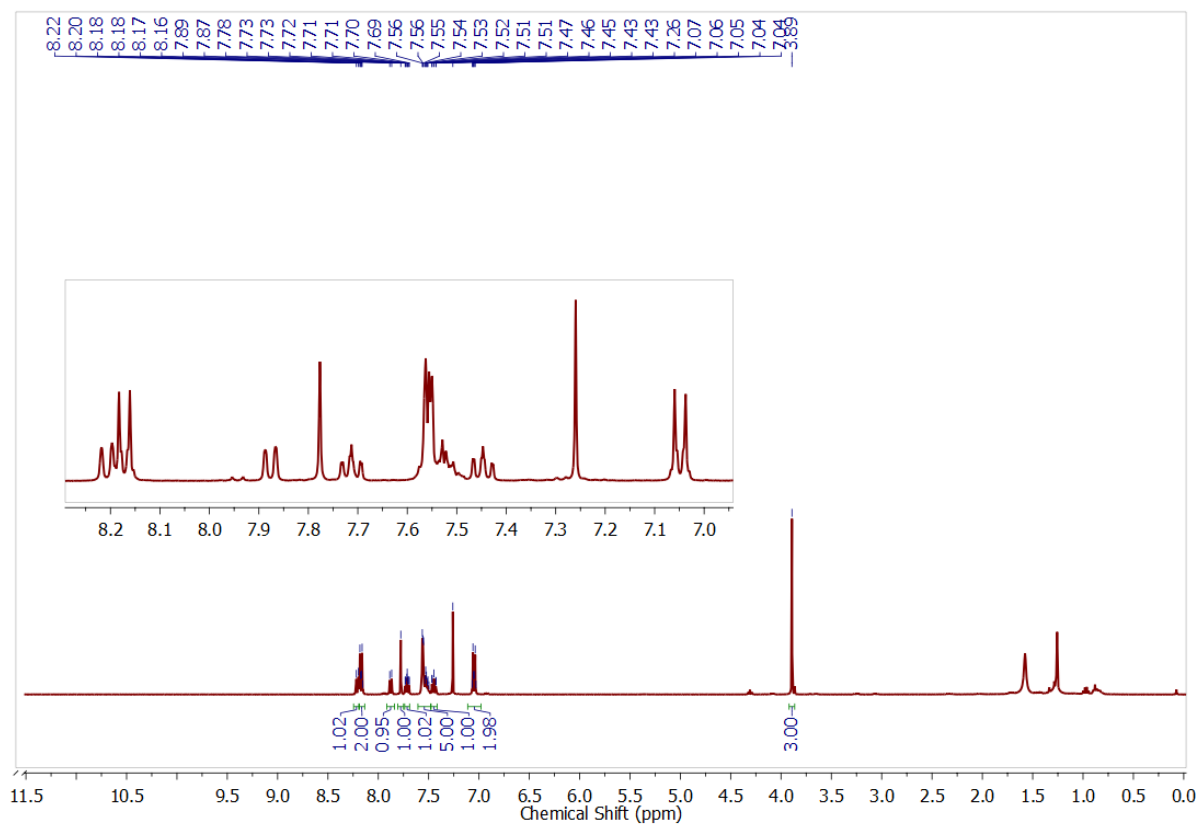


(b)

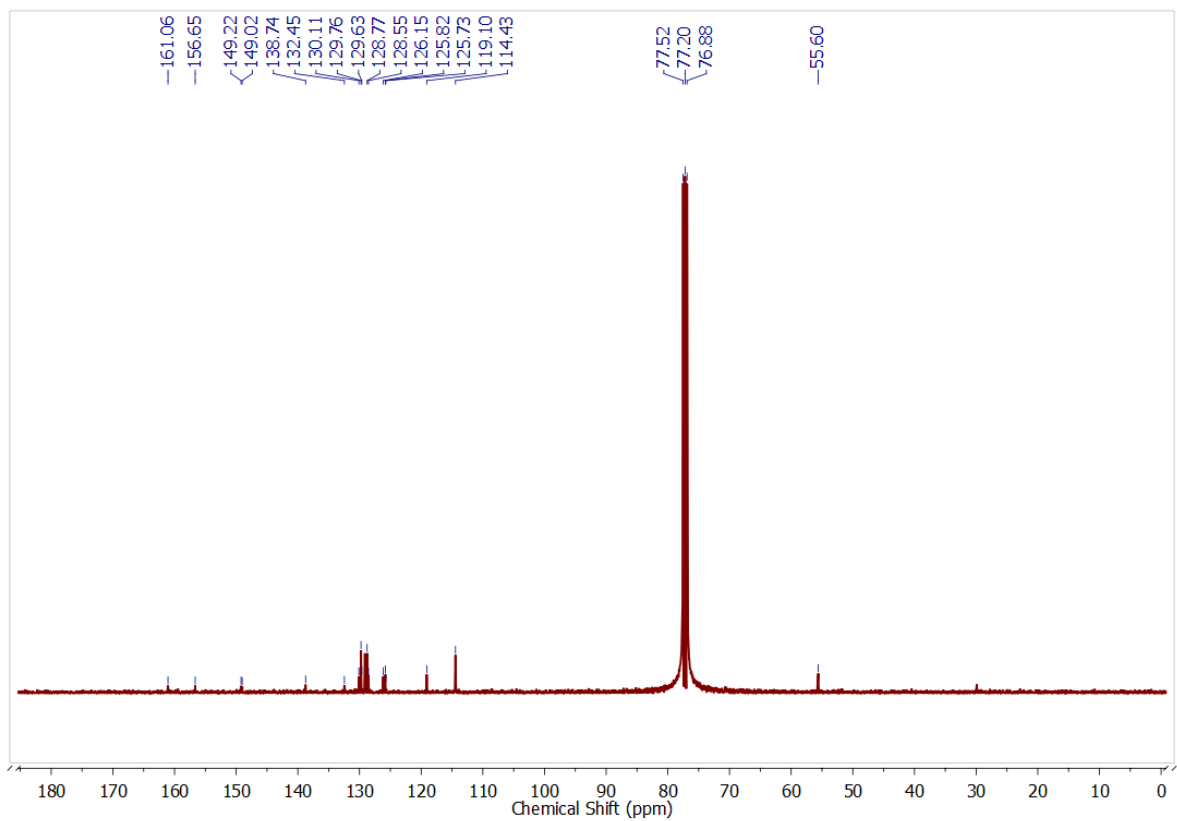


(c)

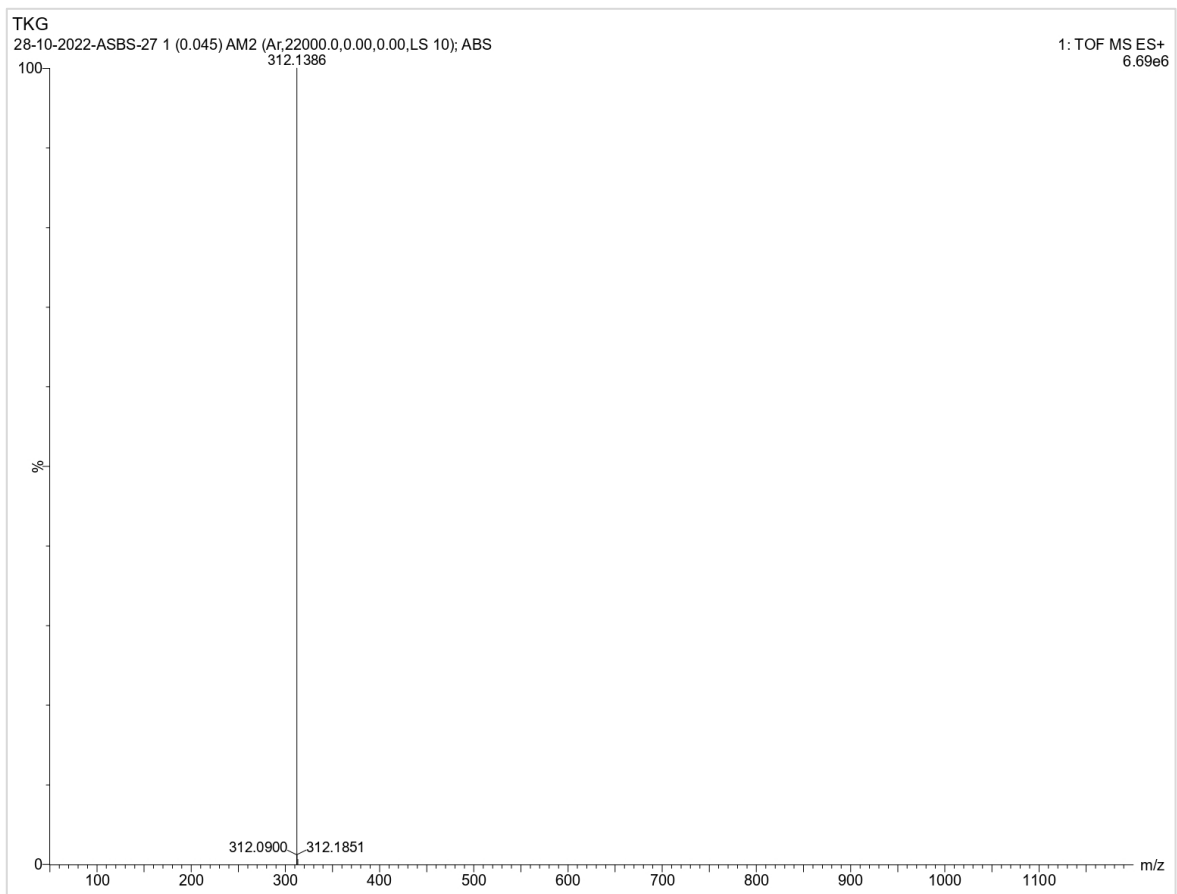
Figure S26. (a)  $^1\text{H}$ , (b)  $^{13}\text{C}\{^1\text{H}\}$  NMR and (c) HRMS of **6p**.



(a)



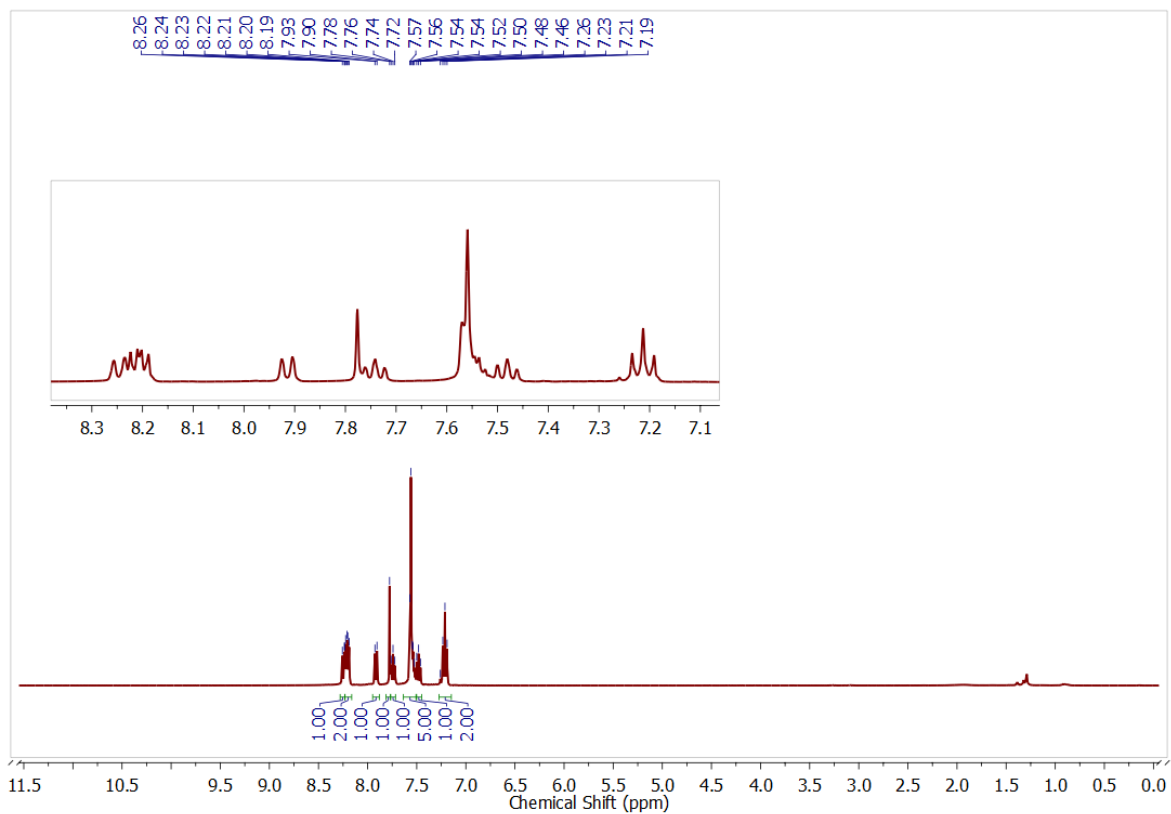
(b)



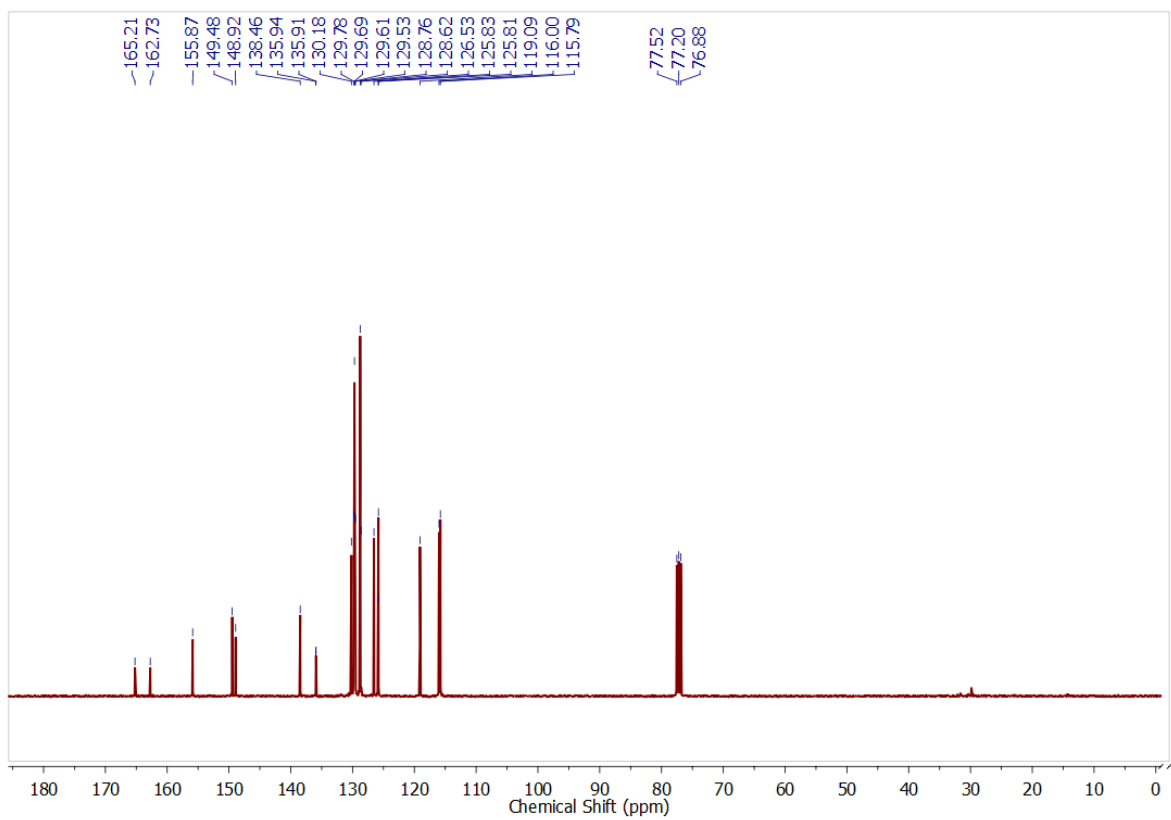
(c)

Figure S27. (a)  $^1\text{H}$ , (b)  $^{13}\text{C}\{^1\text{H}\}$  NMR and (c) HRMS of **6q**.

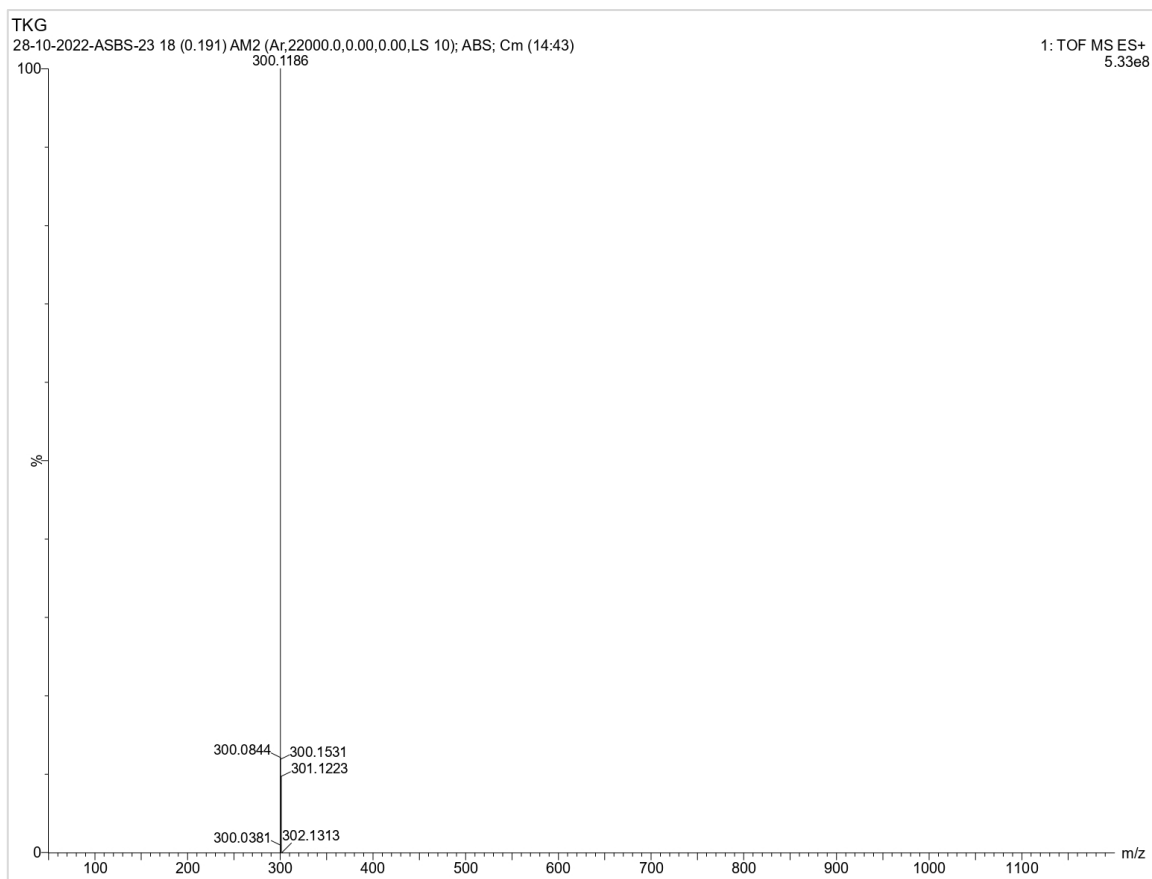




(a)

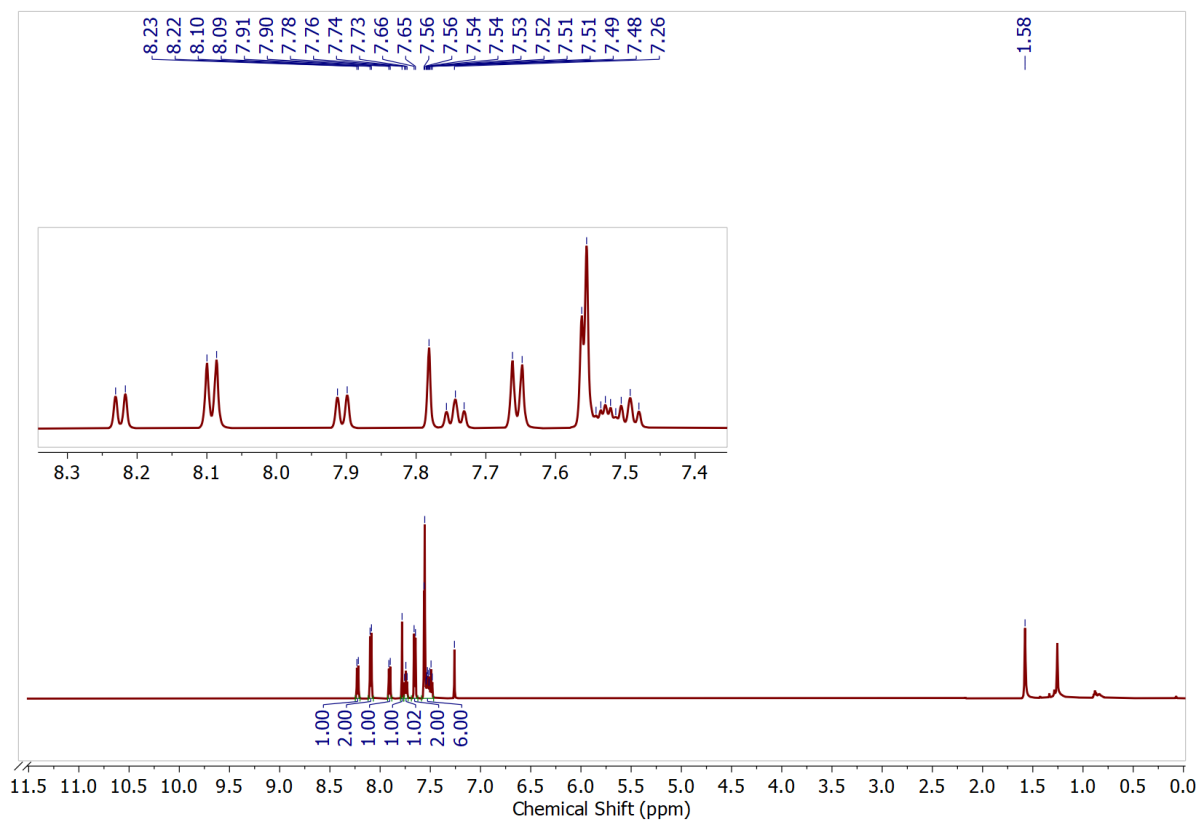


(b)

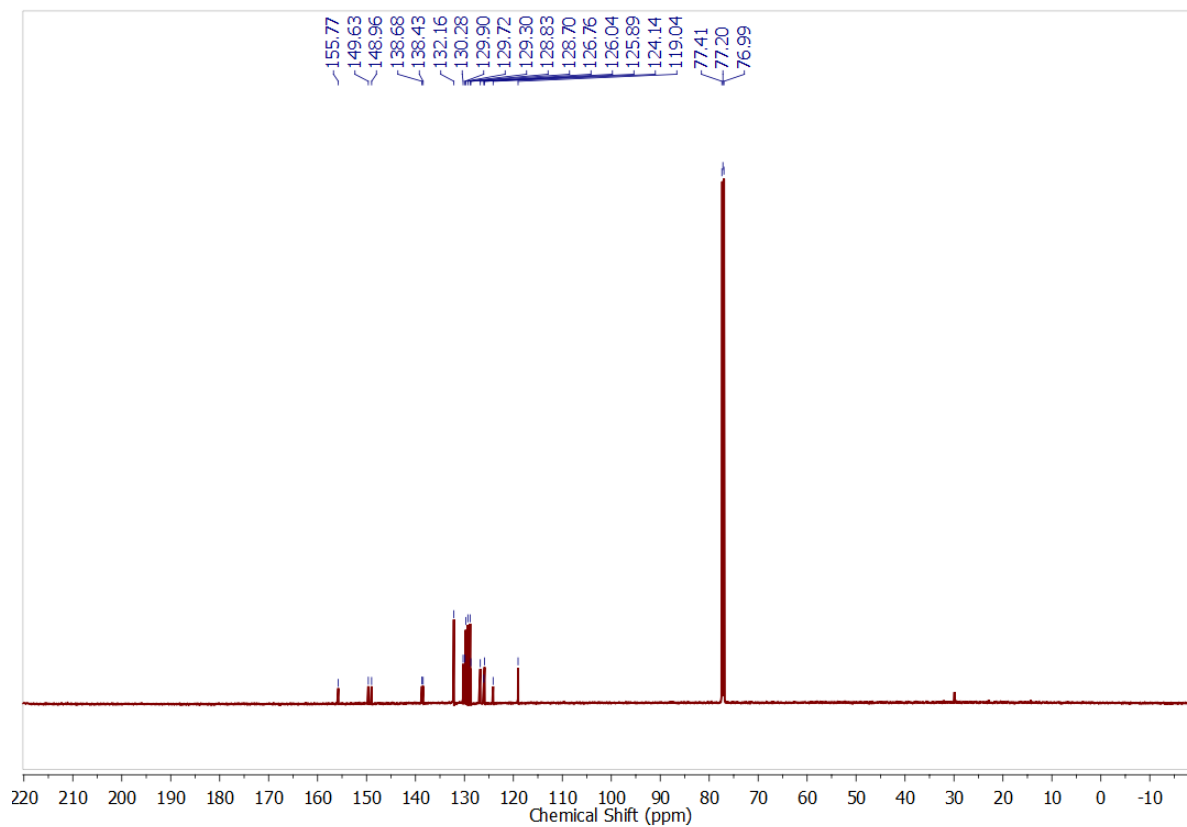


(c)

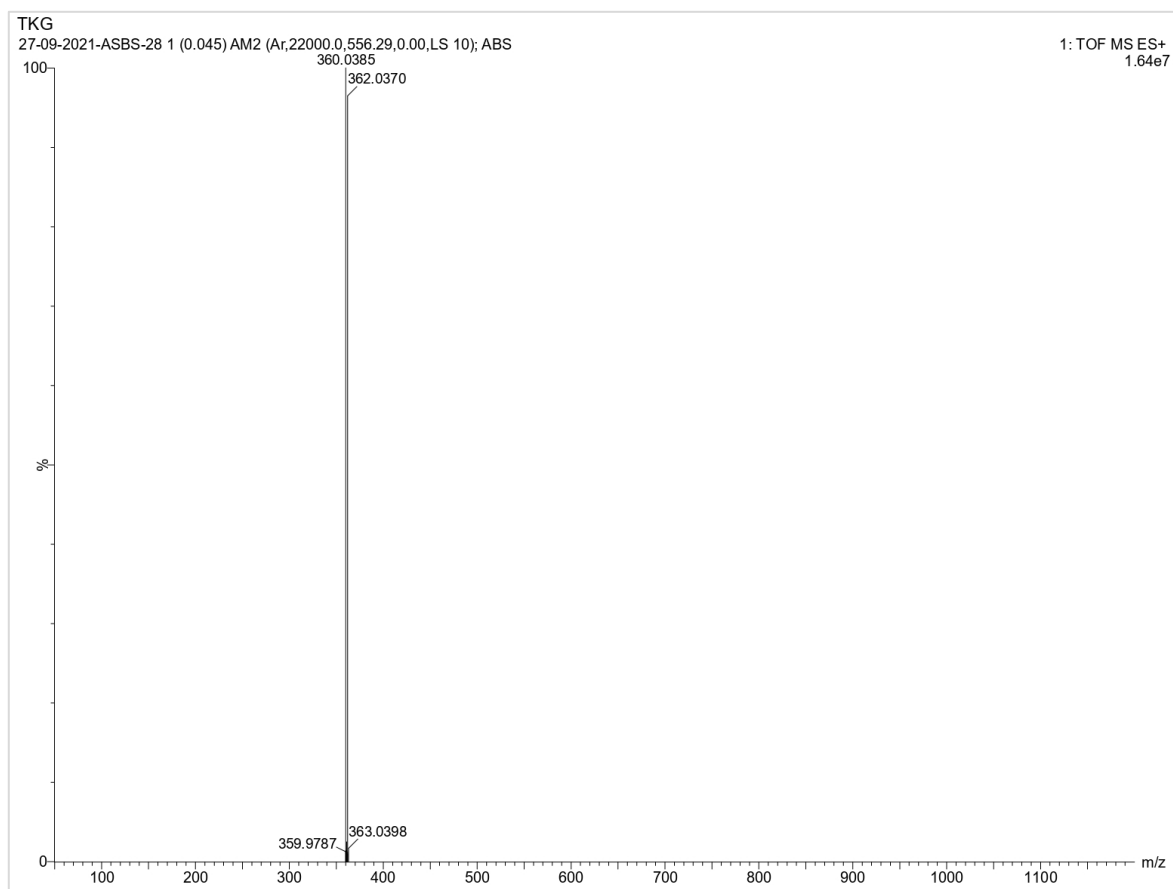
Figure S28. (a)  $^1\text{H}$ , (b)  $^{13}\text{C}\{^1\text{H}\}$  NMR and (c) HRMS of **6r**.



(a)

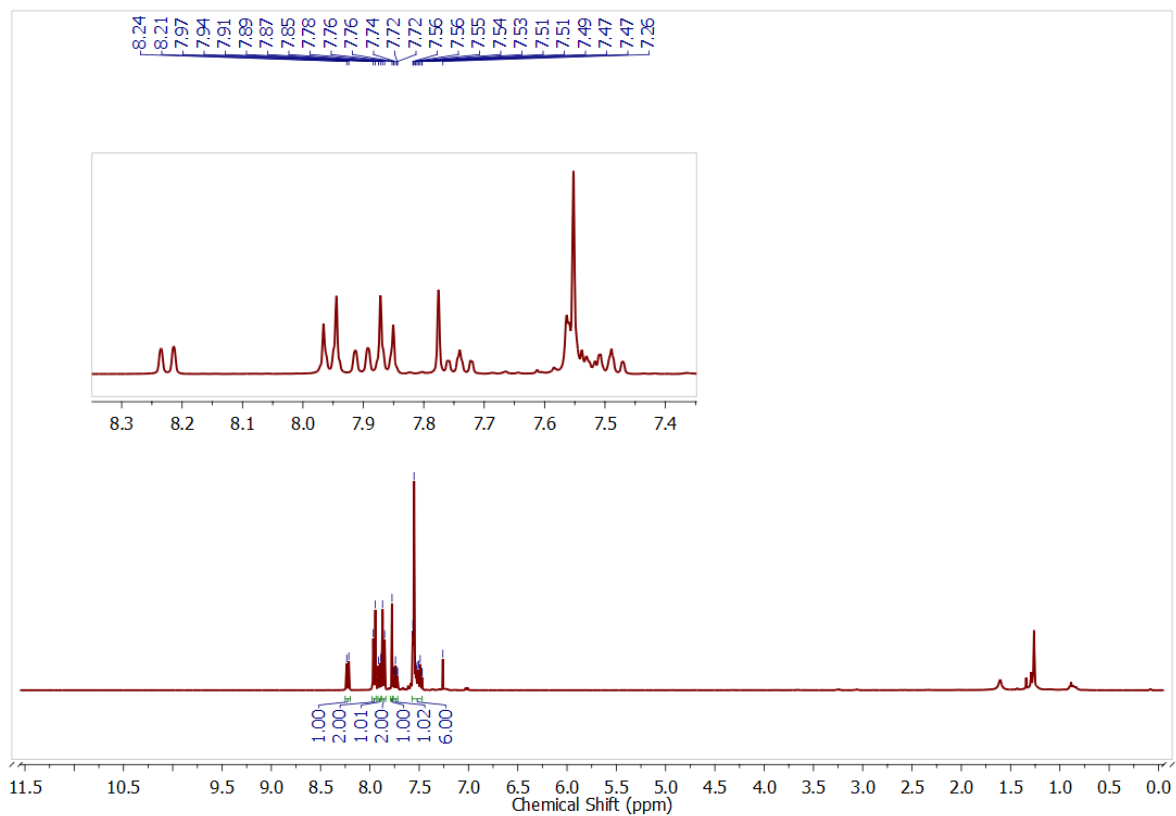


(b)

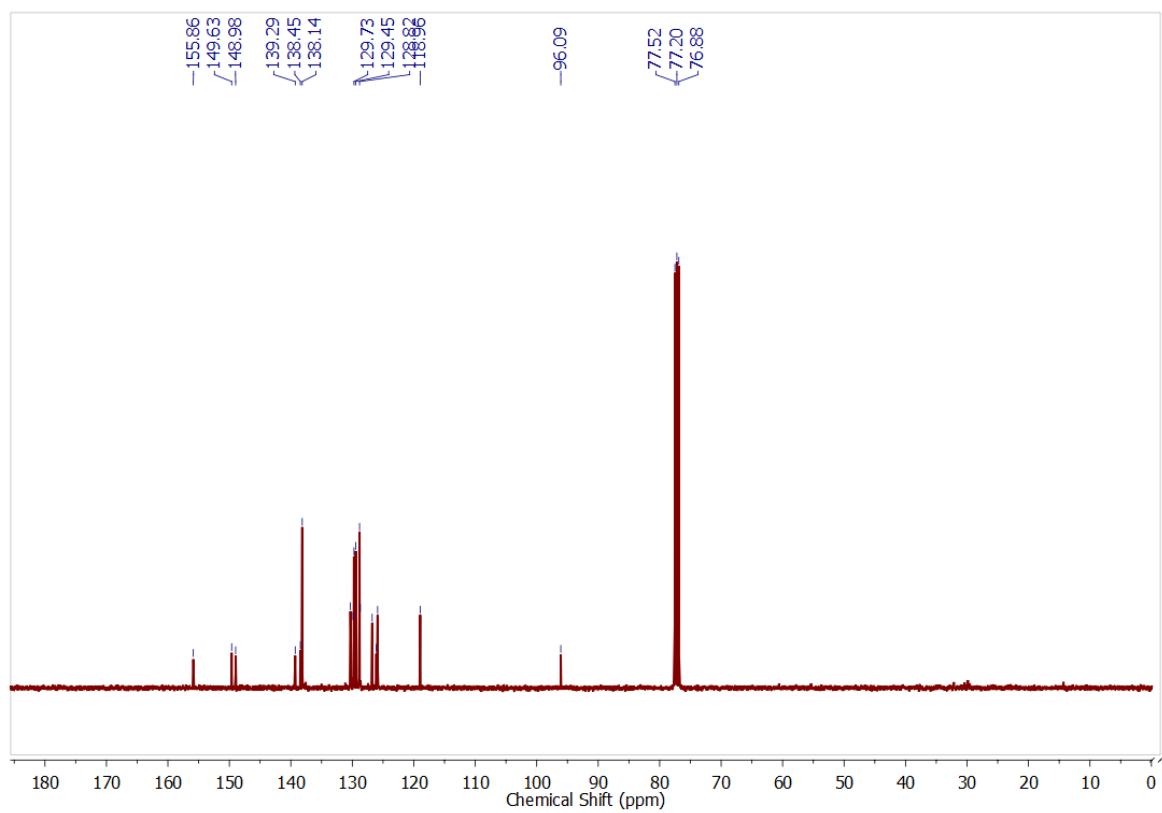


(c)

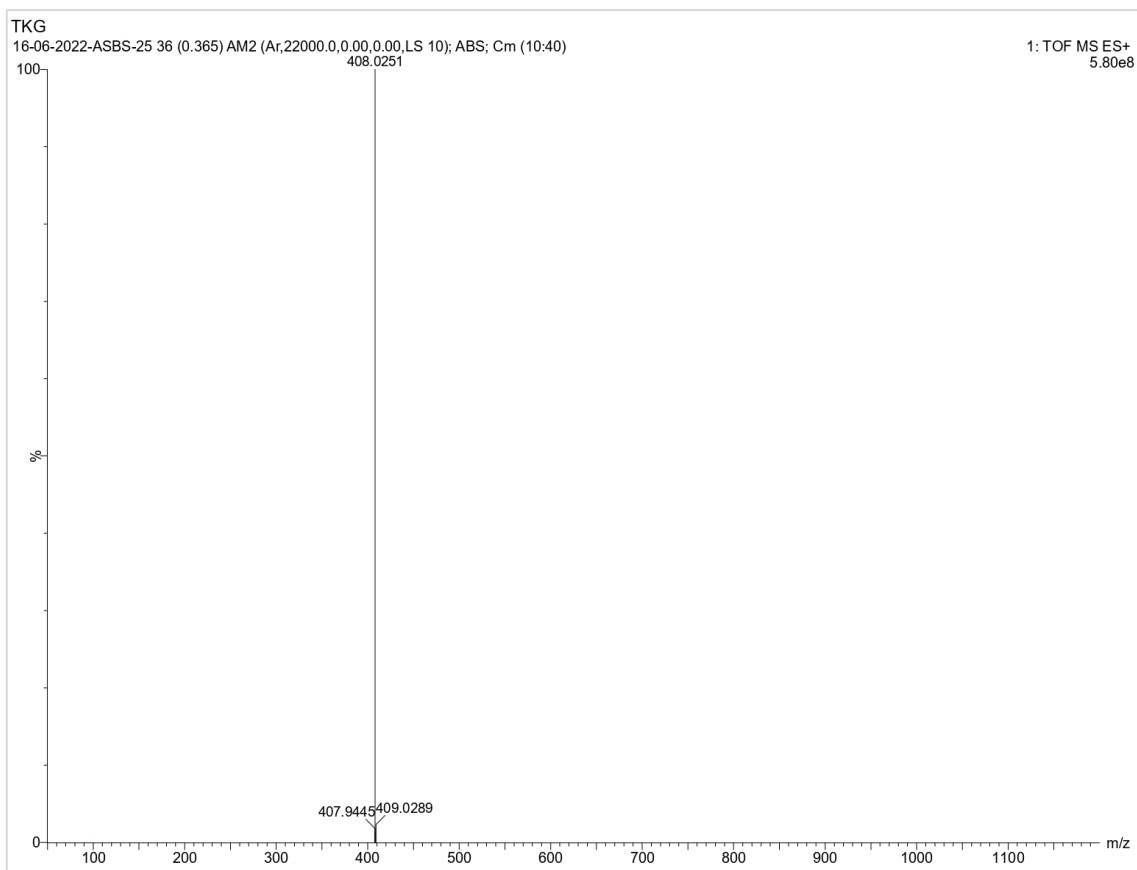
Figure S29. (a)  $^1\text{H}$ , (b)  $^{13}\text{C}\{^1\text{H}\}$  NMR and (c) HRMS of **6s**.



(a)

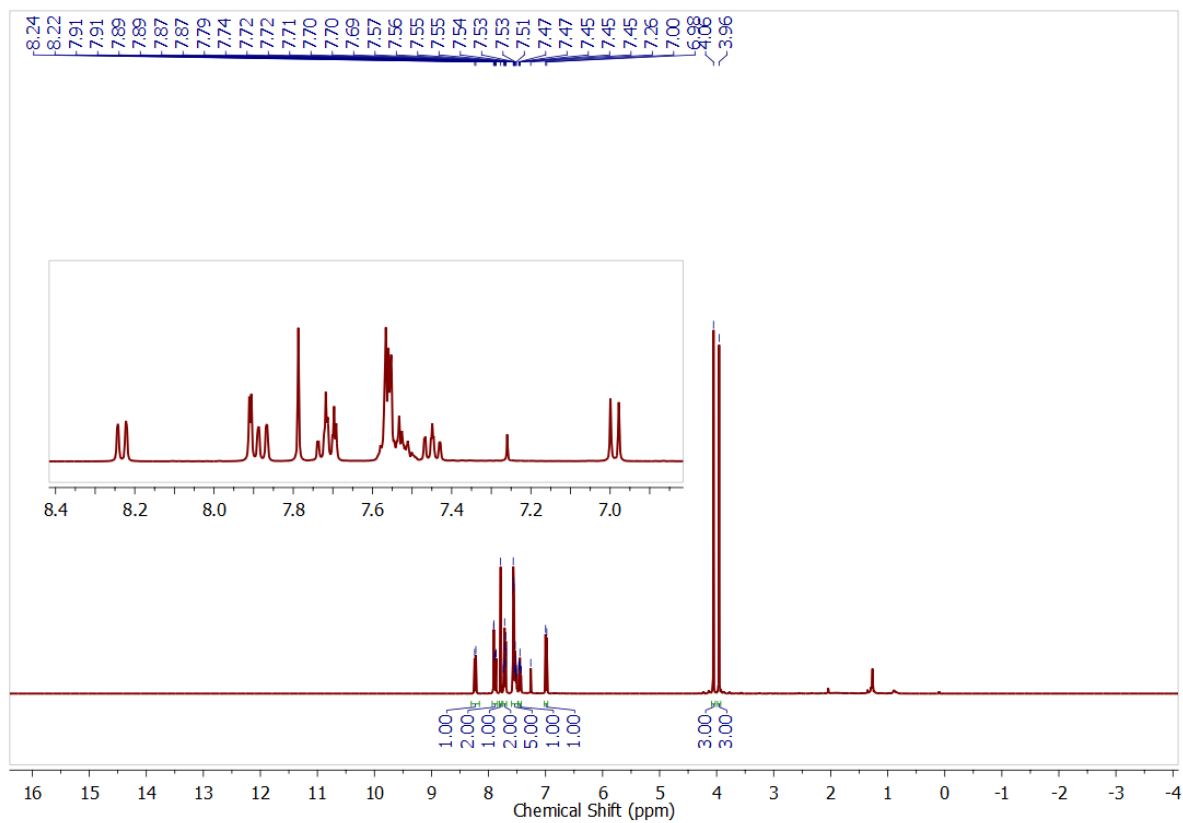


(b)

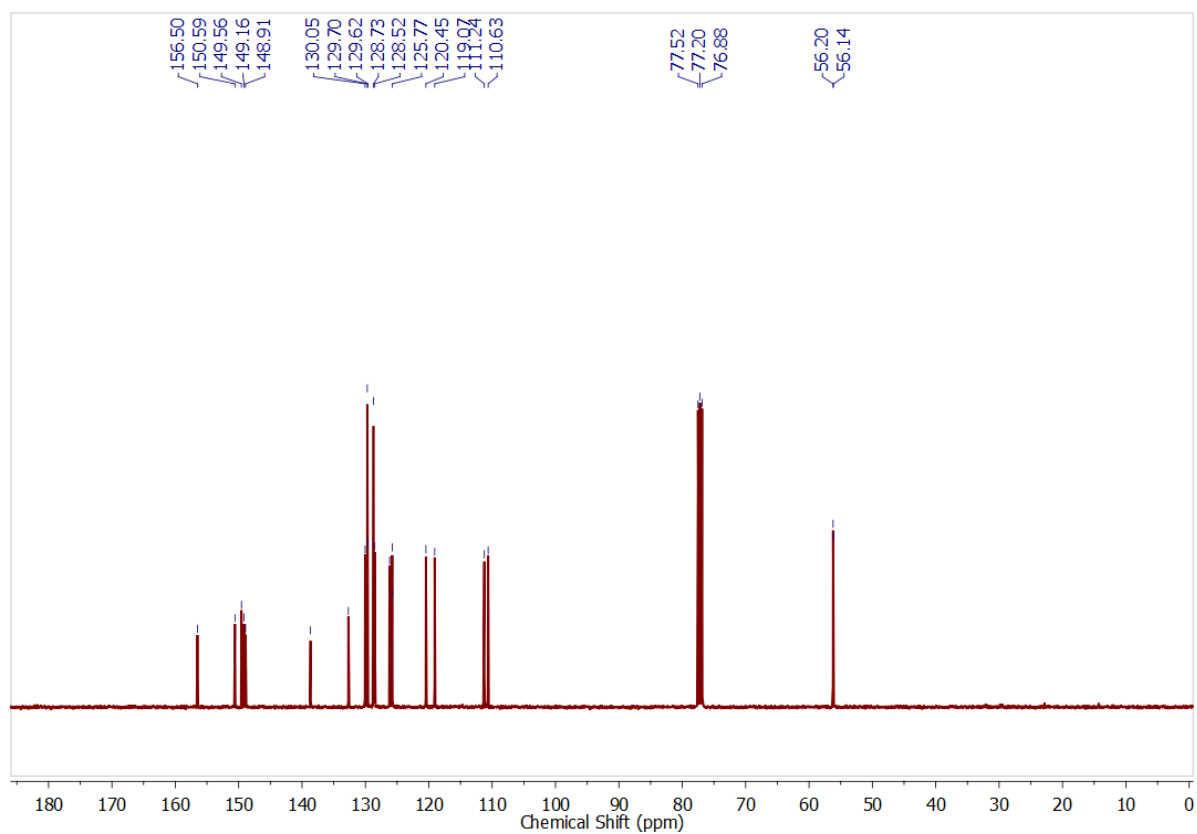


(c)

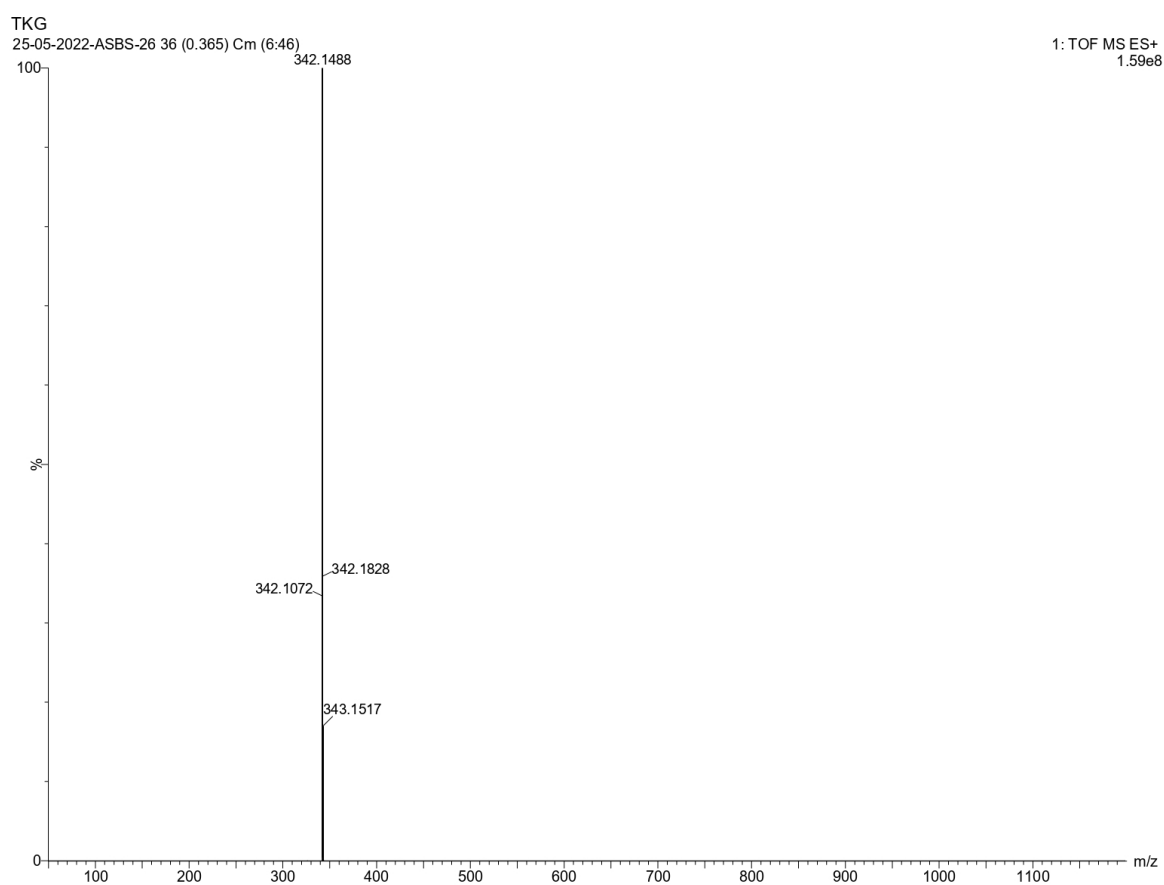
Figure S30. (a)  $^1\text{H}$ , (b)  $^{13}\text{C}\{^1\text{H}\}$  NMR and (c) HRMS of **6t**.



(a)

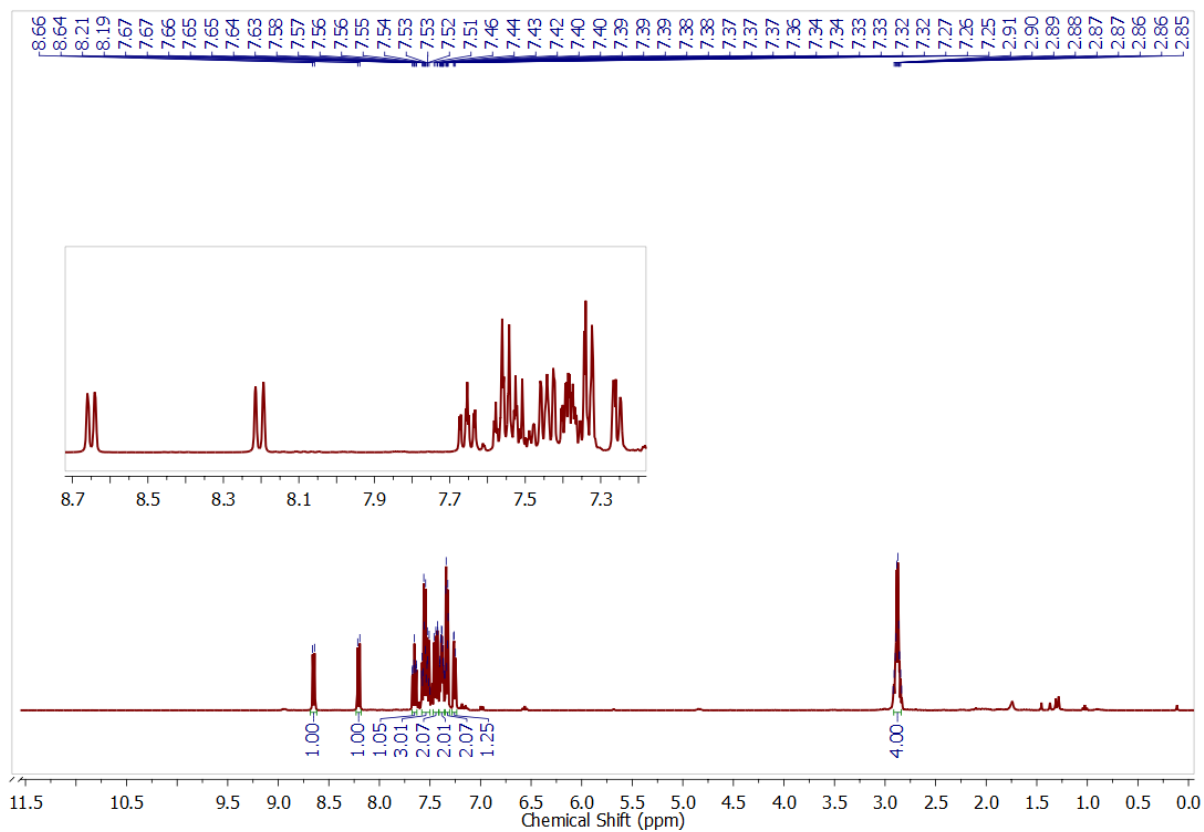


(b)

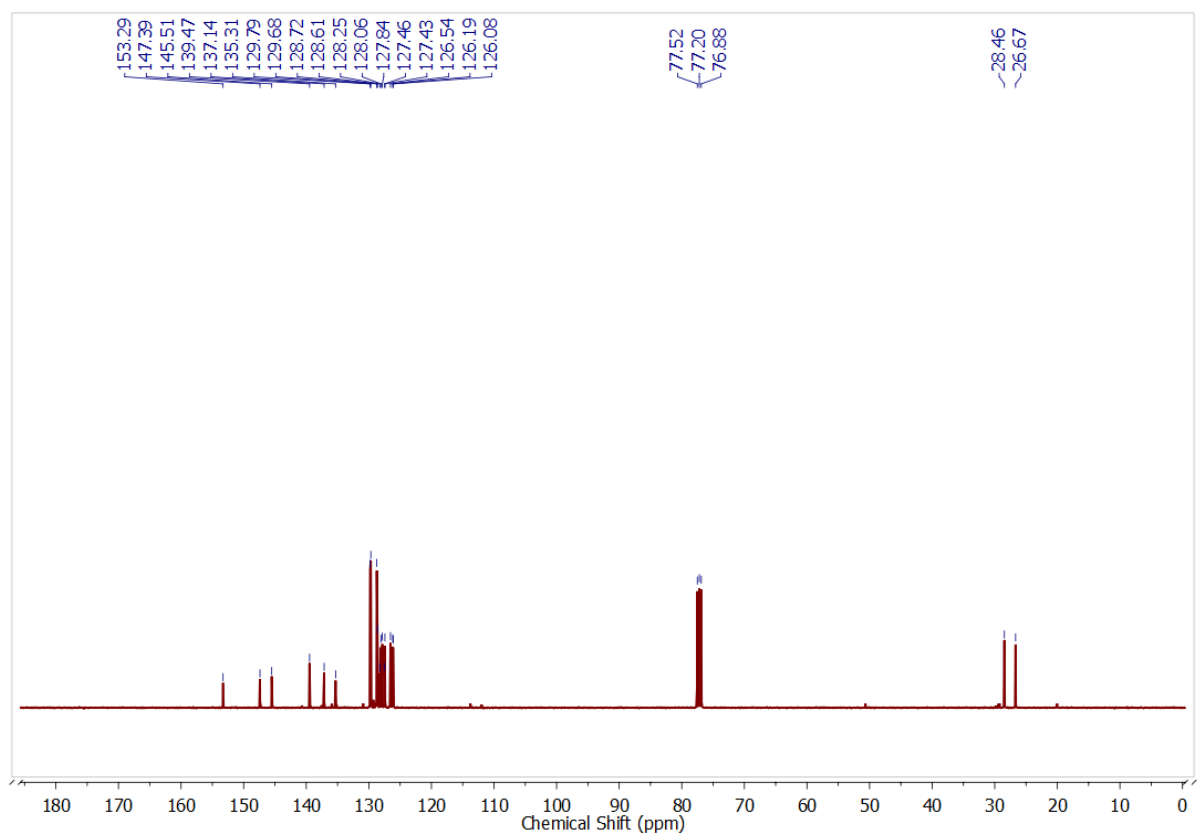


(c)

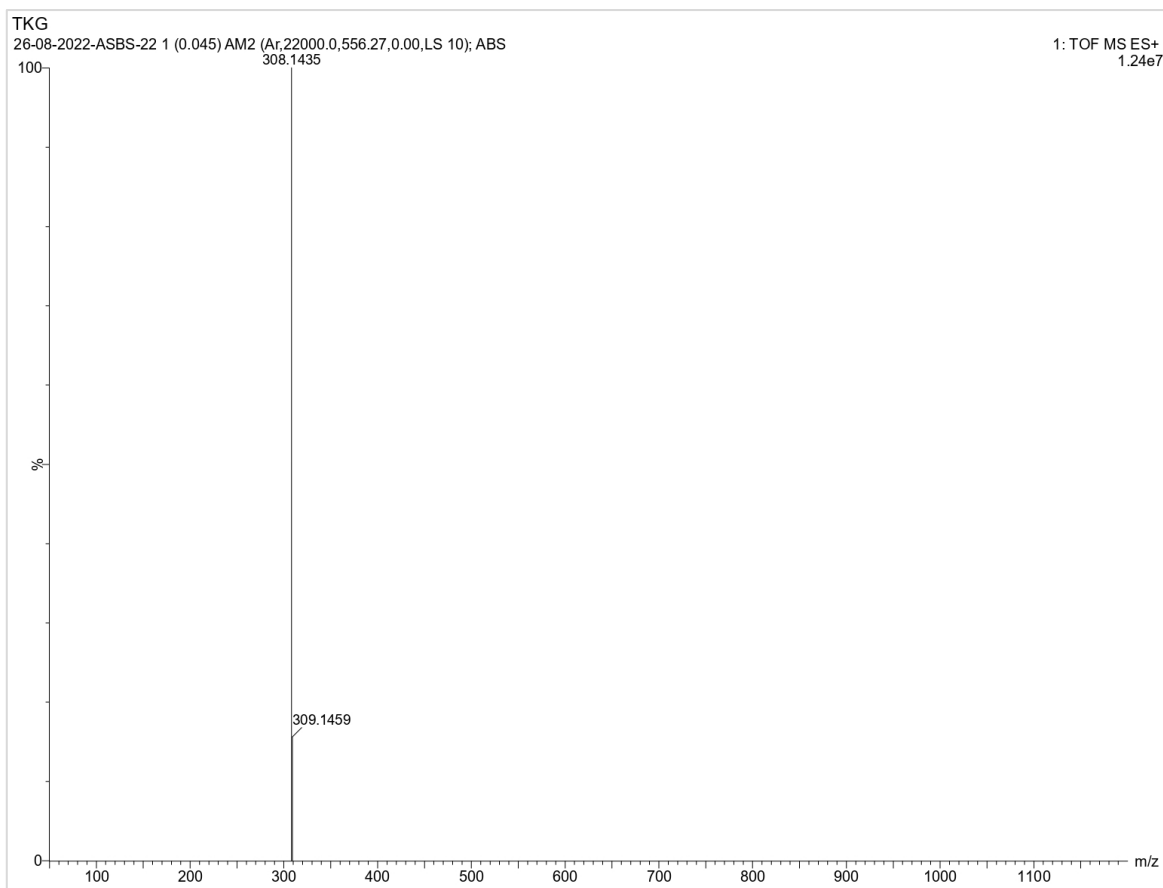
Figure S31. (a)  $^1\text{H}$ , (b)  $^{13}\text{C}\{^1\text{H}\}$  NMR and (c) HRMS of **6u**.



(a)



(b)



(c)

Figure S32. (a)  $^1\text{H}$ , (b)  $^{13}\text{C}\{^1\text{H}\}$  NMR and (c) HRMS of **6v**.

#### References:

1. G. Chelucci and A. Porcheddu, *Chem. Rec.*, 2017, **17**, 200–216.
2. L. Yang and J. P. Wan, *Green Chem.* 2020, **22**, 3074–3078.
3. R. Pothikumar, V. T. Bhat and K. Namitharan, *Chem. Commun.*, 2020, **56**, 13607–13610.
4. Salunkhe, N., Thakare, N., Ladole, C. and Aswar, A. J. *Indian Chem. Soc.*, 2015, **92**, 1295–1298.
5. Cho, C. S., Kim, B. T., Choi, H.-J., Kim, T.-J. and Shim, S. C. *Tetrahedron*, 2003, **59**, 7997–8002.
6. Tang, J., Wang, L., Mao, D., Wang, W., Zhang, L., Wu, S. and Xie, Y. *Tetrahedron*, 2011, **67**, 8465–8469.
7. Lee, S. B., Jang, Y., Ahn, J., Chun, S., Oh, D. C. and Hong, S. *Org. Lett.*, 2020, **22**, 8382–8386.
8. Li, H. J., Wang, C. C., Zhu, S., Dai, C. Y. and Wu, Y. C. *Adv. Syn. Catal.*, 2015, **357**, 583–588.
9. Xu, J. X., Pan, N. L., Chen, J. X. and Zhao, J. W. *J. Org. Chem.* 2021, **86**, 10747–10754.